Entschlüsselung der Funktion des “alten gelben Enzyms” OfrA in der Stressreaktion von *Staphylococcus aureus*

Unraveling the function of the old yellow enzyme OfrA in *Staphylococcus aureus* stress response

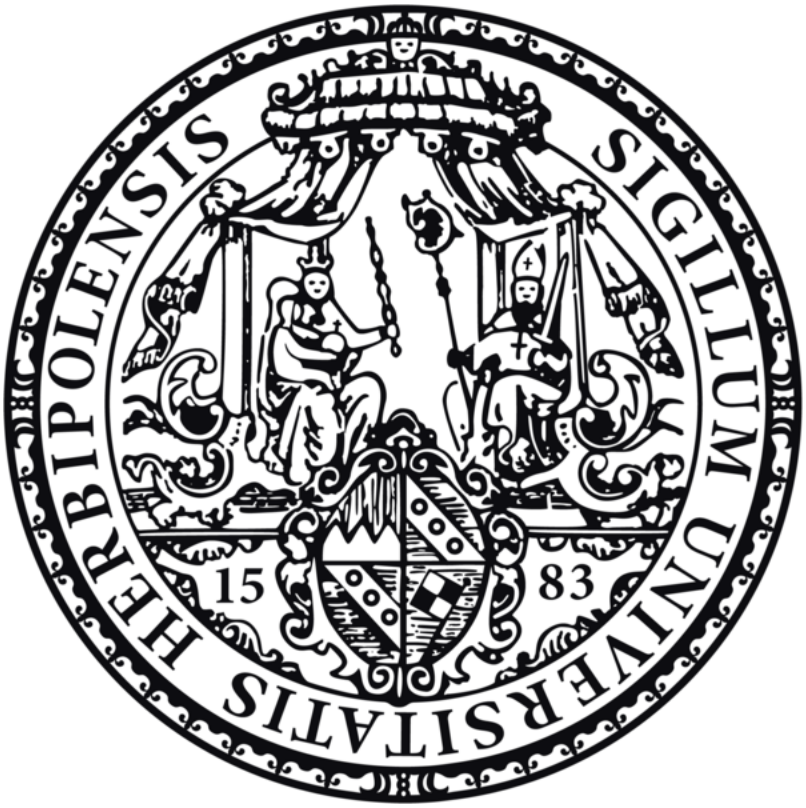

Doctoral thesis for a doctoral degree

at the Graduate School of Life Sciences,

Julius-Maximilians-Universität Würzburg,

Section Infection and Immunity

submitted by

Eslam Samir Ragab Ibrahim

from Cairo, Egypt

Würzburg 2022

Submitted on: ……..……..

Office stamp

Members of the Thesis Committee

Chairperson: Prof. Dr. Christoph Sotriffer

Primary Supervisor: PD. Dr. Knut Ohlsen

Supervisor (Second): PD. Dr. Wilma Ziebuhr

Supervisor (Third): PD. Dr. Martin Fraunholz

Date of Public Defence: ……

Date of Receipt of Certificates: ……..

Contents

Acknowledgment

I would like to express my grateful appreciation to my supervisor, PD Dr. Knut Ohlsen. Dr. Ohlsen offered me an example of how ideal mentorship could be. He was always supporting me and giving attention to my ideas. Because of his guidance, I owe him a lot to be a better member of the scientific field. He encouraged me to join many conferences and scientific projects so that I learnt a lot. He shared with me his huge experience about staphylococcal research, especially, in infection biology. During our conversations, the study conceptualization exponentially progressed. I cannot express how I am glad to be one of his PhD students.

I gained a plethora of insightful thoughts and discussions with PD Dr. Wilma Ziebuhr and PD Dr. Martin Fraunholz. I would like to express my thankfulness for sharing their expertise and resources with me. Dr. Ziebuhr helped us by drawing blood from donors for the whole human blood killing assay.

I would like to thank Dr. Tobias Hertlein and Liane Dreher for their help. Dr. Tobias offered me suggestions regarding the manuscript preparation. Dr. Tobias shared his great expertise with me regarding the host-pathogen interface.

In the beginning of my PhD studies, Dr. Gabriella Marincola and Dr. Freya Wencker offered me stimulating discussions and advices to go through the PhD experience. They were always there whenever I needed to ask for technical advice.

I am thankful for all the support from the working group of PD Dr. Knut Ohlsen, PD Dr. Wilma Ziebuhr, and PD Dr. Martin Fraunholz. I would like to especially thank Jessica Brock for the technical assistance in whole human blood killing assay and Johannes Stumpf and Melina Stockheimer for their assistance in German translation of the thesis summary. I acknowledge Dr. Adriana Moldovan, Tessa Marciniak, Stefanie Stirl, Laura Cecchino, and Stella Cavicchioli for their support and discussions.

I would like to thank the whole supporting members of IMIB institute for the nice scientific niche especially Dr. Elisa Venturini, Dr. Svetlana Durica-Mitic, and Dr. Kristina Popova.

In addition, I am grateful for my family (my mother, my wife, and my brother) for supporting me during the whole PhD journey. Special thanks go to my friends; Muhammed El-Hossary, Dr. Ebaa El-Hossary, Dr. Mariam Hassan, Dr. Abdelrahman Mahomud, Dr. Ammar Abdelrahman, Dr. Eslam Khatab, and Dr. Karim Mersal.

I. Summary

Biological systems are in dynamic interaction. Many responses reside in the core concepts of biological systems interplay (competition and cooperation). In infection situation, the competition between a bacterial system and a host is shaped by many stressors at spatial and temporal determinants. Reactive chemical species are universal stressors against all biological systems since they potentially damage the basic requirements of these systems (nucleic acids, proteins, carbohydrates, and lipids). Either produced endogenously or exogenously, reactive chemical species affect the survival of pathogens including the gram-positive *Staphylococcus aureus* (*S. aureus*). Therefore, bacteria developed strategies to overcome the toxicity of reactive species.

S. aureus is a widely found opportunistic pathogen. In its niche, *S. aureus* is in permanent contact with surrounding microbes and host factors. Deciphering the deterministic factors in these interactions could facilitate pinpointing novel bacterial targets. Identifying the aforementioned targets is crucial to develop new strategies not only to kill the pathogenic organisms but also to enhance the normal flora to minimize the pathogenicity and virulence of potential pathogens. Moreover, targeting *S. aureus* stress response can be used to overcome bacterial resistance against host-derived factors. In this study, I identify a novel *S. aureus* stress response factor against reactive electrophilic, oxygen, and hypochlorite species to better understand its resilience as a pathogen.

Although bacterial stress response is an active research field, gene function is a current bottleneck in characterizing the understudied bacterial strategies to mediate stress conditions. I aimed at understanding the function of a novel protein family integrated in many defense systems of several biological systems.

In bacteria, fungi, and plants, old yellow enzymes (OYEs) are widely found. Since the first isolation of the yellow flavoprotein, OYEs are used as biocatalysts for decades to reduce activated C=C bonds in α,β-unsaturated carbonyl compounds. The promiscuity of the enzymatic catalysis is advantageous for industrial applications. However, the physiological function of OYEs, especially in bacteria, is still puzzling. Moreover, the relevance of the OYEs in infection conditions remained enigmatic.

Here, I show that there are two groups of OYEs (OYE flavin oxidoreductase, OfrA and OfrB) that are encoded in staphylococci and some firmicutes. OfrA (SAUSA300_0859) is more conserved than OfrB (SAUSA300_0322) in staphylococci and is a part of the staphylococcal core genome.

A reporter system was established to report for *ofrA* in *S. aureus* background. The results showed that *ofrA* is induced under electrophilic, oxidative, and hypochlorite stress. OfrA protects *S. aureus* against quinone, methylglyoxal, hydrogen peroxide, and hypochlorite stress. Additionally, the results provide evidence that OfrA supports thiol-dependent redox homeostasis. At the host-pathogen interface, OfrA promotes *S. aureus* fitness in murine macrophage cell line. In whole human blood, OfrA is involved in *S. aureus* survival indicating a potential clinical relevance to bacteraemia.

In addition, *ofrA* mutation affects the production of the virulence factor staphyloxanthin *via* the upper mevalonate pathway. In summary, decoding OfrA function and its proposed mechanism of action in *S. aureus* shed the light on a conserved stress response within multiple organisms.

II. Zusammenfassung

Biologische Systeme unterliegen ständig dynamischen Interaktionen. Diese werden geprägt von Konkurrenz und Kooperation. Im Falle einer Infektion wird die Konkurrenz zwischen einem bakteriellen Organismus und dem infizierten Wirt von der Einwirkung vieler Stressoren in allen biologischen Nischen geprägt. Eine fundamentale Rolle spielen dabei reaktive chemische Verbindungen die als universale Stressoren alle biologischen Systeme mit ihren fundamentalen Makromolekülen (Nukleinsäuren, Proteine, Kohlenhydrate und Lipide) potenziell schädigen. Reaktive chemische Verbindungen, entweder endogen oder exogen gebildet, beeinträchtigen das Überleben aller Pathogene, auch das Überleben des in dieser Arbeit behandelten gram-positiven Bakteriums *Staphylococcus aureus* (*S. aureus*). Um die lebensbedrohende Toxizität der reaktiven Verbindungen zu umgehen, haben Bakterien eine Vielzahl hoch spezialisierter Überlebensstrategien entwickelt.

S. aureus ist ein weit verbreiteter opportunistischer Krankheitserreger. Er unterliegt dem permanenten Kontakt mit dem umgebenden Mikrobiom und den verschiedenartigen Wirtsfaktoren. Das Wissen um die Mechanismen der bakteriellen Stressabwehr während einer Pathogen-Wirts-Beziehung könnte als Grundlage für die Identifizierung neuer antibakterieller Zielstrukturen dienen. Eine spezifische Inaktivierung solcher Strukturen könnte dann den pathogenen Organismus schädigen ohne die normale Flora zu schwächen. Ferner können Untersuchungen an der Stressantwort von *S. aureus* genutzt werden, um die bakterielle Resistenz gegen wirtseigene Faktoren zu schwächen.

Im Mittelpung dieser Arbeit steht die Charakterisierungeines neuartigen Faktors in der Stressantwort von *S. aureus*, der sowohl gegen elektrophilen Stress als auch gegen reaktive Sauerstoff- und Hypochlorit-Verbindungen aktiv ist. Die Ergebnisse der Arbeiten tragen zu einem besseren Verständnis der Stressantwort von dem wichtigen pathogenen Bakterium *S. aureus* bei.

Trotz der Tatsache, dass die Untersuchung bakterieller Stressantworten Gegenstand der aktuellenForschung ist, sind viele Prozesse und die daran beteiligten Faktoren nur unzureichend charakterisiert. Daher war die Zielsetzung dieser Thesisdie Funktion eines Vertreters einer neuen Proteinfamilie, die mglw. in vielen Abwehrsystemen gegen chemische Stressoren eine wichtige Rolle spielt, zu untersuchen. Die von Otto Warburg erstmalig als “old yellow enzymes” (OYEs) bezeichnete Proteinfamilie ist im Bakterien-, Pilz- und Pflanzenreich weit verbreitet. Nach der erstmaligen Isolation des gelben Flavoproteins, werden OYEs seit

vielen Jahrzehnten als Biokatalysatoren verwendet, um aktivierte C=C-Doppelbindungen in α,β-ungesättigte Carbonylverbindungen zu reduzieren. Die Promiskuität der enzymatischen Katalyse ist für industrielle Anwendungen sehr vorteilhaft. Nichtsdestotrotz konnte die physiologische Funktion von OYEs besonders in Bakterien bislang nur ansatzweise aufgeklärt werden und die Beteiligung der OYEs unter Infektionsbedingungen ist weiterhin unbekannt.

In dieser Arbeit wurden zwei Vertreterder OYEs (OYE flavin oxidoreductase OfrA und OfrB) im Genom von Staphylokokken und Firmicuten identifiziert. OfrA (SAUSA300_0859) ist in Staphylokokken stärker konserviert als OfrB (SAUSA300_0322) und ist Teil des Kerngenoms. Es wurde ein Reportersystem etabliert, um die Expression von *ofrA* in *S. aureus*-Stämmen zu untersuchen. Die Daten dieser Arbeit zeigen, dass *ofrA* unter elektrophilen, oxidativen und hypochloriten Stressbedingungen induziert wird. OfrA schützt *S. aureus* vor Stress durch Quinone, Methylglyoxal, Wasserstoffperoxid und Hypochlorit. Weiterhin liefern die Ergebnisse Evidenz, dass OfrA die Thiol-abhängige Redox-Homöostase unterstützt. Weiterhin ist OfrA an der Fitness und dem Überleben von *S. aureus* nach Phagozytose in murinen Makrophagen beteiligt. Das Überleben von *S. aureus* in humanem Vollblut war ebenfalls sehr stark von der OfrA Expression abhängig. Somit kann auf eine wichtige Rolle von OfrA während des Infektionsgeschehens z.B. bei Bakteriämie geschlossen werden.

Weiterhin zeigt sich, dass Mutationen in *ofrA*, die Produktion des Virulenzfaktors Staphyloxanthin über den oberen Mevalonatweg beeinflussen. Insgesamt liefert die vorliegende Arbeit neue Einblicke in die Funktion und Verbeitung von OfrA, einem neuen Vertreter aus der Klasse der OYEs. Die vorliegenden Ergebnisse ermöglichen somit auch ein besseres Verständnis konservierter Strategien der Stressantwort bei Bakterien und deren Bedeutung während des Infektionsgeschehens.

1 Introduction

1.1 *Staphylococcus aureus* is a successful opportunistic pathogen

Staphylococcus is a gram-positive bacterial genus. Staphylococci belong to the phylum Firmicutes from which they inherit the cell wall structure. Under microscope, staphylococcal species has cocci- (spheres) shaped cells. The genomes of staphylococci contain low G+C content (roughly around 33%) together with many other genera of Firmicutes (including *Bacillus*, *Listeria*, *Enterococcus*, *Clostridium*, and *Streptococcus*).

Staphylococcus aureus (*S. aureus*) is a biologically and clinically important species that has the ability to inhabit humans as a part of the normal microbiota of skin and upper respiratory system. The first report of *S. aureus* as a pathogen was released in 1880 by the surgeon Alexander Ogston (Guo et al., 2020). *S. aureus* cells are averaged to be 0.8 µm in diameter (Guo et al., 2020). On blood agar, *S. aureus* colonies have a diameter of 1-2 mm and most of *S. aureus* strains are haemolytic (Sato et al., 2019).

S. aureus is characterized by the ability to produce a golden pigment (staphyloxanthin) as a metabolite from carotenoid biosynthesis. The golden pigmentation showed a characteristic phenotype in the subsequent naming of the organism. *S. aureus* are capsulated to avoid the phagocytic clearance in their host (Kuipers et al., 2016). Another phenotype of *S. aureus* that showed clinical relevance is their ability for bacterial colonization (Krismer et al., 2017). In the mode of pathogen, *S. aureus* can cause a variety of minor infections (skin and soft tissue) and major infections (pneumonia, osteomyelitis, and bacteraemia) (Klevens et al., 2007; Tong et al., 2015). *S. aureus* is one of the ESKAPE pathogens which are brought up as increasingly resistant to the commonly known antibiotics (Renner et al., 2017).

1.1.1 *S. aureus* virulence factors and pathogenesis

To be a successful human pathogen, *S. aureus* is able to produce many virulence factors including adhesins, enzymes, and toxins that affect the host-pathogen interplay (Thammavongsa et al., 2015). *S. aureus* aims at utilizing the host tissue as a resource for bacterial growth and benefits *via* exoproteins include enzymes, toxins, and surface proteins (Smith et al., 2016).

S. aureus produces surface components such as the polysaccharide capsule and adhesins (Lacey et al., 2016). The ability to produce capsular polysaccharide is linked to the ability of invasive infections (Portolés et al., 2001; Rausch et al., 2019). Microbial surface

components recognizing adhesive matrix molecules (MSCRAMM) are an integral part of *S. aureus* virulence factors for host-attachment (Foster, 2019). MSCRAMM, in *S. aureus*, include surface Ig-binding protein (SpA) (Votintseva et al., 2014), fibronectin-binding proteins (FnbpA and FnbpB) (Speziale and Pietrocola, 2020), collagen adhesion (CNA) (Arora et al., 2021), and clumping factors (ClfA, ClfB) (Speziale and Pietrocola, 2020).

S. aureus is a coagulase positive *Staphylococcus*. Coagulation can be a strategy for immune evasion and can be achieved *via* expression of coagulases (Coa and vWbp) (McAdow et al., 2012). Staphylokinase interact with plasminogen resulting in active proteolytic plasmin in some lysogenic *S. aureus* strains (BOKAREWA et al., 2006). Staphylococcal lipase (Lip) aims at evading granulocytes and affects *S. aureus* pathogenesis (Hu et al., 2012). Furthermore, hyaluronic acid (abundant in skeletal tissues, lungs, skin, and heart valves) is a substrate for the hyaluronidase enzyme (HysA) as a spreading factor for *S. aureus* infections (Duran-Reynals, 1933; Ibberson et al., 2014). *S. aureus* is able to escape the host defence neutrophil extracellular traps (NETs) *via* nuclease production (Berends et al., 2010).

A plethora of *S. aureus* toxins are pathogenesis determinants under infection conditions (Berends et al., 2010). *S. aureus* can produce three major categories of toxins; 1) pore-forming, 2) exfoliative, and 3) superantigens (Oliveira et al., 2018). Examples of pore-forming toxins are haemolysin-α, haemolysin-β, leukotoxin, and phenol-soluble modulins (Oliveira et al., 2018). Some serine proteases are examples of exfoliative toxins and associated with keratinocytes junction cleavage (Bukowski et al., 2010). So far, 23 superantigens were discovered in *S. aureus*, some of them are famous for inducing food-poising symptoms (Grumann et al., 2014).

Overall, the disease progression caused by *S. aureus* infections involve many bacterial virulence factors. These factors are highly regulated through different molecular mechanisms to achieve a multifactorial virulence according to the site of infection. However, some toxins can solely cause toxic syndromes such as food poisoning, and toxic shock syndrome.

S. aureus regulates its virulence machinery *via* a complicated network of regulators (Jenul and Horswill, 2019). Two-component systems (TCSs) such as AgrAC, SaeRS, SrrAB, and ArlRS sense and respond to the external stimuli surrounding *S. aureus* (**Table 1**). In addition, the transcriptional regulators SarA, Rot, and MgrA control *S. aureus* virulence at the host-pathogen interface (**Table 2**). The alternative sigma factor (SigB) is critical in *S. aureus*

infections *via* affecting the transcriptional initiation of stress-mediating proteins and some virulence determinants (Tuchscherr et al., 2015).

Table 1: Virulence regulating TCS examples in *S. aureus*.

TCS	Characteristics	References
AgrAC	• *agr* is a qurom sensing system in *S. aureus*. • *agr* system controls numerous exoenzymes and exotoxins.	(Dunman et al., 2001; Cheung et al., 2011)
SaeRS	• SaeRS system controls α-toxin, β- and γ-hemolysins, coagulase, LukGH, and other virulence factors. • Copper and zinc inhibit the signal transduction from SaeS to SaeR.	(Giraudo et al., 1999; Mainiero et al., 2010; Cho et al., 2015)
SrrAB	• SrrAB system senses the available level of oxygen. • SrrAB is important in nitrosative and oxidative stress.	(Throup et al., 2001; Ulrich et al., 2007)
ArlRS	• ArlRS system controls *S. aureus* autolysis for cell wall remodeling. • ArlRS affects *S. aureus* clumping phenotype. • ArlRS is important in cell wall stress response.	(Fournier et al., 2001; Memmi et al., 2012; Walker et al., 2013)

Table 2: Virulence transcriptional regulators examples in *S. aureus*.

Regulator	Characteristics	References
SarA	• SarA is one of a family of regulators including SarR, SarT, SarU, and SarS. • SarA has positive and negative regulation on some virulence factors in close interaction with *agr* system.	(Liu et al., 2006; Morrison, 2012)
Rot	• Rot was discovered as “repressor of toxins” from SarA-like family. • Rot interacts with *agr* system and SaeRS for some virulence genes regulation.	(Manna and Ray, 2007; Benson et al., 2012)
MgrA	• MgrA controls a wide variety of virulence genes such as coagulase, Protein A, and extracellular serine proteases. • MgrA is partly controlled by ArlRS system.	(Luong et al., 2003; Crosby et al., 2016)

1.1.2 *S. aureus* and antibiotic resistance and tolerance

Clinically important antibiotics have one of five main mechanisms of action (Foster, 2017). 1) β-Lactams, vancomycin, daptomycin, and their analogues target the cell envelope (Arbeit et al., 2004; Peacock and Paterson, 2015; Zeng et al., 2016). 2) 30S ribosomal subunits protein synthesis inhibitors are exemplified with tetracyclines and aminoglycosides (Davis et al., 1986; Wilson, 2009). 3) Linezolid, chloramphenicol, clindamycin, macrolides, streptogramins, and their analogues are 50S ribosomal subunits protein synthesis inhibitors (Wilson, 2014). 4) Other protein synthesis inhibitors such as fusidic acid (elongation factor G inhibitor)

and mupirocin (isoleucyl-tRNA synthetase inhibitor) are of high therapeutic values against *S. aureus* infections (Thomas et al., 2010; Fernandes, 2016). 5) Nucleic acid synthesis inhibitors (fluoroquinolones, antifolates, rifampicin, and analogues) are widely used antibiotics (Campbell et al., 2001; Hooper, 2002; Oefner et al., 2009). Furthermore, fatty acid biosynthesis, cell division, ClpP protease, and teichoic acid synthesis are proposed as important and/or potentially important basis for new therapeutics development as a proxy to overcome the increasing *S. aureus* resistance (Foster, 2017).

Since the usage of penicillin in the clinical setting, in 1940s, reports pointed out penicillin resistant *S. aureus* (Imsande, 1978). The main mechanism was the production of penicillinase enzyme (Rosdahl, 2009). Semi-synthetic penicillin (methicillin) was developed in a way to overcome the bacterial resistance. After two years after introducing methicillin in clinics, *mecA* in SCCmec was reported to cause a methicillin-resistance phenotype in *S. aureus*. SCCmec is a chromosomal mobile genetic element causing the appearance of the methicillin-resistant *S. aureus* (MRSA) lineages (Liu et al., 2016). Importantly, methicillin-resistant *S. aureus* (MRSA) increased prevalence leads to treatment failure due to multiple drug resistance (Fischbach and Walsh, 2009). Overall, the mortality rate are higher in MRSA infections than in methicillin-susceptible *S. aureus* (MSSA) (Cosgrove et al., 2003).

Due to important differences in the pathogenesis, epidemiology, and microbiological characteristics, MRSA is further classified into three types. MRSA includes hospital acquired (HA-MRSA), community acquired (CA-MRSA), or livestock-associated (LA-MRSA) (Lindsay, 2013; Otto, 2013; Anjum et al., 2019). One important difference in the genotypes between HA- and CA-MRSA is the SCCmec typing (SCCmec type I-III or SCCmec type IV-V) (Bukharie, 2010). HA-MRSA is considered an opportunistic pathogen, however, CA-MRSA is able to establish an infection in people with no predisposing comorbidities (Naimi et al., 2003).

In minor infections of CA-MRSA, incision and drainage improves the outcome of the therapy (Lee et al., 2004). However, in more complicated infections, antibiotic treatment is the favourable curative option (besides the surgical drainage if possible). Trimethoprim-Sulfamethoxazole, doxycycline, clindamycin, rifampicin, and tetracycline can be used to treat *S. aureus* infections as monotherapy or in combination depending on the clinical situation and the possibility of co-infections (Kaplan, 2005).

Antibiotic resistance in *S. aureus* can be classified into two main categories; 1) intrinsic and 2) acquired resistance. Intrinsic resistance could be due to membrane permeability, efflux

systems, and β-lactamases production (Guo et al., 2020). Acquired resistance could be due to mutations, horizontal gene transfer, and heteroresistance (Guo et al., 2020). Although, the heteroresistance phenomenon is unstable and could be reversed by the removal of antibiotic, the clinical outcome of the therapy could be affected with the presence of heteroresistant sub-population (Kayser et al., 1970; El-Halfawy and Valvano, 2015). Recent reports illustrated that heteroresistance is caused by gene amplification in monoclonal or polyclonal sub-populations (El-Halfawy and Valvano, 2015; Nicoloff et al., 2019).

Recently, the scientific community is looking at the antibiotic tolerance as another therapeutic determinant in the failure of *S. aureus* eradication (Levin-Reisman et al., 2019). Antibiotic tolerance is the ability of the microorganism to survive transient exposure of a bactericidal antibiotic without change in the minimum inhibitory concentration (MIC) of the antibiotic against the strain (Brauner et al., 2016). Non-inherited tolerance can be caused by stress response from starvation, oxidative stress, host factors, and/or the antibiotic (Bigger, 1944; Nguyen et al., 2011; Johnson and Levin, 2013; Rowe et al., 2020). However, activation of some stress response mechanisms, such as efflux pumps, could result in increasing MIC against the bactericidal antibiotic in a mixed resistance and tolerance phenotype (Nguyen et al., 2011; Brauner et al., 2016). *In-vitro* analysis of the tolerant phenotype of *S. aureus* shows a plethora of factors including: *agr*, ATP, *ileS*, TCA cycle, ppGpp, Clp, MazF/MazE, *msaABCR*, and SOD as targets (Kuehl et al., 2020). The presence of many factors in redox homeostasis mechanisms of *S. aureus* illustrates the *in-vivo* role of redox homeostasis in the overall clinical outcome of the therapy (Rowe et al., 2020).

In conclusion, the understanding of *S. aureus* resistance and tolerance mechanisms against the host immune response and antibiotics will lead to new drug target discovery, better designing new antibiotics, and potentiating the existing antibiotic toolbox.

1.2 Redox-related stresses in *S. aureus* at the host-pathogen interface

During bacterial growth and infection, *S. aureus* is exposed to numerous types of reactive species. Reactive oxygen (ROS), electrophilic (RES), chlorine (RCS), nitrogen (RNS), and sulfur species (RSS) are possible redox homeostasis threats with which *S. aureus* needs to cope with (Van Loi et al., 2015; Peng et al., 2017). Oxidants can interact with numerous targets within the bacterial cells including amino acids, nucleic acids, carbohydrates, and/or fatty acids (Marnett et al., 2003; Delmastro-Greenwood et al., 2014). Although stresses are intracellularly interconvertible due to sequential reactions, *S. aureus* maintains numerous

stress response as separate and/or integrated network to quench their toxic effects and repair the damaged biomolecules (Guerra et al., 2017; Reichmann et al., 2018; Linzner et al., 2020).

1.2.1 Oxidative stress

Reactive oxygen species (ROS) are by-products of oxygen metabolism and include superoxide ($O_2^{-\cdot}$), hydrogen peroxide (H_2O_2), organic peroxides, singlet oxygen ($^1O_2$), and the highly toxic hydroxyl radical ($^{\cdot}OH$). ROS interact with all types of cellular resources including nucleic acids, proteins, and lipids to cause cellular toxicity (Imlay, 2013). In addition, ROS production is amplified within the bacterial cells. For example, $O_2^{-\cdot}$ and H_2O_2 destabilize Fe-S clusters in enzymatic systems, such as aconitase and serine dehydratase. The released Fe interacts with H_2O_2 to produce hydroxyl radicals *via* Fenton chemistry (Jang and Imlay, 2007).

In bacteria, energy is produced *via* a series of redox reactions. Electrons move through biomolecules and oxygen be their final acceptor in aerobic respiration (Imlay, 2019). An inevitable cost of cellular respiration, oxygen metabolism produces ROS *via* the electron transport chain (ETC). However, ETC is not the only source of bacterial-derived ROS (Seaver and Imlay, 2004). Cellular metabolism contributes to ROS production in bacteria indicating the necessity of conserved ROS detoxification and repair systems (Brynildsen et al., 2013). Moreover,

in *S. aureus*, the phenol soluble modulins (PSMs) virulence factor and the stringent response cause increased intracellular oxidative stress (Horvatek et al., 2020). In addition, the host utilizes ROS as an effective killing mechanism against many bacteria including *S. aureus*. In phagocytic cells, NADPH oxidase (NOX_2), which is located in the phagosome membrane, produces ROS in the oxidative burst process to kill invading bacteria (Pidwill et al., 2021). Furthermore, antibiotic treatment results in substantial production of endogenous ROS, which contribute to many bactericidal mode of action (Kohanski et al., 2007; Brynildsen et al., 2013; Hung and Helmann, 2013). In summary, *S. aureus* encounters ROS through cellular metabolism, aerobic respiration, host factors, bacterial virulence factors, and antibiotics.

1.2.2 Electrophilic stress

RES is employed by chemical compounds that contain an electron-deficient carbon center (Farmer and Davoine, 2007). *S. aureus* has to cope with endogenous RES (menaquinones, siderophores, and methylglyoxal), RES generated secondarily to ROS and RNS, and RES from the host-pathogen interface (formaldehyde) (Chakraborty et al., 2014; Groitl and Jakob, 2014; Chen et al., 2016; Linzner et al., 2020). During infection, reactive aldehydes and methylglyoxal

are excessively produced as toxic molecules against the invading organism (Hazen et al., 1998). RES target the labile proteins through protein *S*-alkylation at cysteine, lysine, and arginine residues (Linzner et al., 2020). Protein *S*-alkylation could result in function inhibition, initiation, or modulation, being interesting at transcriptional regulators (Reichmann et al., 2018; Ray et al., 2020; Van Loi et al., 2021).

1.2.3 Hypochlorite stress

S. aureus infections could be hospitably acquired that we need to eradicate in healthcare settings through disinfectants usage. Sodium hypochlorite (NaOCl) dissociates into hypochlorous acid (HOCl) which is highly oxidizing agent producing reactive chlorine species (RCS) (da Cruz Nizer et al., 2020). Moreover, disinfection using NaOCl is superior to ethanol against *S. aureus* biofilms (Tiwari et al., 2018b). Host immune response exploits the sensitivity of *S. aureus* towards hypochlorite stress in the activated macrophages and neutrophils. Myeloperoxidase generates HOCl from Cl^- and H_2O_2 in the oxidative burst process. ROS and RCS are the main bacterial killing mechanisms in the phagolysosome (Chapman et al., 2002; Klebanoff et al., 2013).

1.2.4 Nitrosative stress

Nitric oxide (NO) is a product from the host immune response *via* nitric oxide synthase (Bogdan, 2015). In *S. aureus*, the lipophilic gas NO diffuses through the bacterial membrane and causes the nitrosative stress. NO interacts with metal centers of bacterial enzymes including Fe-S clusters, heme, and transition metal cofactors (Richardson et al., 2011). Thus and at high concentration, NO can inhibit the bacterial respiration due to cytochrome heme iron interaction (Richardson et al., 2008). In addition, NO encounters protein-thiols causing protein *S*-nitrosylation (Foster et al., 2003). However, the NO-based control against *S. aureus* is not as critical as against *Salmonella enterica* (Gaupp et al., 2012). RNS is expanded by the reaction of NO with other reactive species such as O_2^- to yield the strong oxidant ($ONOO^-$) (Tharmalingam et al., 2017).

1.2.5 Sulfhydryl stress

Some of sulfur-based compounds have the ability to oxidize protein-thiols with increasing the oxidation status of the sulfur atoms (Giles and Jacob, 2002). RSS are exemplified with polysulfides, persulfides, and thiosulfates. Intracellular H_2S production is mediated with cystathionine-β-synthase or cystathionine-γ-lyase in *S. aureus* from sulfur metabolism (Linzner et al., 2020). RSS exposure and sulfur metabolism manipulate important phenotypes in *S. aureus* including the biofilm formation and antibiotic resistance (Soutourina et al., 2009;

Shatalin et al., 2011). Moreover, RSS levels and H_2S homoeostasis affect the protein *S*-sulfhydration and thus virulence genes regulation (Peng et al., 2017). Furthermore, defective sulfur cysteine and homocysteine metabolism strains show compromised survival in leukocytes clearance (Toliver-Kinsky et al., 2019).

1.3 Redox homeostasis in *S. aureus*

Many biomolecules act as potential targets of oxidant-toxicities. Fe-S clusters of certain enzymes (aconitase and serine dehydratase) are oxidized leading to the enzymatic activity loss (Flint et al., 1993).

Hydroxyl radial that is generated from Fenton reaction can interact with the first encountered molecule. Ironically, Fe^{2+} cations, the Fenton chemistry essential, are attracted to DNA due to charges difference which causes higher hydroxyl radical production rate in close proximity to DNA. Therefore, DNA becomes a sensible target for oxidative damage (Keyer and Imlay, 1996).

In addition, amino acids in free form and/or in protein residues, including cysteine, methionine, and tryptophan, are amenable to oxidation (Chouchani et al., 2011). Although protein modification can be considered as oxidative damage, some modifications can actually cause functional gain or modulation as exemplified by many oxidative-stress resistance mechanisms (Reichmann et al., 2018). The modification can be a secondary product of the LMW thiol redox buffering system including SarR, PerR, CtsR, and SarS (Linzner et al., 2020). Therefore *S. aureus* has to continually maintain intracellular redox homeostasis *via* metal homeostasis response, metabolic response, DNA protection and repair, thiol-independent detoxification, and thiol-dependent detoxification. Indeed, the classification does not employ clear cutoffs; rather, all systems harmonically operate to defend against oxidative threats.

Oxidative stress response affects many physiological functions in *S. aureus*. However, the stress response has different modes depending on the nature of the stressor (hydrogen peroxide, organic peroxide, hypochlorite, alkylating agents, electron-deficient species, etc.) (Wolf et al., 2008). Within the host, the response is more complicated due to the complex nature of the stressors and the interference with other kinds of stress responses such as stringent response (Chen et al., 2016; Moldovan and Fraunholz, 2019; Horvatek et al., 2020). Therefore, it is important for *S. aureus* to build a complicated regulatory network to increase the survivability against the expected stressors and better using its resources.

1.3.1 Metal homeostasis

Transition metals have particular importance in redox homeostasis due to their roles in enzymatic functions, hydroxyl radical formation, electron transfer, and protein structures. Fe, Cu, Mn, and Zn are the most important intracellular transition metals. Therefore, *S. aureus* developed strategies to control the intracellular levels of each metal (Gaupp et al., 2012).

Iron is stored, in *S. aureus*, after interaction with ferritin (*ftnA*). Moreover, bacterioferritin comigratory protein (Bcp) and metallo regulated gene A (MrgA) act as iron chelators (Poole, 2005).

In general, Mn^{2+} is less likely to cause oxidative stress compared to Fe^{2+} due to higher reducing potential. However, lower intracellular Mn^{2+} affects SodA and SodM activities (Clements et al., 1999; Valderas and Hart, 2001). Therefore, both MntH and MntABC transporters are encoded in *S. aureus* genome to regulate Mn^{2+} homeostasis (Coady et al., 2015; Grunenwald et al., 2019).

When ion homeostasis is disrupted, Zn can compete with other transition metals in protein centers creating toxicities. Therefore, *zntRA* and *cadCA* exporter systems help to maintain Zn homeostasis (Singh et al., 1999).

Like Fe, Cu can cause harmful electron cycling between two oxidation status Cu^{2+} and Cu^{+}. To counteract the possible oxidative damage from high levels of free copper, *S. aureus* has P1-type ATPase CopA and copper chaperone CopZ under the regulation of CsoR (Singh et al., 1999).

1.3.2 Metabolic response

Bacterial metabolism is adapted according to the stress encountered. Metabolic adaptation resembles a core bacterial strategy to re-focus the cellular aim towards certain metabolites. Therefore, *S. aureus* responds to redox homeostasis imbalance by metabolic adaptation.

Glucose catabolism results in increased NADH/NAD^{+} ratio which enhances the cellular respiration and, hence, ROS production. However, glyoxylate shunt bypasses two NADH formation and overall decrease the oxidative status (Dolan and Welch, 2018). Different carbon sources (glucose, glycerol, citrate, malate, glutamate, and histidine) are metabolized into α-ketoacids (pyruvate and α-ketoglutarate). In oxidative stress, bacteria can increase the flux of non-enzymatic decarboxylation of the formed α-ketoacids in order to decrease the oxidative stress (Li et al., 2021). Furthermore, redirection of glucose utilization into the pentose phosphate pathway (PPP), instead of pyruvate formation *via* glycolysis,

increases NADPH/$NADP^+$ ratio in the cells (Christodoulou et al., 2018). NADPH acts as reducing equivalent for BSH, Brx, and Trx regeneration to combat oxidative stress (see section 1.3.5). In addition, NADPH is also important in mevalonate pathway to produce IPP. IPP condenses into FPP which then produce staphyloxanthin, an important ROS quenching metabolite (see section 1.3.4).

1.3.3 DNA protection and repair

Due to the broad effects of oxidative damage to the cells, *S. aureus* developed stress response to counteract the resulting damage according to the targeted biomolecule. Hence, we found DNA protection and repair stress response.

In *S. aureus*, the Dps orthologue (MrgA), which is a member of ferritin super family, is involved in nucleoid organization and compacting. Therefore, MrgA participates in oxidative stress resistance (Morikawa et al., 2006, 2019). However, genetic integrity is essential to maintain overall species identity. Hence, excision and recombinational repair mechanisms are encoded within *S. aureus* genome to combat possible DNA lesions including oxidative damage (Gaupp et al., 2012). Furthermore, SOS-response has been reported as a significant player in *S. aureus* survival against oxidative stress and antibiotic-generated ROS (Clarke et al., 2021).

1.3.4 Thiol-independent detoxification and repair

In *S. aureus*, several detoxification systems tackle the expected oxidants. Some of them quench the toxicity such as staphyloxanthin. Others directly catalyze the conversion of the toxic species into less toxic or harmless compounds such as superoxide dismutase, catalase, and flavohemoglobin. Repair mechanisms are important either to increase the expected survival after the damage or to decrease further toxicities such as Fe-S cluster repair.

S. aureus is known to produce a golden-colored pigment staphyloxanthin (STX). STX is one of the carotenoid pigments that is produced from farnesyl pyrophosphate (FPP) *via crtOPQMN* operon (Wieland et al., 1994). FPP is a condensation product of isopentenyl pyrophosphate (IPP) which is the main product of mevalonate pathway (MVA). Thus, STX is highly linked to the bacterial metabolism *via* MVA (Matsumoto et al., 2016). STX quenches ROS, RCS, and RNS due to the extended double-bond conjugation (Clauditz et al., 2006).

S. aureus acquired several detoxification enzymes to detoxify certain species. Superoxide dismutase (SOD) catalyzes the conversion of O_2^- to H_2O_2 and contains one of transition metals (Cu/Zn, Mn, Fe, or Ni) (Gaupp et al., 2012). *S. aureus* genomes encode

for two SODs (SodA and SodM) (Clements et al., 1999; Valderas and Hart, 2001). *sodA* transcription is induced by internal oxidants and *sodM* by exogenous oxidants.

However, the dismutation of superoxide into peroxide is still problematic due to increased intracellular H_2O_2. Therefore, *S. aureus* has *katA* which encodes the heme-tetrameric catalase enzyme which detoxifies H_2O_2 into the harmless H_2O (Sanz et al., 2000).

Flavohemoglobin (Hmp) family exhibits three activities; 1) alkyl-hydroperoxide reductase, 2) NO-reductase, and 3) NO-dioxygenase (Bonamore and Boffi, 2008). As expected from the naming, Hmp contains N-terminal globin domain, which is attached to heme, and C-terminal NAD- and FAD- binding domains. Therefore, Hmp is important in nitrosative stress to convert NO into nitrate *in-vivo* and *in-vitro* (Kinkel et al., 2013).

In oxidative stress, Fe-S clusters are destabilized and it is important to recover these clusters otherwise the freed Fe enhances the fatal Fenton reaction. Therefore, the *sufCDSUB* system maintain healthy Fe-S cluster assembly (Roberts et al., 2017). In addition, IscS was reported to maintain the Fe-S cluster in AirSR redox TCS (Sun et al., 2012). Furthermore, the di-iron ScdA is involved in Fe-S clusters repair especially in Aconitase and Fumarase enzymes (Overton et al., 2008).

1.3.5 Thiol-dependent detoxification and repair

The reducing nature of bacterial cytoplasm, in redox hemostasis, is mediated *via* redox buffering system containing LMW thiols and thiol-dependent enzymes. However, under oxidative conditions, proteins' sensitive thiol residues could be oxidized or over-oxidized (Ezraty et al., 2017). Therefore, it is vital to *S. aureus* to maintain its redox buffering as strong as possible. To do so, LMW thiols, such as CoASH and bacillithiol (BSH), are predominant intracellular metabolites (Dahl et al., 2015).

S. aureus synthesizes coenzyme A from pantothenate (vitamin B_5) and utilize it in many metabolic functions such as metabolites activation for TCA cycle (Leonardi et al., 2005). CoASH is the reduced form of coenzyme A and is in balance with its oxidized form $CoAS_2$ (Tsuchiya et al., 2018). CoASH disulfide reductase (Cdr) maintain this balance *via* reducing the disulfide form back to the free thiol (DelCardayré and Davies, 1998). After protein thiols oxidation, both CoASH and BSH interchangeably produce mixed disulfides with the oxidized sulfenic acid residue (Linzner et al., 2020). Protein CoAlation causes disruption of function such as GAPDH, AldA, Trx, and AhpC (Tsuchiya et al., 2018).

In most gram-negative bacteria, like *E. coli*, glutathione maintains the reducing nature of the bacterial cytoplasm. In *S. aureus* and Firmicutes, bacterial cells synthesize another

analogue (BSH) to maintain the function. *S. aureus* synthesizes BSH (L-cysteinyl-D-glucosamine-L-malic acid) using glycosyltransferase (BshA) as the first step in biosynthesis. Then, the deacetylase (BshB) and the Cysteine ligase (BshC) produce the final product (BSH) (Gaballa et al., 2010). Analogous to CoASH, BSH is the reduced form of bacillithiol and, upon oxidation, mixed disulfides (RSSB) and/or disulfide oxidized form (BSSB) are produced (Dickerhof et al., 2020). The balance of BSH/BSSB is restored back by the disulfide reductase YpdA (Linzner et al., 2019; Mikheyeva et al., 2019).

Gram-negative bacteria utilize thiol-dependent redox systems to maintain the reduced nature of the bacterial cytoplasm; namely thioredoxin (Trx) and glutaredoxin (Grx) systems (Prinz et al., 1997). In *S. aureus* and related Firmicutes, bacilliredoxin (Brx) is the analogue system to Grx. Trx and Brx systems are important hydrogen donors supports regeneration of oxidized methionine (*via* methionine sulfoxide reductases), bacillithiolated and coAlated proteins (*via* mixed disulfide reductases) (Linzner et al., 2019). Moreover, Trx and Brx are ROS scavengers as oxidizable metabolites that could be further regenerated rather than critical nucleic acids and proteins.

In *S. aureus*, Trx (*trxA*-encoded and other Trx-like protein) and the two paralogous Brxs (BrxA and BrxB) function as electron providers to ribonucleotide reductases and peroxidases (Chandrangsu et al., 2018). Trx is re-reduced *via* thioredoxin reductase (TrxB) which is regenerated by $FADH_2$ 2-electron reduction (Peng et al., 2018). Eventually, NADPH is used to recycle the utilized $FADH_2$. The maintenance of Brx in reduced/oxidized ratio is possible *via* BSH which is further regenerated through NADPH-dependent flavoenzyme YpdA (Linzner et al., 2019). Therefore, the two efficient redox pathways are Trx/TrxB/$FADH_2$/NADPH and Brx/BSH/YpdA/NADPH.

In addition to *katA*, peroxiredoxins convert peroxides into their corresponding alcohols using reducing equivalents NAD(P)H. This mechanism is dependent on the cysteine residue of AhpC. The disulfide reductase (AhpF) works to regenerate the oxidized AhpC cysteine active site (Poole, 2005). Although the supraphysiological levels of peroxides are detoxified using KatA, physiological levels of peroxides are kept under control using the peroxiredoxin AhpC/AhpF system (Cosgrove et al., 2007). Interestingly, the iron-chelator (Bcp) has an additional thiol-dependent peroxidase activity as a peroxiredoxin from AhpC family (Jeong et al., 2000).

Methionine is the first encoded amino acid in the protein biosynthesis and susceptible to oxidation which could disrupt the structure and the function of many proteins.

Methionine sulfoxide in *R*- and *S*- diastereomeric forms are the expected oxidation products. Therefore, *S. aureus* encodes for methionine sulfoxide reductases (Gaupp et al., 2012). Since the configuration of the oxidation products are different, *S. aureus* uses MsrA to reduce the *S*-form and MsrB for the *R*-form (Moskovitz et al., 2002). To function, both MsrA paralogues and MsrB utilizes thiol-dependent redox systems such as thioredoxin as discussed earlier (Singh et al., 2015).

1.4 Old yellow enzymes as biocatalysts with unknown physiological role

Old yellow enzymes (OYEs a.k.a. ene-reductases) belong to flavoproteins (proteins bound to the nucleic acid derivative riboflavin). Flavoproteins contain flavin adenine dinucleotide (FAD) or flavin mononucleotide (FMN) as a prosthetic group or a cofactor. Of all studied flavoproteins, more than 90% function as oxidoreductases (Macheroux et al., 2011).

The first identified old yellow enzyme (OYE1) was isolated from *Saccharomyces pastorianus* in 1932. OYE enzymatic activity was established by Warburg in 1930s (Warburg and Christian, 1938). Later, the yellow color of the enzyme was attributed to the flavin mononucleotide (FMN) prosthetic group which was proven to be a functional determinant of the activity.

Mechanistically, FMN group act as a cofactor through which the reducing electrons land to substrates from NAD(P)H *via* redox-cycling of FMN. Overall, OYEs use NAD(P)H as reducing equivalents to reduce activated C=C bonds in α,β-unsaturated carbonyl compounds including quinones and N-ethylmaleimide (NEM). Therefore, OYEs were assigned to the E.C. number 1.6.99.1 (Matthews and Massey, 1969). In addition, OYEs have type-I nitroreductase activity which was proven important in xenobiotics degradation and/or inactivation such as 2,4,6-trinitrotoluene (TNT) (Williams et al., 2004) and the novel antibacterial compound MT02 (El-Hossary et al., 2018).

OYEs adopt a conserved ubiquitous TIM-barrel $(\alpha\beta)_8$ structure. Eight α-helices and central β-strands with β-hairpin lid (at N-terminal) and FMN-binding (at C-terminal of the β-strands) are characteristics for OYEs (Scholtissek et al., 2017). The conserved structure allows for broad substrate specificity which is different from other OYEs and then the physiological relevance to the encoding organism (Shi et al., 2020). Therefore, it is common to find different paralogues encoded in the same organism with different transcriptional controls (Nizam et al., 2015). Hence, we cannot consider them as isoenzymes.

Since OYEs convert the planar C=C bond into saturated bond with chiral centers, there are two possibilities of the resulting compound (*R*/*S*-enantiomers). OYEs have

stereoselectivity to certain product enrichment such as OYE1 and OYE3 from *Saccharomyces cerevisiae* (Powell, III et al., 2018). Hence, OYEs become an important focus for protein engineering as biocatalysts for reduction reactions (Amato and Stewart, 2015). This research niche enhances OYEs in using NADH or even cheaper reducing equivalents as co-substrates. Moreover, creating or enhancing stereoselectivities towards more valuable isomers of the product is also an important sub-field. Furthermore, researchers optimize the reaction conditions, use novel OYEs, or modify the enzyme for broader substrate specificities or enhanced reaction kinetics. All of these improvements made OYEs an integral node in biocatalysis and biotechnology, alone or in combination with complementary enzymes (Shi et al., 2020).

Although OYEs are found across bacteria, fungi, and plant kingdoms, they are rarely found in higher animals. Phylogenetically, eukaryotic and prokaryotic OYEs are classified into three classes: Class-I (from plants and bacteria), Class-II (from fungi), and Class-III (thermophilic-like and mesophilic from bacteria) (Scholtissek et al., 2017).

In gram-positive bacterium, YqiG and YqjM are two OYEs isolated from *Bacillus subtilis* (Kitzing et al., 2005; Sheng et al., 2016). YqjM was first isolated from *B. subtilis* based on sequence homology with the yeast OYE (Fitzpatrick et al., 2003). *In-vitro* analysis showed that YqjM preferentially utilizes NADPH for reducing α,β-double bonds in nitroester and nitroaromatic aldehydes and ketones. Additionally, *yqjM* is induced after exposure to H_2O_2 and 2,4,6-trinitrotoluene (TNT) (Fitzpatrick et al., 2003). YqiG was shown to has low tolerance towards organic solvents but high tolerance against pH and elevated temperature (Sheng et al., 2016). Despite OYEs are industrially useful biocatalysts, the physiological role of bacterial OYEs is still uncovered (Toogood et al., 2010).

1.5 Aims and objectives

Although OYEs are widespread in many (micro)organisms including a wide variety of prokaryotes and eukaryotes, OYE function is still enigmatic without prior information about a proposed mode of action. Moreover, the transcriptional regulation has never been associated to an OYE orthologue in the gram-positive bacteria. Here, I aim at functional analysis of the staphylococcal conserved SAUSA300_0859 (old yellow enzyme flavin oxidoreductase A, *ofrA*) and the relevance in infection situation of the important human pathogen *S. aureus*. Furthermore, I intend to unravel a mechanism by which *ofrA* causes the associated phenotypes. I also aim at decoding the regulation network that transcriptionally controls *ofrA* in *S. aureus*.

2 Materials

2.1 Chemicals

Table 3: Chemicals and reagents used in this study.

No	Chemicals and reagents	Supplier
1	4-Methylumbelliferyl-β-D-galactopyranoside (MUG)	Carl Roth
2	Agar	Becton, Dickson and Company
3	Agarose	Biozym
4	Ambion water	Invitrogen
5	ATP	New England BioLabs
6	Brain Heart Infusion (BHI)	Sigma-Aldrich
7	$CaCl_2$	Carl Roth
8	Cumene hydroperoxide	Sigma-Aldrich
9	Diamide	MP Biomedicals
10	Dimethyl Sulfoxide (DMSO)	Sigma Aldrich
11	dNTPs	New England BioLabs
12	Ethanol	Carl Roth
13	Fetal Bovine Serum (FBS)	Biochrom GmbH
14	Formaldehyde	Sigma Aldrich
15	Gel Loading Dye Purple (6x)	New England Biolabs
16	Glycerol	Carl Roth
17	Hydrogen peroxide	Sigma Aldrich
18	Isopropanol	Carl Roth
19	K_2HPO_4	Carl Roth
20	Lysostaphin	Bharat Biotech International
21	Methanol	Carl Roth
22	Methylglyoxal	Sigma Aldrich
23	Methylhydroquinone	Sigma Aldrich
24	Midori Green	Nippon Genetics
25	N-acetylcysteine	Hölzel Diagnostika
26	NaCl	Carl Roth
27	Pepton/Trypton	Carl Roth
28	RiboLock	Thermo Fisher Scientific
29	Sodium Hypochlorite (NaOCl)	Alfa Aesar
30	Thiourea	Carl Roth
31	TSB	Sigma-Aldrich
32	Yeast extract	Carl Roth

2.2 Consumables

Table 4: Plastic consumables used in this study.

No	Item	Supplier
1	24-well cell culture plates	VWR International
2	96-well microtiter plates (U- and flat bottom)	Greiner Bio-One International
3	Absorbance cuvettes	Ratiolab GmbH
4	Cell scrapers (16, 25, 39 cm)	Sarstedt AG & Co. KG
5	Cryo-tubes	Thermo Fisher Scientific
6	DNA-free and RNA-free microfuge tubes	Brand GmbH & Co. KG
7	Eppendorf tubes (2, 1.7 ml)	Sarstedt AG & Co.KG
8	Falcon tubes (50, 15 ml)	Sarstedt AG & Co.KG
9	Parafilm	A.Hartenstein GmbH
10	Petri dishes (20 ml)	Nerbe plus GmbH & Co.KG
11	Pipette tips (1000, 200, 10 µl)	Sarstedt AG & Co.KG
12	Single use pipettes (25, 10, 5 ml)	Sarstedt AG & Co. KG
13	Sterile filter (0.22, 0.45 µm)	PALL Life Sciences
14	Syringes (20, 5 ml)	Becton, Dickson and Company

Table 5: Glass consumables used in this study.

No	Item	Supplier
1	Beakers	A.Hartenstein GmbH
2	Electroporation cuvettes	Biorad
3	Flasks	A.Hartenstein GmbH
4	Measuring cylinders	Witeg Labortechnik
5	Pipettes	Sarstedt AG & Co.KG

2.3 Antibiotics

Table 6: Antibiotics used in this study.

No	Antibiotics	Supplier
1	Ampicillin	Carl Roth
2	Chloramphenicol	AppliChem GmbH
3	Fosfomycin	TCI Deustchland
4	Gentamicin	AppliChem GmbH
5	Kanamycin	Carl Roth
6	Streptonigrin	Biomol

2.4 Kits and enzymes

Table 7: Kits used in this study.

No	Kits	Supplier
1	Biozym Blue S'Green qPCR kit	Biozym
2	DNeasy Blood&Tissue kit	Qiagen
3	NucleoSpin ® Gel and PCR Clean-up kit	Macherey-Nagel
4	NucleoSpin® Plasmid kit	Macherey-Nagel
5	RapidOut DNA removal kit	Thermo Fisher Scientific
6	RNeasy Mini kit	Qiagen
7	SuperScript IV Reverse Transcriptase	Thermo Fisher Scientific

Table 8: Enzymes used in this study.

No	Enzymes	Supplier
1	Antarctic Phosphatase	New England BioLabs
2	Catalse	MP Biomedicals
3	GoTaq Polymerase	Promega
4	Q5 High Fidelity Polymerase	New England BioLabs
5	Restriction Enzymes	New England BioLabs
6	RPPH	New England BioLabs
7	T4 DNA ligase	New England BioLabs
8	T4 Polynucleotide Kinase	New England BioLabs
9	T4 RNA ligase I	New England BioLabs

2.5 Bacterial growth Media

Table 9: Media composition used in this study.

No	Medium	Composition (per liter)
1	B-medium	10 g peptone/tryptone 5 g yeast extract 5 g NaCl 1 g K_2HPO_4
2	BHI	37 g Brain-Heart-Infusion
3	LB	10 g pepton/trypton 5 g yeast extract 5 g NaCl
4	RPMI 1640 + GlutaMAX	Catalog number 72400021
5	TSB	30 g TSB powder mixture
6	Solid form of any medium	Composition 15 g Agar-Agar
7	$CaCl_2$-TSB	30 g TSB powder mixture 5 ml (100 mM) $CaCl_2$ 15 g Agar-Agar
8	Phage Top Agar	3 g peptone/tryptone 3 g yeast extract 4.44 g NaCl 7.52 g Agar-Agar

9	TSA Top Agar	15 g TSB powder mixture 2.5 g Agar-Agar

2.6 Buffers and solutions

Table 10: Buffer and solutions used in this study.

No	Item	Composition
1	EC (electrical conductivity) buffer	0.5 M Sucrose in 10% Glycerol
2	MUG solution	1 mg/ml in DMSO
3	PBS (Phosphate buffered saline, 10x)	17.8 g $Na_2HPO_4.2H_2O$ 2.4 g KH_2PO_4 80 g NaCl 2 g KCl To 1000 ml distilled water, pH 6.8
4	Stop reaction solution	52.99 g Na_2CO_3 to 500 ml water
5	TAE buffer (50x)	242 g Tris 57.1 ml Acetate 100 ml 0.5 M EDTA (pH 8) To 1000 ml distilled water
6	Z-buffer	16 g $Na_2HPO_4.12H_2O$ 6.25 g $NaH_2PO_4.H_2O$ 0.75 g KCl 0.25 g $MgSO_4.7H_2O$ To 1000 ml distilled water
7	Lysis buffer for genomic DNA isolation	20 mM Tris.HCl (pH 8) 20 mM Na.EDTA 1.2% TritonX-100

2.7 Bacterial strains

Table 11: Bacterial strains used in this study.

Strain	Genotype / Description	Reference
E. coli DH5α	F-, *end*A1, *hsd*R17 (rk-, mk-), *sup*E44, *thi*-1, *rec*A1, *gyrA*96, *rel*A1, λ-, Δ(*argF-lac*)U169, Φ80*dlacZ* ΔM15	MBI Fermentas
E. coli IM08B	*mcrA* Δ(*mrr-hsdRMS-mcrBC*) ϕ80*lacZ*ΔM15 Δ*lacX*74 *recA1* araD139 Δ(ara-leu)7697 *galU galK rpsL endA1 nupG* Δdcm ΩPhelp-*hsdMS* (CC8-2) ΩPN25-*hsdS* (CC8-1)	(Monk et al., 2015)
S. aureus JE2	*S. aureus* LAC (USA300_FPR3757) cured from pUSA01, pUSA02, and pUSA03, ErmS	(Fey et al., 2013)
S. aureus NewmanΔ*crtM*	*S. aureus* NewmanΔ*crtM::cat*	(Clauditz et al., 2006)
Created *E. coli* strains		
DH5α pES3	Reporter system based on pKO10 by replacing P_{hla} with EcoRI, HindIII sites	
DH5α pES2::SAUSA300_0857-0860	Cloning and mutagenesis aid vector	This study
DH5α pES3::P_{ofrA}-*lacZ*	Construction of reporter plasmid	This study
DH5α pBASE6Δ*ofrA*	Construction of deletion plasmid	This study

DH5α pRB473::*ofrA*	Construction of complementation plasmid	This study
IM08B pES3::P_{ofrA}-*lacZ*	Reporter plasmid	
IM08B pBASE6Δ*ofrA*	Deletion plasmid	This study
IM08B pRB473::*ofrA*	Complementation plasmid	This study
Created *S. aureus* strains		
JE2 pES3::P_{ofrA}::*lacZ*	Temperature sensitive reporter plasmid in *S. aureus* JE2 strain	This study
EI011	*S. aureus* JE2::P_{ofrA}::*lacZ*	This study
JE2 pBASE6Δ*ofrA*	*S. aureus* JE2 + the deletion plasmid	This study
EI046	*S. aureus* JE2Δ*ofrA*, marker-less deletion	This study
EI047	*S. aureus* JE2Δ*ofrA* pRB473::*ofrA*, complemented strain	This study
JE2Δ*crtM::cat*	Deletion mutant of JE2 strain in *crtM*	This study
JE2Δ*ofrA*Δ*crtM::cat*	Deletion mutant of EI046 strain in *crtM*	This study
EI011Δ*sigB::ermB*	Deletion mutant of EI011 strain in *sigB*	Laura Cecchino
EI013	*S. aureus* NewHG::P_{ofrA}::*lacZ*	Laura Cecchino
EI013Δ*arlR::ermB*	Deletion mutant of EI013 strain in *arlR*	This study
EI013Δ*ccpA::tetL*	Deletion mutant of EI013 strain in *ccpA*	This study

2.8 Oligonucleotides

Table 12: Oligonucleotides used in this study.

Primers' overhangs are underlined. Ribonucleic acids are in bold.

Oligonucleotide	Sequence	Purpose
Δ*ofrA*_seq	ATTGGAGAATGAAAAAATTACATG	Sequencing
pKO10_seqR	CGATTAAGTTGGGTAACGC	
pBASE forward	AAATTACGCCCCGCCCTG	
pBASE reverse	CATCAACAATCCGTTCTGC	
*ofrA*_report_up	GCAATCTCAATATATTTATCAAGAAAGC	
pRB473::P_{xyl}	TAGATATCTCGGACCGTC	
pES_seq	TCCTTCATTACAGAAACGGC	
ofrA.del.1	GATAAATCAATTCTTTTGCTTGTAATCATTTAAGTAATTATGTCATTATAAATGTAAGGG	PCR-mediated plasmid deletion
ofrA.del.2	TAAATGATTACAAGCAAAAGAATTGATTTATCTGTTCCTTTAGTCGTTTCGAATTGCTCG	
P_{ofrA}_pKO10.1	GGCCCTTTCGTCTTCAATTAAAGATAATAGTTGAGGTTGC	Cloning
P_{ofrA}_pKO10.2	CAACAAGCTGGGGATCTTTACTTAATTCCTCCTTAAAATTATTGAG	
0857_0860_pES2.BamHI.1	CCGGGATCCGGACATCGTCTCCATTTTCTTCAACAATCGTGACACC	
0857_0860_pES2.XhoI.2	CCGCTCGAGGTGCCATCATCCATTCGTACAGGGATACGCAC	
*ofrA*_up_pBASE6.SacI.1	CCGGAGCTCGTGGCTGGCCTCAACC	
*ofrA*_down_pBASE6.NheI.2	CCGGCTAGCCTAATACAACAGAAATTGGGAAGACTC	

*ofrA*_pRB473.EcoRI.1	CCGGAATTCAACAGAAAAATATGGGTTTC AAAC	
*ofrA*_pRB473.BamHI.2	CCGGGATCCAGAATTGATAATTTTACACT TAATCAAAAG	
tag.*ofrA*.cDNA	ACTTAGCGCGGGAACACGCATGATGTATT TGTACGAGTGC	cDNA synthesis
tag.qPCR	ACTTAGCGCGGGAACACG	RT-qPCR
ofrA.qPCR	GCCATCAATCGCGCATGACA	
rpoB.qPCR.1	CTAAGCACAGAGGTCGT	
rpoB.qPCR.2	ACGGCATCCTCATAGT	
rho.qPCR.1	GAAGCTGCTGAAGTCG	
rho.qPCR.2	CGTCCATACGTGAACCC	
acuA.qPCR.1	TGGGGGCAATTGAAGTCAGC	
acuA.qPCR.2	CACCAGTTGCCATTAACCGCT	
crtM.qPCR.1	GCAACATGCTGAAGCGCCA	
crtM.qPCR.2	TCAAAGAAAAGCGGTTTGGGCA	
rocD.qPCR.1	AGCAGGATTAGGTCGTTCGGG	
rocD.qPCR.2	TGAACCATGTGAGCCAGGTGT	
crtQ.1	GCACGTTCATATGGTGCGAC	Transduction confirmation
crtN.2	GATTCATACGCCCGCCTACA	
cat.3	ACCAGCAAACTACGTATAGCA	
cat.4	GCATGATGAAGCTGTAAGGCA	
ErmB10	CACCTGCAATAACCGTTACC	
arlR.up	TAGTGAAAAGTCAGTATATGACAAC	
ccpA.up	TTTACATATAGCGAGTTGGTAC	
tetL.1	TTGTGTCGTAAATTCGATTGTG	
RNA_adaptor	**CUAGUACUCCGGUAUUGCGGUACCCUUGU ACGCCUGUUUUAUA**	5'RACE

2.9 Plasmids

Table 13: plasmids used in this study.

Plasmid	Characteristics	Reference
pET28a(+)	His_6 overexpression vector - Kan^R	Novagen
pKO10	Shuttle vector – Amp^R (*E. coli*), Cm^R (*S. aureus*) – Ori^{TS} (*S. aureus*) – *lacZ* reporter	(Ohlsen et al., 1997)
pBASE6	Shuttle vector – Amp^R (*E. coli*), Cm^R (*S. aureus*) – Ori^{TS} (*S. aureus*) – anti-*secY* counter-selection	(Geiger et al., 2012)
pRB473	Shuttle vector – Amp^R (*E. coli*), Cm^R (*S. aureus*)	PD.Dr. Wilma Ziebuhr
pES2	pET28a(+) with deleted transcriptional terminator, induction system (*lacI*, P_{lac}), and f1 replication origin - Kan^R	This study
pES3	Shuttle vector – Amp^R (*E. coli*), Cm^R (*S. aureus*) – Ori^{TS} (*S. aureus*) – *lacZ* reporter	This study
pRB473::P_{xyl}::*ofrA*	Xylose inducible expression of *ofrA*	This study
pRB473::P_{ofrA}::*ofrA*	Natural promoter induced expression of *ofrA*	This study

pES3::P_{ofrA}::*lacZ*	Shuttle vector – Amp^R (*E. coli*), Cm^R (*S. aureus*) – Ori^{TS} (*S. aureus*) – *lacZ* reporter	This study
pES2:: SAUSA300_0857-0860Δ*ofrA*	Deletion plasmid construction	This study
pBASE6Δ*ofrA*	Deletion plasmid	This study

2.10 Instrument

Table 14: Instrument and machines used in this study.

No	Item	Company
1	FastPrep®-beadbeater	MB Biomedicals, Eschwege, Germany
2	NanoDrop®-Spectrophotometer	Thermo Fisher, Darmstadt, Germany
3	Synergy H1	Agilent,Frankfurt, Germany
4	TECAN Infinite F200 Pro	Tecan Group Ltd., Männedorf, Switzerland
5	Thermocycler	PEQLAB Biotechnologie GmbH, Erlangen, Germany

2.11 Databases, software, visualization and genetic analysis, packages, and servers

Table 15: Databases used in this study.

No	Database	Link
1	AlphaFold	https://alphafold.ebi.ac.uk/
2	Aureolib	http://www.aureolib.de/
3	AureoWiki	https://aureowiki.med.uni-greifswald.de/Main_Page
4	Genome Browse	https://www.ncbi.nlm.nih.gov/genome/browse/
5	KEGG	https://www.kegg.jp/
6	Microbes Online	http://www.microbesonline.org/
7	PubMed	https://pubmed.ncbi.nlm.nih.gov/
8	*S. aureus* Expression Data Browser	http://genome.jouy.inra.fr/cgi-bin/aeb/index.py
9	SAMMD	https://satmd.org/
10	Uniprot	https://www.uniprot.org/uniprot/
11	Web of Science	https://www.webofscience.com/wos/woscc/basic-search

Table 16: Analysis software used in this study.

No	Software	Link / Reference
1	BLAST ncbi-blast-2.11.0+	https://ftp.ncbi.nlm.nih.gov/blast/executables/blast+/2.11.0/
2	Clustal Omega	https://www.ebi.ac.uk/Tools/msa/clustalo/
3	Cutadapt	https://cutadapt.readthedocs.io/en/stable/
4	FastQC	https://www.bioinformatics.babraham.ac.uk/projects/fastqc/
5	OligoAnalyzer	https://eu.idtdna.com/pages/tools/oligoanalyzer
6	Python 3.7.1	https://www.python.org/downloads/release/python-371/
7	R 3.6.1	https://cran.r-project.org/bin/windows/base/old/3.6.1/
8	RAxML 8.0.0	https://cme.h-its.org/exelixis/web/software/raxml/
9	READemption	https://reademption.readthedocs.io/en/latest/
10	SDDC v3.2	https://github.com/Eslam-Samir-Ragab/Sequence-database-curator/releases/tag/v3.2

Table 17: Maintenance and version control software used in this study.

No	Software	Link / version
1	Git	git version 2.26.2.windows.1
2	Github	https://github.com/Eslam-Samir-Ragab
3	Mendeley	https://www.mendeley.com/
4	Microsoft Office 2016	https://www.office.com/
5	PyScripter 4.1.1	https://sourceforge.net/projects/pyscripter/
6	Rstudio 1.1.463	https://www.rstudio.com/
7	tmux	https://github.com/tmux/tmux/wiki

Table 18: Visualization and genetic analysis software used in this study.

No	Software	Link
1	Benchling	https://www.benchling.com/
2	Biorender App	https://biorender.com/
3	Genome compiler	https://designer.genomecompiler.com/
4	Integrated Genome Browser	https://www.bioviz.org/
5	Snapgene	https://www.snapgene.com/

Table 19: R-packages used in this study.

No	R package	Link
1	clusterProfiler	https://bioconductor.org/packages/release/bioc/html/clusterProfiler.html
2	gggenes	https://cran.r-project.org/web/packages/gggenes/index.html
3	ggplot2	https://cran.r-project.org/web/packages/ggplot2/index.html
4	ggpubr	https://cran.r-project.org/web/packages/ggpubr/index.html
5	ggtree	https://bioconductor.org/packages/release/bioc/html/ggtree.html
6	rstatix	https://cran.r-project.org/web/packages/rstatix/index.html

Table 20: Servers used in this study.

No	Server	System information
1	Cuba	Ubuntu 18.04.6 LTS
2	Julia	Ubuntu 18.04.6 LTS
3	Local machine	Ubuntu 16.04.7 LTS

3 Methods

3.1 Bacterial growth and stocks

If otherwise not specified, LB broth or agar was used to grow *E. coli* strains at 37°C. When necessary, antibiotic (100 µg/ml ampicillin or 50 µg/ml kanamycin) supplemented LB was used to maintain plasmids. *S. aureus* strains were grown in B-medium with antibiotic (10 µg/ml chloramphenicol) in case of plasmid bearing strains at 37°C. If the plasmids have a temperature sensitive origin of replication, the permissive temperature (30°C) was used for plasmid propagation and the non-permissive temperature (43°C) was used for chromosomal integration.

For short-term storage (less than one week), agar plates were kept in 4°C. For long-term storage, overnight cultures were stored in -80°C freezers using 25% glycerol as a cryoprotectant.

3.2 RAW 264.7 cell line maintenance

RAW 264.7 cell line were grown in cell culture flasks using RPMI 1640 GlutaMAX – HEPES medium supplemented with 100 units/ml penicillin and 50 µg/ml streptomycin and 10% fetal bovine serum (FBS). Cells were grown in 37°C and with 5-10% CO_2. In each passage, the cells were split into fresh pre-warmed medium (1:10 dilution) every 3 days when confluent. Frequently, the cell-line cultures were inspected to ensure the absence of contamination. Passages 12 to 15 were used for the macrophage survival assay.

3.3 DNA isolation and manipulation

3.3.1 Genomic DNA isolation

S. aureus strains were grown in B-medium from a well-isolated colony. 2-ml overnight culture were collected with centrifugation (16000 x g for 2 minutes) then resuspended in 360 µl lysis buffer. Lysostaphin was added to a final concentration 200 µg/ml. After incubation at 37°C for 30 minutes, 50 µl was added from proteinase K (10 mg/ml) and 400 µl AL-buffer (Qiagen DNeasy blood and tissue kit). After incubation at 56°C for 30 minutes, 400 µl of 96% ethanol was added and mixed. The released genomic DNA was retained on the DNA-binding column from the mentioned kit and washed with 500 µl AW1 buffer then 500 µl AW2 buffer. After drying the column from excess ethanol, the genomic DNA was eluted using pre-warmed DNase-free water.

3.3.2 Plasmid isolation

E. coli strains were grown in LB-medium supplemented with the selective antibiotic from a well-isolated colony. 3-ml overnight culture were collected with centrifugation (16000 x g for 2 minutes) then resuspended in 250 µl A1 buffer (Macherey-Nagel Nucleospin plasmid isolation kit). 250 µl A2 buffer was added, gently mixed, and incubated with the bacterial suspension at room temperature for 5 minutes. The alkaline pH was then neutralized with 300 µl A3 buffer. The plasmid DNA was retained on the DNA-binding column from the mentioned kit and washed with 500 µl A4 buffer. After drying the column from excess ethanol, the plasmid DNA was eluted using pre-warmed DNase-free water.

3.3.3 Bacterial lysis for colony PCR

This method was used to screen for a desired genotype. For *E. coli* strains, one colony is resuspended in 40 µl DNase-free water and boiled for 5 minutes at 95^{o}C. For *S. aureus* strains, one colony is resuspended in 30 µl DNase-free water and boiled for 5 minutes at 95^{o}C. After cooling the bacterial lysates on ice for 2 minutes, the cell debris were collected with centrifugation (16000 x g for 2 minutes). 1 µl of the supernatant was used as a template DNA for further analysis using polymerase chain reaction (PCR).

3.3.4 Measuring DNA concentration

1 µl of the isolated and purified nucleic acids were used to determine the concentration using A_{260}. The success of purification was determined *via* the A_{260}/A_{280} and A_{260}/A_{230} ratio measured by Nanodrop spectrophotometer.

3.3.5 Polymerase Chain Reaction (PCR)

In general, PCR was performed using the following: DNase-free water, polymerase buffer, DNA template, dNTPs, a forward and a reverse primer, and a DNA-polymerase. For screening a certain genotype, GoTaq DNA polymerase in green reaction buffer was used. For sequencing, cloning, and long-range amplification, Q5 DNA polymerase was used. The overall primers incompatibilities (inter- and intra-molecular interaction) were checked using oligoanalyzer program from IDT.

In case of long-range amplification from *S. aureus* templates, dNTPs mixture was customized (dATP:dTTP:dCTP:dGTP = 3:3:1:1 molar ratio) to facilitate the Q5 polymerase activity from the low-GC template.

The general thermal protocol was as follows:

Initial denaturation	98°C	3 minutes
35-40 Cycles:		
Denaturation	98°C	30 seconds
Primers' annealing	55°C	30 seconds
Extension	72°C	0.5-4.5 minutes
Final extension	72°C	20 minutes
Storage	16°C	

PCR-mediated plasmid deletion was used to generate pES2 cloning aid vector from pET28a(+). The designed primers have 20 bp 5' overhangs to pair with the overlapping fragment in the linked primer. PCR-mediated plasmid deletion is a form of long-range PCR with annealing sequences in outward direction. For this application, the PCR thermal protocol was modified for both annealing and extension temperature = 68°C.

3.3.6 Oligonucleotides phosphorylation and hybridization

This protocol was used to generate a short insert (less than 60 bp) replacing an unused cloned fragment with a multiple cloning site (pES3). The oligonucleotides were designed to be hybridized by simple thermal treatment with overhangs identical to restricted sites to the matched sequence on the backbone (Penewit et al., 2018). The oligonucleotides were first phosphorylated by T4 polynucleotide kinase (from New England Biolabs) using the T4 DNA ligation buffer as a donor of phosphorylation mixture. The following recipe was incubated for 40 minutes at 37°C:

Oligo 1 (100 µM)	0.5 µl
Oligo 2 (100 µM)	0.5 µl
T4 ligation buffer	2.5 µl
T4 PNK	0.5 µl
ddH_2O	21 µl

The phosphorylation reaction was then stopped and a complete denaturation of the 5'-phosphorylated oligonucleotides was established by incubation at 95°C for 5 minutes. The mixture was then cooled down gradually to 20°C over 45 minutes. The template was used in a ligation reaction to generate the intended vector.

3.3.7 DNA clean-up and purification

The excess oligonucleotides, enzyme, and salts from PCR products as well as DNA fragments of interest trapped in agarose gel were cleaned and purified with NucleoSpin® Gel and PCR Clean-up Kit (from Marcherey-Nagel). The manufacturer's instructions were applied in both PCR and gel clean-up. The purified DNA was eluted in 20 µl of DNase-free water.

3.4 Molecular Cloning

3.4.1 DNA restriction and dephosphorylation

Enzymatic hydrolysis was used to restrict 2-5 µg purified PCR products and plasmids. In 20 µl reaction, the double digestion was performed using the manufacturer's manual instructions except using 1 µl of each restriction enzyme instead of 0.4 µl. After one hour of incubation at 37°C, the restriction products were purified with NucleoSpin® Gel and PCR Clean-up Kit directly or after gel electrophoresis and gel-purification of the DNA fragment of interest.

In case of plasmid restriction, after the restriction reaction, the Antarctic phosphatase in phosphatase buffer was used to dephosphorylate the restriction products to prevent plasmid self-ligation.

3.4.2 DNA ligation

The restricted insert and vector were mixed in 3:1 or 5:1 ratio (insert:vector) based on 50 ng of the vector. The ligation reaction was done in 20 µl using the manufacturer's manual instructions except using 1 µl of each restriction enzyme instead of 0.4 µl. The ligation mixture was incubated for 16 hours at 16°C. The T4 DNA ligase was then inactivated by heating for 10 minutes at 65°C. 5 µl of the ligation products was transformed into home-made competent *E. coli* DH5α *via* heat-shock transformation to screen for successful cloning.

3.4.3 *In-vivo* assembly (IVA)

This protocol was used to generate plasmids without the need of *in-vitro* ligation to decrease the timing, the costs, and the effort to include suitable cloning sites not present in the original backbone (García-Nafría et al., 2016). First, the vector backbone was linearized by double digestion. Second, the insert was amplified using primers containing 15-20 bp 5'-overhangs which overlapped the linearized vector. The purified insert and linearized vector were mixed as 3:1 ratio based on 50 ng of the vector, respectively. The mixture was then transformed into home-made competent *E. coli* DH5α *via* heat-shock transformation to screen for successful cloning.

3.5 Horizontal DNA transfer

3.5.1 Transformation

3.5.1.1 Preparation of chemically competent cells from *E. coli*

An overnight culture of *E. coli* strain was 1:100 diluted in 100 ml LB. The fresh culture was incubated at 37°C with shaking. At the OD_{600}= 0.4-0.5, the culture was chilled on ice

for 20 minutes. The bacterial cells were collected with centrifugation for 10 minutes at 4000 rpm at 4°C. The collected pellets were resuspended in 25 ml ice-cold $CaCl_2$ solution and re-collected with centrifugation (same conditions). A second resuspension in 5 ml ice-cold $CaCl_2$ solution was performed before the cells were re-collected with centrifugation (same conditions). Finally, the competent cells were resuspended in 2.5 ml ice-cold $CaCl_2$ solution and incubated on ice for 30 minutes. 520 µl of 86% glycerol was added as a cryoprotectant. The competent cells were then stored in -80°C in 100 µl aliquots.

3.5.1.2 Transformation *via* heat-shock method

After thawing the chemically competent *E. coli* cells on ice, 45 µl of the cells were added to 1-7 µl of the transforming DNA and mixed gently. The transformation mixture was incubated on ice for 45 minutes. A heat-shock was performed by heating the transformation mixture for 2 minutes at 45°C then incubating on ice for 5 minutes. 950 µl of LB was added to the transformation mixture. The transformants were allowed to grow for one hour in 37°C with shaking then plated on selective LB-plates based on the resistance marker of the plasmid.

3.5.2 Electroporation

3.5.2.1 Preparation of electro-competent cells from *S. aureus*

An overnight culture of *S. aureus* strain was 1:100 diluted in 100 ml TSB. The fresh culture was incubated at 37°C with shaking. At the OD_{600}= 0.8-1, the bacterial cells were collected with centrifugation for 10 minutes at 4000 rpm at room temperature. The collected pellets were resuspended in 50 ml ddH_2O and re-collected with centrifugation (same conditions). A second resuspension of two bacterial pellets in 50 ml ddH_2O was performed before the cells were re-collected with centrifugation (same conditions). The third wash was performed with 16 ml ddH_2O. The fourth wash was performed with 10 ml 10% glycerol. Finally, the competent cells were resuspended in 5 ml 10% glycerol and incubated at room temperature for 15 minutes. To concentrate the cells, the competent cells were collected with centrifugation (same conditions) then resuspended in 1.5 ml 10% glycerol. The competent cells were then stored in -80°C in 100 µl aliquots.

3.5.2.2 Electroporation

After thawing the electro-competent *S. aureus* cells at room temperature for 5 minutes, 50 µl of the cells were incubated at room temperature for 20 minutes. The competent cells were resuspended with 500 µl of EC buffer (0.5 M sucrose in 10% glycerol) and collected

with centrifugation (5000 rpm for 5 minutes at room temperature). The competent cells were resuspended gently with 1.5 µg DNA and 85 µl EC buffer and incubated at room temperature for 30 minutes. Electroporation was performed using 2 mm gap electroporation cuvette (2.9 kV, 100 Ω, and 25 µF) or 1 mm gap electroporation cuvette (2.3 kV, 100 Ω, and 25 µF).

After electroporation, 900 µl of pre-warmed TSB was added to the cuvette and mixed with the electroporation mixture to extract the electroporants. The electroporants were allowed to grow for 1.5 hours in 37°C with shaking then plated on selective TSA-plates based on the resistance marker of the plasmid. When the plasmids have temperature-sensitive origin of replication, the plates were incubated in 30°C. Successful electroporants were assessed after 1-3 days incubation.

3.5.3 Transduction

3.5.3.1 Preparation of phage lysates from *S. aureus*

In this study, the generalized transduction was performed using ϕ11 which was propagated by Liane Dreher. A freshly grown bacterial colony was resuspended in 500 µl phage buffer. 50 µl of 1:10 dilution of ϕ11 stock was added to donor strain suspension. The mixture was incubated at room temperature for 10 minutes. 4 ml TSA top agar (kept at 50°C) was added to the mixture with gentle mixing. The whole suspension was poured on $CaCl_2$-TSA plates to activate the bacterial lysate formation. A negative control plate was done exactly as the previous protocol except that ϕ11 was excluded. A sterility control plate was done exactly as the previous protocol except that the bacterial colony was excluded. The plates were incubated in upright position at 37°C for 6 hours or until the bacterial growth was lysed with ϕ11. 4 ml TSB was added to the lysate plate to facilitate scraping and collecting the bacterial lysate. The bacterial lysate was then incubated for 10 minutes at 50°C to liberate the phages from the agar. A centrifugation step (5000 x g for 10 minutes at 4°C) was performed to clarify the lysate. The lysate was then filter sterilized using 0.45 µm syringe filter and stored at 4°C until use.

3.5.3.2 Generalized phage transduction

A freshly grown colony of the acceptor strain was resuspended in 200 µl phage buffer. 100 µl bacterial lysate was added. The transduction mixture was then incubated for 10 minutes at 37°C with shaking. A sterility control plate was done exactly as the previous protocol except that the bacterial lysate was not added. 3.5 ml of phage top agar (kept at 50°C) was added and gently mixed with the transduction mixture.

The whole suspension was poured on selective TSA-plates based on the resistance marker. Successful transductants were assessed after 1-3 days incubation.

3.6 Bacterial mutagenesis

3.6.1 Chromosomal reporter

To construct the reporter strain (EI011 = JE2::P_{ofrA}::*lacZ*), pES3 was constructed by replacing P_{hla} in pKO10 with a multiple cloning sequence using oligonucleotides phosphorylation and hybridization followed by ligation with the restricted pKO10 backbone. pES3 was then used to clone 1 kb fragment upstream *ofrA* with IVA cloning strategy.

After confirming the correct cloning with PCR and sequencing, the reporter plasmid (pES3::P_{ofrA}::*lacZ*) was transformed into *E. coli* IM08B. The reporter plasmid was then electroporated into *S. aureus* JE2 strain. *S. aureus* JE2 + pES3::P_{ofrA}::*lacZ* strain was grown in non-permissive temperature (43°C) to select for single crossover event on TSA-chloramphenicol plate (Ohlsen et al., 1997). The single crossover was confirmed by PCR with primer in the plasmid and another primer in upstream of the 1 kb cloned fragment to ensure the successful single crossover. Sequencing the chromosomal integration site confirmed the reporter system.

3.6.2 Chromosomal mutation

Allelic replacement in *S. aureus* was mediated with homologous recombination using pBASE6 vector. First, the whole DNA region containing *ofrA* (SAUSA300_0857 to SAUSA300_0860) was cloned in pES2 cloning aid vector with restriction-ligation strategy. PCR-mediated deletion was used to delete *ofrA* coding sequence in pES2 vector in *E. coli* DH5α.

After confirming the correct deletion with sequencing, 1 kb upstream and 1 kb downstream fragment to *ofrA* was cloned in pBASE6 shuttle vector in *E. coli* DH5α using restriction-ligation strategy. After confirming the correct cloning with PCR, restriction analysis, and sequencing, the deletion plasmid (pBASE6Δ*ofrA*) was transformed into *E. coli* IM08B. The deletion plasmid was then electroporated into *S. aureus* JE2 strain.

S. aureus JE2 + pBASE6Δ*ofrA* strain was grown in non-permissive temperature (43°C) to select for single crossover event on TSA-chloramphenicol plate. A big well-isolated colony was grown in TSB in the permissive temperature (30°C) to allow the double crossover event. Inducible counter-selection was used to enrich for the plasmid curation after the double crossover by plating on B-plate supplemented with anhydrotetracycline (final concentration = 100 ng/ml) (Bae and Schneewind, 2006). Several colonies

were screened for chloramphenicol sensitivity. The candidates were then screened using colony PCR to check for the genotype (Δ*ofrA*). Later, the genomic DNA of both the WT and the mutant (EI046 = JE2Δ*ofrA*) were isolated and subjected to whole genome sequencing *via* MicrobesNG company.

3.7 β-Galactosidase assay

The early stationary phase cells of the reporter strain (OD_{600} = 1.25 ± 0.05) in RPMI medium supplemented with 10 µg/ml chloramphenicol. The stressors were added to 500 µl of the bacterial culture at the pre-defined concentrations. Untreated controls were done without the addition of a stressor. The bacterial cultures were then incubated for 2 hours at 37°C with shaking. β-Galactosidase assay was performed as indicated in a previous study (Vidal-Aroca et al., 2006). 40 µl of the cultures was added to 160 µl of Z-buffer. OD_{600} was then recorded for normalization. 50 µl of 1 mg/ml MUG solution was added to each well and mixed with pipetting. After 15 minutes incubation at room temperature, 60 µl of the stop solution was added to each well and mixed with pipetting. Fluorescence of the generated MU was measured using 360 nm excitation and 460 nm emission. Arbitrary MUG units were calculated for each well as follows: $\frac{F_{360/460}}{15 \times A_{600}}$.

3.8 Minimum inhibitory concentration (MIC)

Dilutions (1:100) of the overnight cultures of *S. aureus* strains into fresh cultures were allowed to grow in 37°C with shaking until logarithmic phase (OD_{600} = 0.4-0.6). The bacterial cultures were then adjusted to OD_{600} = 0.05 by fresh medium and incubated with serial dilutions of the stressors for 24 hours in a microtiter plate with shaking. The growth was then monitored in microtiter plate reader each 20 minutes by measuring OD_{500}. The MIC was considered as the minimum concentration that prevents the bacterial growth (final OD_{500} less than 0.1).

3.9 Bacterial growth assay

S. aureus strains were conditioned in RPMI medium by growth overnight. Dilutions (1:100) of the overnight cultures into fresh cultures were allowed to grow in 37°C with shaking until logarithmic phase (OD_{600} = 0.4-0.6). The bacterial cultures were then adjusted to OD_{600} = 0.35 by fresh pre-warmed medium. The growth was then monitored in microtiter plate reader for 20 minutes by measuring OD_{500}. When, OD_{500} reached 0.5, stressor compounds were added to the pre-determined final concentrations. Further, the OD_{500} was continuously measured each 20 minutes for 10-15 hours with the microtiter plate reader.

3.10 Growth inhibition assay

Dilutions (1:100) from overnight cultures into fresh RPMI medium were allowed to grow in 37°C with shaking until mid-logarithmic phase (OD_{600} = 0.5). The bacteria were diluted down to 5 x 10^5 cells. Different concentrations of streptonigrin (0-2 µg/ml) were added to the cultures. OD_{600} were continuously measured each 20 minutes for 24 hours with the microtiter plate reader.

3.11 Survival assays

3.11.1 *In-vitro* survival assay

After pre-conditioning *S. aureus* strains in RPMI medium by growth overnight, 1:100 dilutions of the overnight cultures into fresh cultures were allowed to grow in 37°C with shaking. Until mid-logarithmic phase (OD_{600} = 0.4-0.6), the cultures were then adjusted to OD_{600} = 0.4 by fresh medium after collecting the bacterial pellets with centrifugation (4000 rpm for 10 minutes). The calculated amounts of the stressors (dissolved in sterilized water) were added to the bacterial culture and incubated at 37°C for the indicated time. Controls without adding any stressors were used for normalization. After incubating the bacterial cultures +/- stressors in 37°C, the viable bacterial counts were determined with single plate-serial dilution spotting method on LB agar (Thomas et al., 2015).

3.11.2 Bacterial infection stocks preparation

This protocol was used to prepare bacterial infection stocks to ensure the homogeneity of *ex-vivo* and *in-vivo* assays. A well isolated colony of each strain freshly grown on BHI-plate was used to inoculate an overnight culture in BHI. The next day, a fresh culture was constructed by diluting the overnight culture 1:10 in fresh BHI. The bacteria were allowed to grow by incubation at 37°C with shaking until mid-logarithmic phase (3.5 hours). The bacterial culture was collected with centrifugation (4000 rpm for 10 minutes). The pellet was then resuspended in 20 ml fresh BHI and 4 ml of 86% glycerol (as a cryoprotectant). The infection stock was then stored in -80°C as 2 ml aliquots. For each infection stock prepared, a standard calibration curve was constructed to predict the CFU/ml as a function of OD_{600} (see below).

3.11.3 Standard calibration curve

A 2-ml aliquot of the stored infection stock was thawed at room temperature. The bacterial cells were then washed with 50 ml 1 x PBS and collected with centrifugation (4000 rpm for 10 minutes). The washed bacterial cells were then resuspended with 3 ml 1 x PBS

and diluted 1:2, 1:1, and 2:1 with 1 x PBS. From each of the four concentrations of the cells, OD_{600} was recorded and the viable cells were counted using single plate-serial dilution spotting method on LB agar (Thomas et al., 2015). A calibration curve was constructed with OD_{600} on the X-axis and CFU/ml on the Y-axis.

3.11.4 RAW 264.7 macrophage survival assay

RAW 264.7 macrophage cell line was prepared by cultivation in RPMI medium supplemented with Pen/Strep and 10% FBS. Bacteria from infection stocks were resuspended in 1 x PBS. $5x10^7$ bacterial cells were added to $5x10^6$ RAW 264.1 cells in 24-well plates (MOI=1:10) and in pre-warmed RPMI medium supplemented with 10% FBS. The bacteria-cells mixtures were incubated for one hour at 37°C to ensure bacterial internalization to RAW macrophages. The extracellular bacteria were killed with 150 µg/ml gentamicin exposure for one hour. The medium was replaced with fresh pre-warmed RPMI medium supplemented with 10% FBS and this was considered zero-time (Flannagan et al., 2018).

Samples were taken at time = 4, 24, and 48 hours. The resuspended RAW macrophages in sterile water were frozen in -20°C. The frozen macrophages were thawed in room temperature and vortexed to ensure cell lysis. The viable bacterial counts were determined with using single plate-serial dilution spotting method on LB agar (Thomas et al., 2015).

3.12 Transcriptome analysis

3.12.1 Total RNA isolation

Overnight cultures were conditioned in RPMI then diluted 1:100 in fresh medium. The fresh cultures were allowed to grow in 37°C with shaking until they reached OD_{600} = 0.5. Samples were taken as a control before adding the stressors. After adding the stressors, the bacterial cultures were incubated in 37°C with shaking for 15 minutes. Once 1-ml samples were drawn, they were immediately put on ice until transfer to -80°C to be stored.

The total RNA isolation was performed using RNeasy Mini Kit based on the manufacturer's instruction. First, the bacterial pellets (collected by centrifugation 16000 x g for 2 minutes in 4°C) were resuspended in 700 µl RLT buffer supplemented with β-mercaptoenthanol. The cells suspensions were then transferred into lysing matrix tubes (MP Biomedicals). The bead-beating machine was set for bacterial lysis at 6.5 m/s for 45 seconds. After incubation on ice for 5 minutes, another round of bead beating lysis was performed with the same parameters. The lysates were then cooled for 5 minutes on ice. After centrifugation for 10 seconds at 16000 x g, 500 µl of supernatants were mixed with 350 µl ethanol. Total RNA samples were then bound to RNA-binding column (RNeasy Mini Kit). Washing once

with 700 µl RW1 and twice with 500 µl RPE buffers was performed. Total RNA was then eluted twice from the column with 15 µl DNase- RNase-free water at 70°C for 3 minutes.

3.12.2 Measuring RNA concentration

In general, 1 µl of 1:10 dilution of the isolated total RNA was used to determine the concentration using A_{260}. For RNA-seq experiment, the total RNA concentrations were measured using Qubit™ RNA Assay Kit (according to the manufacturer manual) to ensure there are no inferences from any co-isolated nucleic acids or proteins.

3.12.3 Total RNA isolation for RNA sequencing

Three independent overnight cultures were used to construct fresh cultures with 1:100 dilution. The fresh cultures were allowed to grow in 37°C with shaking until they reached OD_{600} = 0.5. Samples were drawn from the WT and the mutant strains and immediately put on ice until transfer to -80°C to be stored. Total RNA isolation was performed, as above, using RNeasy Mini Kit. After DNase digestion (see below), RNA samples' quality, rRNA depletion, cDNA library preparation, and next generation sequencing were performed by the Core Unit Systems Medicine Facility at the University Hospital Würzburg.

3.12.4 DNase digestion

To get rid of any co-purified DNA, RapidOut DNA removal kit (from Thermo Fisher) was used. The DNase digestion was done in 30 µl reaction according to the manufacturer's instructions. RNA was heated at 65°C for 5 minutes then cooled on ice for 5 minutes. 3 µl DNase buffer and 2.4 µl DNase I enzyme were added to the RNA sample and incubated at 37°C for 45 minutes. 4.8 µl DNase removal reagent (DRR) was added to RNA sample after vigorous vortex to resuspend DRR. DRR was incubated at room temperature for two minutes. DRR combined with DNase I was collected with centrifugation (1000 x g for one minute). The DNA-free RNA was pipetted out into fresh tube. Negative amplification of 16S rDNA locus was used to control for successful DNase treatment.

3.12.5 Reverse transcription

To perform reverse transcription, SuperScript IV reverse transcriptase kit (from Thermo Fisher) was used according to the manufacturer's instructions. To avoid the interference of anti-sense transcription in *ofrA* locus with RT-qPCR assays, a non-staphylococcal tag / anti-tag pair were developed for strand-specific amplification (Vashist et al., 2012).

The reverse transcription reaction was constructed as follows:

RNA	2 µg
Random hexamers (100 µM)	0.5 µl
tag.*ofrA*.cDNA (10 µM)	0.2 µl
dNTPs (10 mM each)	1 µl
DNase- RNase-free water	up to 13 µl

The reverse transcription mixture was then heated at 65^{o}C for 5 minutes followed by cooling on ice for 1 minute. A reverse transcription master mixture was constructed (per reaction) as follows:

5x SSIV buffer	4 µl
DTT (100 mM)	1 µl
Ribolock	1 µl
SSIV Reverse Transcriptase	1 µl

7 µl of the master mixture was added to the reverse transcription mixture and incubated at 23^{o}C for 10 minutes then 52.5^{o}C for 10 minutes, and finally 80^{o}C for 10 minutes to inactivate SSIV Reverse Transcriptase. After the first strand synthesis, the cDNA sampled were stored in 4^{o}C for RT-qPCR analysis. For long-term storage (more than 3 days) cDNA samples were kept at -20^{o}C.

3.12.6 Quantitative PCR (qPCR)

Quantitative PCR was used to relatively quantify *ofrA* cDNA in bacterial cultures supplemented with stressors compared to untreated control as well as validating the RNA-seq results using Biozym Blue S'Green qPCR Kit. For this purpose, the geometric mean of *rho* and *rpoB* relative cDNA quantities were used as a normalization factor (Sihto et al., 2014).

First, cDNA samples were serially diluted. The 10^{-3} dilutions were used as templates for qPCR reactions. The manufacturer's instructions were followed for constructing 20 µl qPCR reactions:

2x qPCR S'Green Blue Mix	10 µl
Forward Primer (10 µM)	0.8 µl
Reverse Primer (10 µM)	0.8 µl
Template	8 µl
DNase- RNase-free water	0.4 µl

Second, the annealing and extension temperature was optimized for each amplification (*ofrA* and *rocD* = 55^{o}C, *rpoB* and *rho* = 57^{o}C, *acuA* = 58^{o}C, and *crtM* = 63^{o}C).

The recommended thermal cycling for amplification was used:

Initial denaturation	95°C	2 minutes
40 Cycles:		
Denaturation	95°C	5 seconds
Primers' annealing + Extension	$T_{ann/ext}$	20 seconds
Fluorescence measurement		
Melting curve:		
65°C -95°C: increment 0.5°C for 5 seconds / step		
Fluorescence measurement		

3.13 5' Rapid Amplification of cDNA Ends (5'RACE)

5'RACE experiment was done as discussed in (Marincola et al., 2012). Briefly, total RNA was extracted from *S. aureus* JE2 strain, that was grown in B-medium until OD_{600}=0.5, using NucleoZOL reagent (Macherey-Nagel) and isopropanol precipitation as in the manufacturer manual. The total RNA was treated with DNase I using RapidOut DNA removal kit (LIFE Technologies). The primary transcripts in 10 µg total RNA were decapped by RNA 5' Pyrophosphohydrolase (RPPH from NEB) which removes the pyrophosphate from the 5' end to leave a 5' monophosphate RNA.

Both the RPPH-treated and the untreated RNA were subjected to ligation with an RNA adaptor using T4 RNA ligase I (LIFE Technologies). SuperScript IV Reverse Transcriptase (LIFE Technologies) was used for cDNA synthesis with *ofrA*-specific primer. A library was generated (in pES2 vector) of specific RPPH-treated samples compared to the untreated control. Then, 15 colonies were sequenced to determine the transcriptional start site.

3.14 Bioinformatics analysis

3.14.1 Conservation analysis

Completely assembled representative Firmicutes and staphylococcal chromosomes were collected from the NCBI website (https://www.ncbi.nlm.nih.gov/genome/browse/) in May 2021. OfrA sequence (WP_000838037.1) was used to search for possible encoded proteins in the completely assembled chromosomal sequences using TBLASTN from the standalone BLAST ncbi-blast-2.11.0+. Then, BLASTP program was used for pairwise local alignment of OfrA to the encoded proteins from the retrieved loci. To consider the protein as a member of OfrA-class of OYEs, the following cut-offs were used: 1) 35% amino acid identity (Shi et al., 2020) and 2) protein length 375 ± 38 amino acids (10% deviation from OfrA length). Sequence Dereplicator and Database Curator was used to filter out identical proteins (Ibrahim et al., 2017).

3.14.2 Phylogenetic analysis

To build a phylogenetic tree based on protein or DNA sequences, a global multiple sequence alignment of these sequences was constructed using Clustal Omega with the default parameters (https://www.ebi.ac.uk/Tools/msa/clustalo/). The multiple sequence alignment was then used to construct a phylogenetic tree using RAxML 8.0.0 (Stamatakis, 2014). The following parameters were used to search for the maximum-likelihood phylogenetic tree of protein sequences (-f a -# autoMRE -m PROTGAMMAAUTO). The R package (ggtree v2.0.1) was used for tree annotation and visualization (Yu, 2020).

3.14.3 RNA-seq analysis

Adaptor sequence (AGATCGGAAGAGCACACGTCTGAACTCCAGTCAC) was trimmed from the raw reads using cutadapt software with the following parameters (--nextseq-trim=20 -u 12) (Martin, 2011). Quality control of the trimmed reads was then checked using FastQC software. Trimmed reads were then mapped to the reference sequence (NC_007793). Reads mapping, coverage calculations, gene quantification, and differential gene expression analysis were done using READemption pipeline (Förstner et al., 2014).

3.14.4 Gene set enrichment analysis (GSEA) and regulon analysis

R scripts were developed for GSEA and regulon analysis. ClusterProfiler R-package version 3.12.0 was used for GSEA (Wu et al., 2021). Regulons were retrieved from (https://aureowiki.med.uni-greifswald.de/download_gene_specific_information) and the study of (Fritsch et al., 2019) for regulon analysis.

3.15 Staphyloxanthin assay

Overnight cultures were diluted 1:100 in fresh medium (with or without supplementation). The fresh cultures were allowed to grow at 37^{o}C with shaking until stationary phase (16-20 hours). Bacterial pellets were collected with centrifuging 2 ml from bacterial cultures (16000 x g for 2 minutes). The pellets were then washed in sterilized water. OD_{600} were recorded for normalization. Methanolic extraction of the carotenoid pigment were done incubating 400 µl of methanol at 55^{o}C for 3 minutes (Sullivan and Rice, 2021). Cellular debris were removed with centrifugation (16000 x g for 2 minutes). 300 µl of the methanolic extract were added to 700 µl methanol. A_{465} of 200 µl of the solution was measured using methanol as a blank.

3.16 Statistical analysis and visualization

For statistical analysis, R version 3.6.1, rstatix R-package version 0.6.0, and ggpubr R-package version 0.4.0 were used. In each figure legend, the statistical test is indicated. *P*-value < 0.05 is considered the statistical significance cut-off in this study.

3.17 Data availability

Whole genome sequencing raw reads are deposited in the SRA database (https://www.ncbi.nlm.nih.gov/bioproject/PRJNA812552). The analysis of RNA sequencing reads is deposited in the NCBI's Gene Expression Omnibus (https://www.ncbi.nlm.nih.gov/geo/query/acc.cgi?acc=GSE196683).

4 Results

4.1 OfrA is a staphylococcal old yellow enzyme flavin oxidoreductase

SAUSA300_0859 gene product was proved responsible for MT02 (a novel DNA-binding anti-MRSA) inactivation *via* nitroreductase activity (El-Hossary et al., 2018). Analysing the amino acid sequence of WP_000838037.1 in InterPro (https://www.ebi.ac.uk/interpro/protein/UniProt/Q2FZU7/), an OYE_like_4_FMN domain was found the only identifiable protein domain in the sequence based on CDD search (Marchler-Bauer et al., 2017). BLASTP analysis of WP_000838037.1 as a query against OYE2 from *Saccharomyces cerevisiae* (NP_012049.1) showed 25% of amino acid identities and 44% similarity.

OYE_like_4_FMN is group 4 of old yellow enzyme related protein domain (https://www.ebi.ac.uk/interpro/entry/cdd/CD04735/). To search for potential paralogous gene(s), TBLASTN of WP_000838037.1 against *S. aureus* USA300_FPR3757 genome showed that OYEs are encoded from two paralogous genes (SAUSA300_0859 and SAUSA300_0322) (**Figure 1A**). WP_000838037.1 and WP_000286485.1 (SAUSA300_0859 and SAUSA300_0322 gene products, respectively) contain an OYE_like_4_FMN domain.

Moreover, WP_000838037.1 and WP_000286485.1 are orthologues to YqiG and YqjM (recently studied OYEs in *Bacillus subtilis*), respectively (Kitzing et al., 2005; Sheng et al., 2016) (**Figure 1A**). Since SAUSA300_0859 and SAUSA300_0322 are two paralogous OYEs in *S. aureus* USA300_FPR3757 genome, we renamed SAUSA300_0859 as **O**YE **f**lavin oxido**r**eductase **A** (*ofrA*) and SAUSA300_0322 as *ofrB* (**Figure 1A**).

Phylogenetic analysis showed that the gram-positive OYEs (OfrA, OfrB, YqiG, and YqjM) are phylogenetically distinct from the gram-negative OYEs (NemA of *E. coli* and XenB of *P. fluorescens*) (**Figure 1B**).

4.2 OfrA conservation in staphylococci and some Firmicutes

To test the conservation of *ofrA* in different *S. aureus* genomes, OfrA-encoding open reading frames were searched in the publicly available 749 fully annotated chromosomes of *S. aureus* strains. OfrA (WP_000838037.1) is encoded in all of the searched genomes with 98% to 100% amino acids identities (**Figure 1C**).

In addition, OfrA is conserved in the fully annotated 28 representative staphylococcal chromosomes (**Figure 1E and Figure 2C**) and wide spread in *Bacillus* species (**Figure 1E and Figure 2A**). BLASTP analysis showed that OfrA orthologues have 55% or more amino acids

identities to OfrA (**Figure 1D**). Unlike *Staphylococcus*, the majority of *Streptococcus*, *Clostridium*, and *Lactobacillus* representative species' chromosomes do not encode for OfrA-like OYEs (**Figure 1E and Figure 2B, 2D**).

Although OfrA is conserved in all the searched staphylococci and *S. aureus* strains, OfrB is only limited to some species of staphylococci (**Figure 1F**). Interestingly, OfrA is more conserved in staphylococci compared to the classical mevalonate pathway (exemplified with MvaA) and staphyloxanthin biosynthesis pathway (exemplified with CrtM) (**Figure 1F**).

CrtM sequences are used as a discriminating orthologue of group B staphylococci (*S. xylosus*, *S. saprophyticus*, and *S. equorum*) (Coates-Brown et al., 2018). Moreover, a recent report showed that staphyloxanthin biosynthesis is ubiquitous across staphylococci (Salamzade et al., 2022).

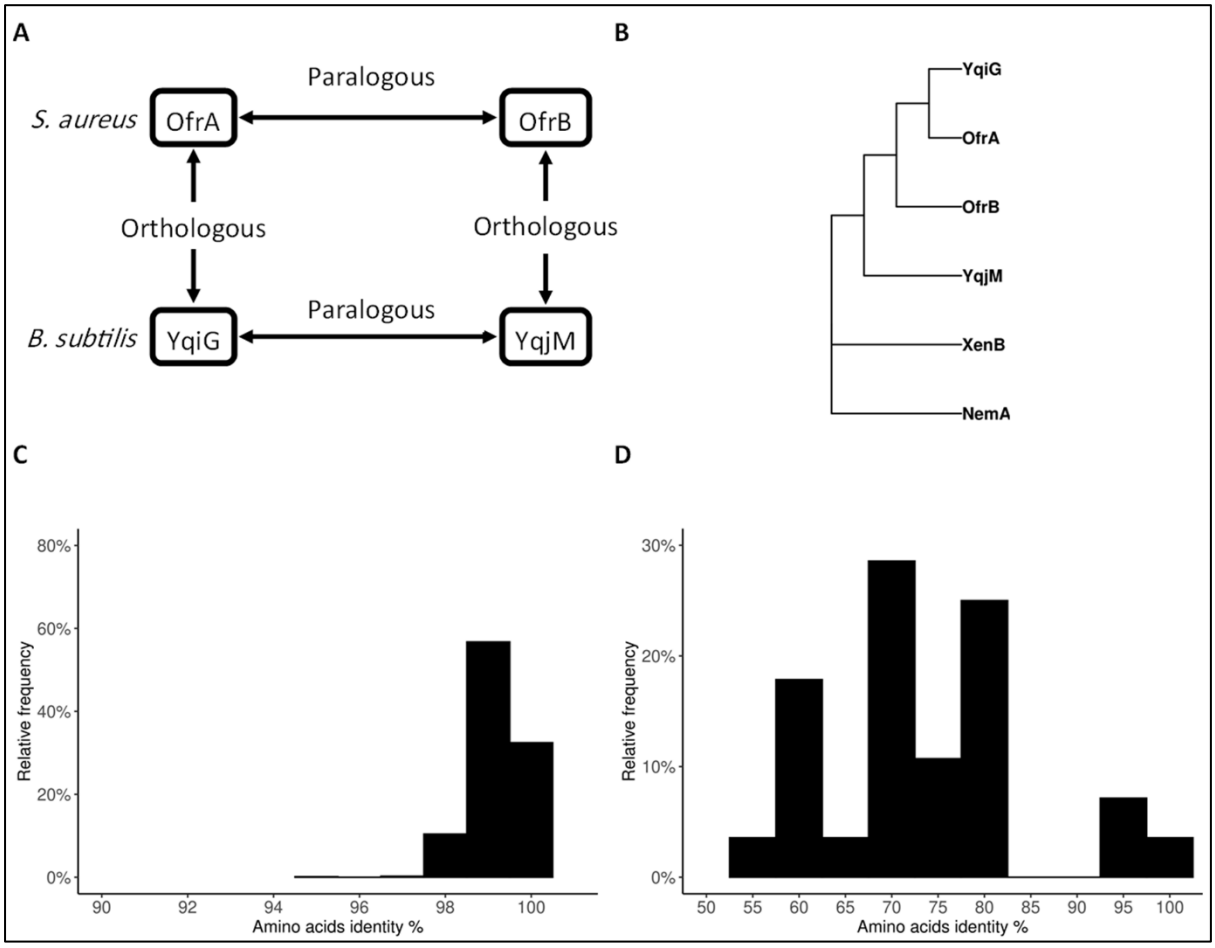

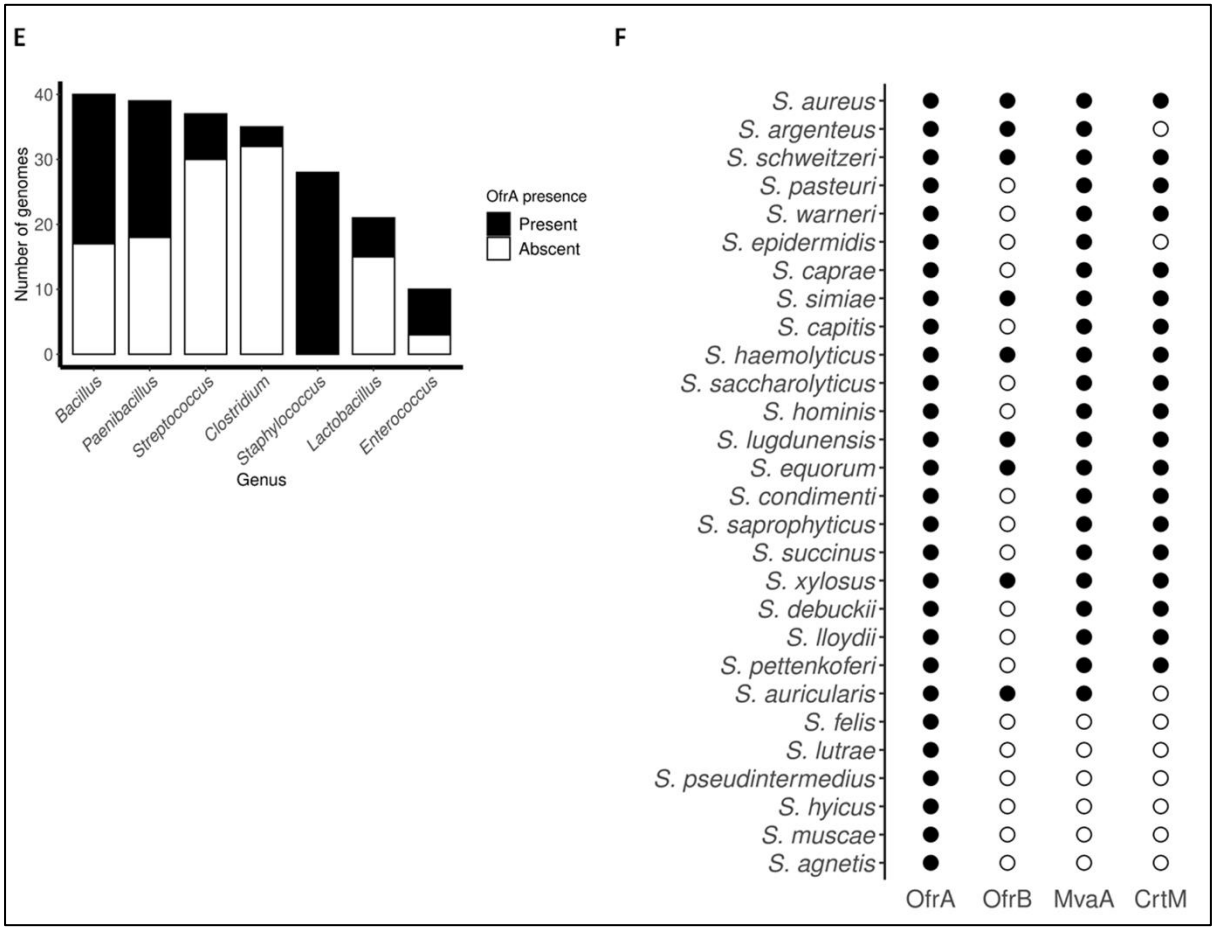

Figure 1| OfrA is a conserved old yellow enzyme encoded in staphylococcal and some Firmicutes' chromosomes. **(A)** OfrA and OfrB are two paralogous OYEs encoded in *S. aureus*. Likewise, YqiG and YqjM are encoded in *B. subtilis*. **(B)** Phylogenetic analysis based on OYEs protein sequences in the Gram-positive [*S. aureus* (OfrA and OfrB) and *B. subtilis* (YqiG and YqjM)] and the Gram-negative (*E. coli* NemA and *Pseudomonas fluorescens* XenB). BLASTP analysis of OfrA amino acid identities compared to its orthologues in **(C)** *S. aureus* strains or **(D)** *Staphylococcus* species. **(E)** The presence or absence of OfrA or OfrA-like orthologues in seven Firmicutes genera. Presence inclusion criteria were based on 35% amino acid identity and protein length = 375 ± 38 amino acids (10% deviation from OfrA length). **(F)** OfrA and OfrB conservation in 28 staphylococcal species compared to MvaA (classical mevalonate pathway) and CrtM (staphyloxanthin biosynthesis). Filled and unfilled circles indicate the presence and the absence, respectively.

4.3 Constructing *ofrA* reporter strain (EI011) and optimizing assay conditions

To screen for possible inducing conditions, a reporter system was constructed based on transcriptional fusion of *ofrA* promoter (P_{ofrA}) to a promoter-less *lacZ*. The chromosomal integration of the reporter system was then confirmed by PCR utilizing a reporter-specific primer and an upstream chromosomal-specific primer followed by sequencing constructing the reporter strain EI011 (**Figure 3A**).

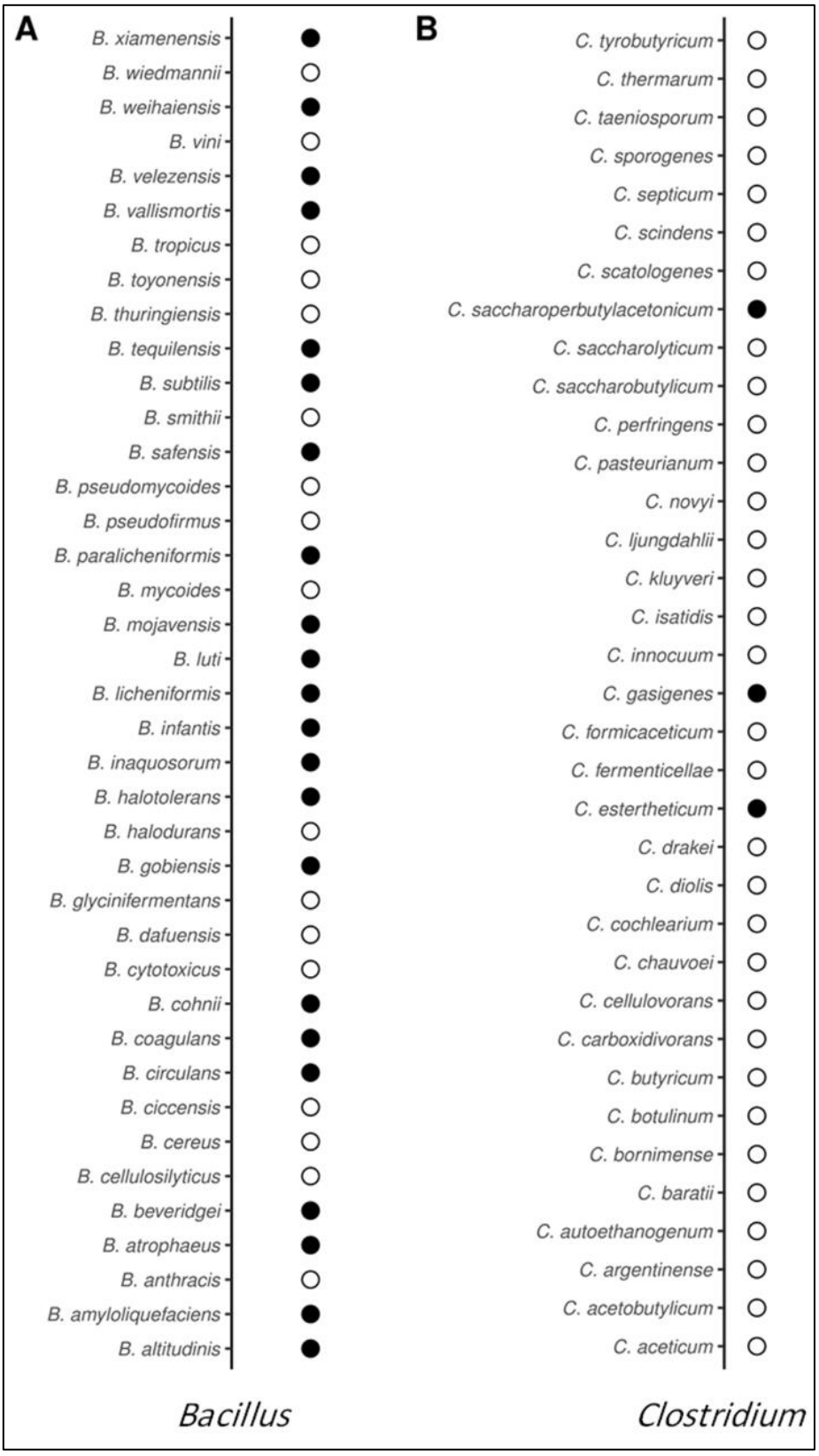
A
B. xiamenensis
B. wiedmannii
B. weihaiensis
B. vini
B. velezensis
B. vallismortis
B. tropicus
B. toyonensis
B. thuringiensis
B. tequilensis
B. subtilis
B. smithii
B. safensis
B. pseudomycoides
B. pseudofirmus
B. paralicheniformis
B. mycoides
B. mojavensis
B. luti
B. licheniformis
B. infantis
B. inaquosorum
B. halotolerans
B. halodurans
B. gobiensis
B. glycinifermentans
B. dafuensis
B. cytotoxicus
B. cohnii
B. coagulans
B. circulans
B. ciccensis
B. cereus
B. cellulosilyticus
B. beveridgei
B. atrophaeus
B. anthracis
B. amyloliquefaciens
B. altitudinis
Bacillus
B
C. tyrobutyricum
C. thermarum
C. taeniosporum
C. sporogenes
C. septicum
C. scindens
C. scatologenes
C. saccharoperbutylacetonicum
C. saccharolyticum
C. saccharobutylicum
C. perfringens
C. pasteurianum
C. novyi
C. ljungdahlii
C. kluyveri
C. isatidis
C. innocuum
C. gasigenes
C. formicaceticum
C. fermenticellae
C. estertheticum
C. drakei
C. diolis
C. cochlearium
C. chauvoei
C. cellulovorans
C. carboxidivorans
C. butyricum
C. botulinum
C. bornimense
C. baratii
C. autoethanogenum
C. argentinense
C. acetobutylicum
C. aceticum
Clostridium

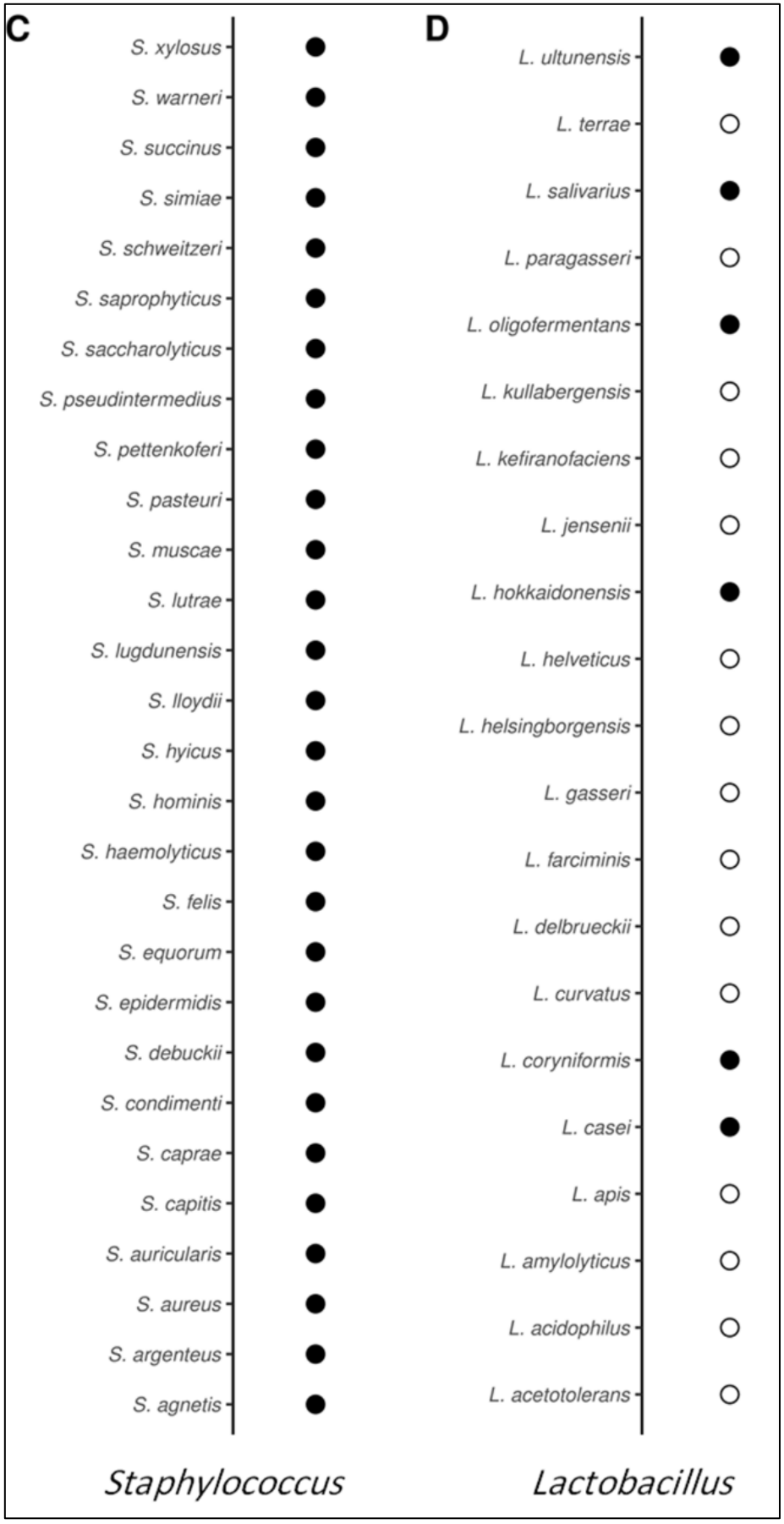

Figure 2 | OfrA distribution in selected Firmicutes. BLASTP analysis of OfrA against **(A)** *Bacillus*, **(B)** *Clostridium*, **(C)** *Staphylococcus*, or **(D)** *Lactobacillus* species. Please, refer to "Methods" section.

OfrA was earlier reported to cause a phenotypic resistance against the novel DNA-binding anti-MRSA compound (MT02) *via* type-I nitroreductase activity (El-Hossary et al., 2018). Furthermore, OYEs are reported to use α, β-unsaturated carbonyl compounds as substrates (Shi et al., 2020). The hypothesis was that these compounds could be possible inducers of *ofrA*. Interestingly, these compounds belong to the reactive electrophilic species which could intracellularly increase the reactive oxygen species. NemA of *E. coli* was also reported to respond to hypochlorite stress and to *in-vitro* reduce the electrophilic stress inducer N-ethylmaleimide (Gray et al., 2013; Lee et al., 2013). Therefore, RPMI-medium was used as a medium for bacterial growth and exposure to stressors to avoid the quenching effect of normal laboratory medium to electrophilic, oxidative, and hypochlorite stress. In addition, RPMI is a well-defined medium that is closer to the host environment than the rich laboratory media (Meerwein et al., 2020).

The β-galactosidase assay was used to determine possible *ofrA* induction conditions with increasing the *ofrA* promoter activity (**Figure 3B**). Since β-galactosidase assay is dependent on functional system of transcription, translation, and functional protein activity, the toxicities of the stressors were first assessed using MIC testing (**Table 21**). Second, the growth of the WT strain (OD_{600} = 0.5) was assessed in the presence or absence of 1x MIC of the stressors in RPMI medium (**Figure 3C**). I tested the β-galactosidase assay after two-hours (4 x doubling time in RPMI) exposure time to the stressors.

In conclusion, the following concentrations were used to test for *ofrA* induction:

Table 21: Testing concentrations of stressors

Compound	Abbreviation/Formula	MIC	Stress
Tetramethylazodicarboxamide	Diamide	0.5 mM	Electrophilic stress
Fosfomycin	Fosfo	8 µg/ml	
Formaldehyde	FA	0.375 mM	
Methylglyoxal	MG	0.25 mM	
Methylhydroquinone	MHQ	60 µM	
Hydrogen peroxide	H_2O_2	0.5 mM	Oxidative stress
Cumene hydroperoxide	CHP	31.25 µM	
Sodium hypochlorite	NaOCl	0.5 mM	Hypochlorite stress

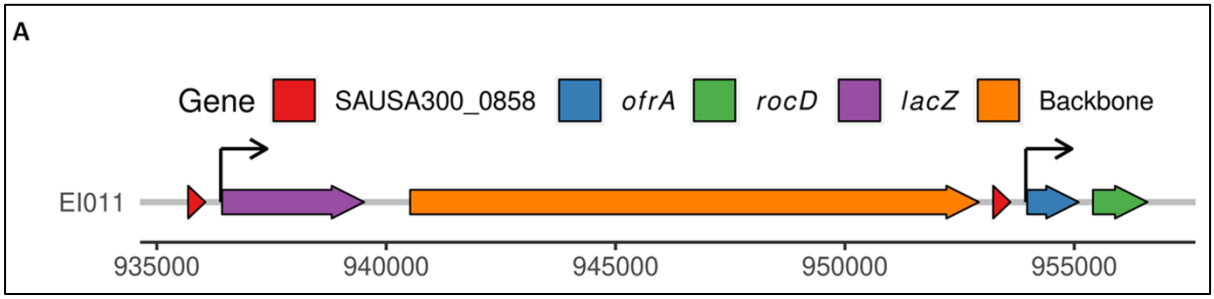
A
Gene
SAUSA300_0858
ofrA
rocD
lacZ
Backbone
EI011
935000
940000
945000
950000
955000

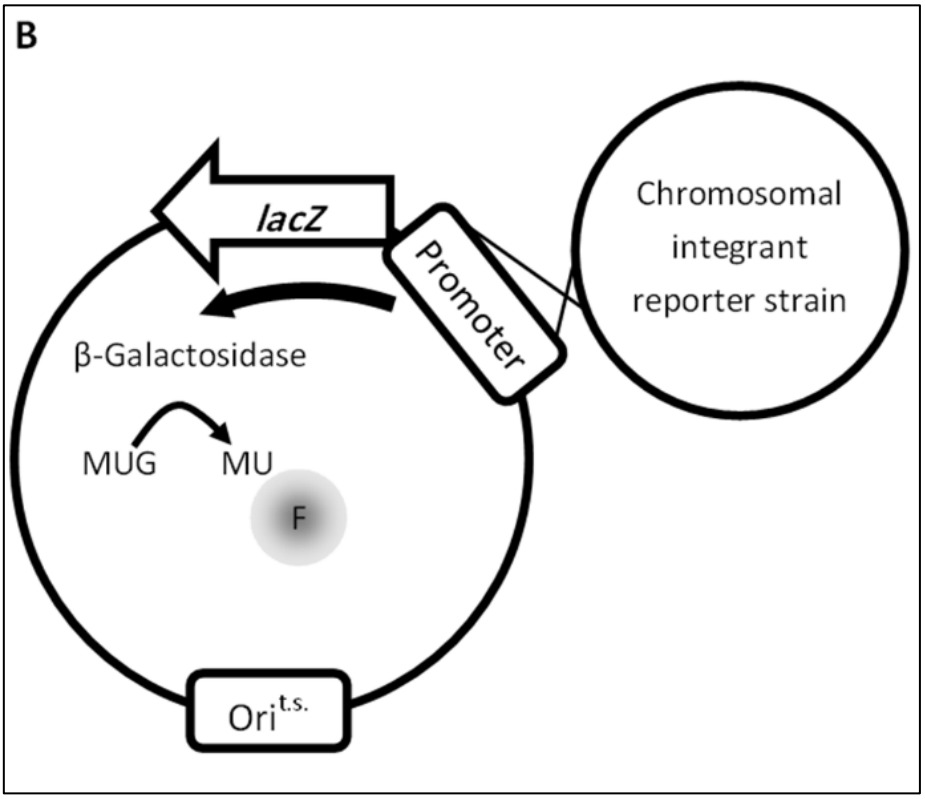
B
lacZ
Promoter
Chromosomal
integrant
reporter strain
β-Galactosidase
MUG
MU
F
Ori t.s.

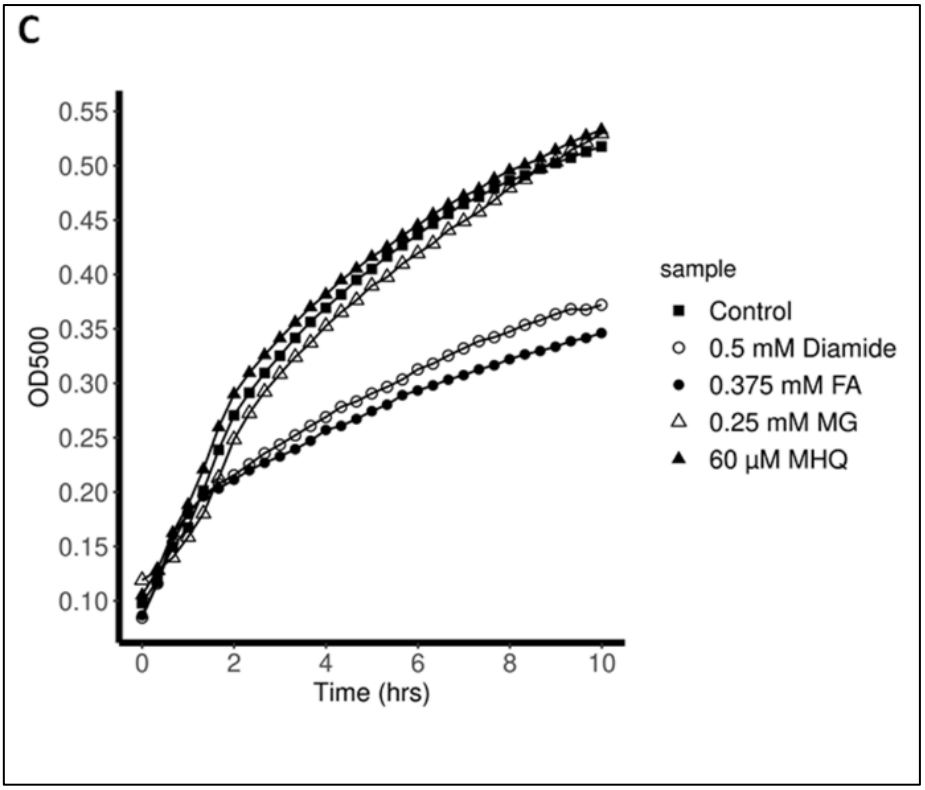
C
OD500
0.55
0.50
0.45
0.40
0.35
0.30
0.25
0.20
0.15
0.10
0
2
4
6
8
10
Time (hrs)
sample
Control
0.5 mM Diamide
0.375 mM FA
0.25 mM MG
60 µM MHQ

Figure 3 | Construction of chromosomal reporter strain (EI011). **(A)** Genetic map shows the single crossover chromosomal integrant genotype. **(B)** Reporter strain construction strategy. P_{ofrA} drives the promoter-less *lacZ* in transcriptional fusion manner. β-Galactosidase assay, converting the non-fluorescent MUG into fluorescent MU, was used to report for *ofrA* induction. **(C)** Growth of *S. aureus* JE2 without (Control) or with different stressors in the stated concentrations that were added at mid-logarithmic phase in RPMI medium. Automatic OD_{500} measurements from the microtiter plate reader were used to track the bacterial growth in three-two biological replicates (average is shown). At least two hours of growth were not significantly inhibited by the added concentrations. FA, formaldehyde; MG, methylglyoxal; MHQ, methylhydroquinone; MUG, 4-methylumbelliferyl-β-D-galactopyranoside; Ori, origin of replication; t.s., temperature sensitive.

4.4 Electrophilic, oxidative, and hypochlorite stress induces *ofrA*

Using β-galactosidase assay suggest that electrophilic, oxidative, and hypochlorite stress conditions result in increased *ofrA* promoter activity (**Figure 4A**). Except fosfomycin, reactive electrophilic species (toxic aldehydes and quinone) induce *ofrA* in *S. aureus*. Diamide, formaldehyde, and methylglyoxal result in roughly four-fold *ofrA* upregulation (**Figure 4A**). MHQ induces *ofrA* up to 21-fold (**Figure 4A**). The inorganic peroxide (H_2O_2) and the organic peroxide (cumene hydroperoxide) cause two- and four- fold upregulation, respectively (**Figure 4A**). Furthermore, hypochlorite stress triggers four-fold induction in *ofrA* reporter system (**Figure 4A**). The induction of *ofrA* follows dose-dependent response with 0.5 x and 1 x MIC of some stressors (**Figure 4B**).

Since diamide is a non-specific and unnatural disulfide-stress inducer, toxic aldehydes (formaldehyde and methylglyoxal) and quinone (MHQ) stress were taken as examples of electrophilic stress. To measure the actual *ofrA* mRNA abundances, RT-qPCR showed that *ofrA* mRNA levels are upregulated in formaldehyde, methylglyoxal, and MHQ after 15 minutes (0.5 x doubling time) of stressors exposure to *S. aureus* JE2 strain in RPMI (**Figure 4C**). The upregulations in *ofrA* mRNA levels are 38-, 4-, and 10-fold in formaldehyde, methylglyoxal, and MHQ stress, respectively.

4.5 Constructing marker-less *ofrA* mutant and whole genome sequencing

To test the effect of *ofrA* mutation on bacterial physiology, a marker-less mutant was constructed in *S. aureus* JE2 strain. The mutant was then complemented using plasmid-based expression of *ofrA* under the control of its natural promoter in the high copy number vector (pRB473). The mutant and the complemented strain are referred as Δ*ofrA* and p*ofrA*, respectively.

A whole genome sequencing was performed on both the WT and Δ*ofrA* strain to confirm the absence of discriminating secondary mutations in Δ*ofrA*. Variant calling

(90% on 10 x coverage) comparing the genome of WT against Δ*ofrA* showed that there are no discriminatory secondary mutations, SNPs, or indels.

4.6 Optimizing *in-vitro* survival assay conditions

In-vitro survivability is dependent on the medium of exposure. To test whether normal laboratory medium quenches the effect of the stressors, the reporter strain EI011 was exposed to MHQ (top inducer) in RPMI medium or in B-medium at 0.5 x and 1 x MIC in the medium. Contrary to RPMI medium, *ofrA* induction could not be seen in B-medium suggesting that B-medium quenches the effect of the stressors (**Figure 4D**).

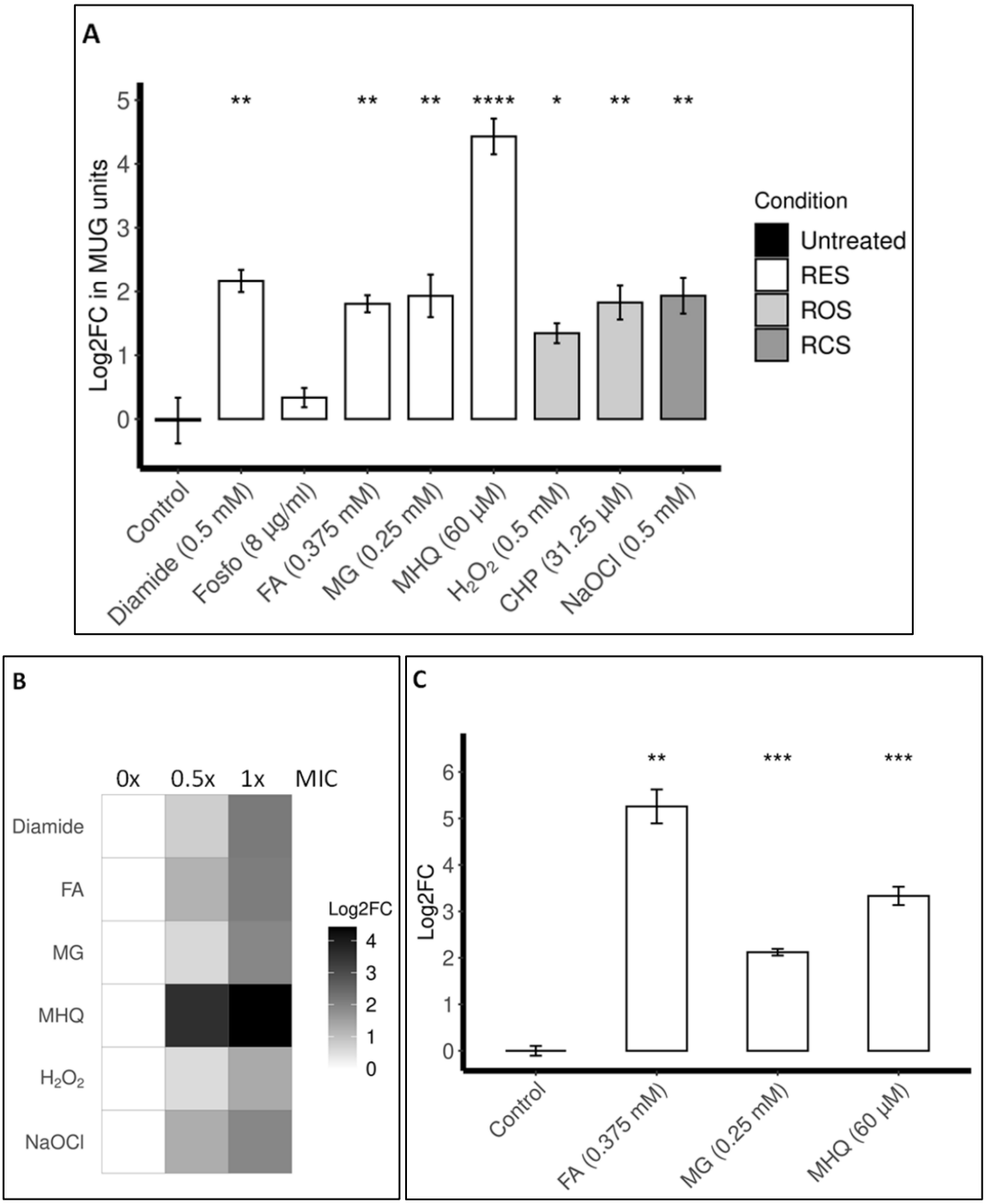

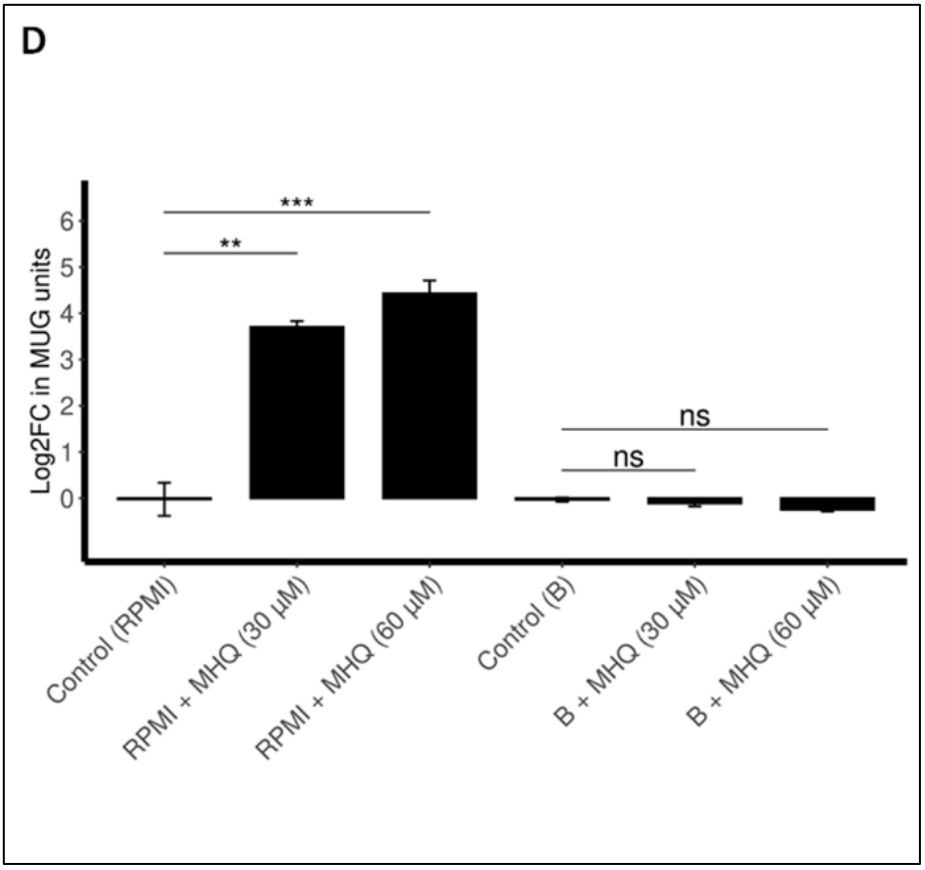

Figure 4 | *ofrA* induction conditions **(A)** β-Galactosidase assays of the reporter strain EI011 culture showing Log2FoldChange in MUG units comparing unstressed control vs stressed cultures with the indicated compounds. The reporter strain grew in RPMI until OD_{600} = 1.25 ± 0.5. Stressors were added to the indicated concentrations and further incubated, along with untreated control, at 37°C for two hours with shaking. The results denote four biological replicates. Error bars represent the standard error of the means. Unpaired two-tailed Student's *t*-test was used for statistical significance inference **(B)** *ofrA* induction, measured with β-galactosidase assays, follows dose response using 0 x MIC (untreated), 0.5 x MIC, or 1 x MIC of the indicated stressors. Data represent the average Log_2FoldChange value of three biological replicates. **(C)** RT-qPCR illustrates increased abundance of *ofrA* mRNA after 15 minutes of mid-logarithmic (OD_{600} = 0.5) phase cells of *S. aureus* JE2 exposure to the indicated stressors in RPMI medium at 37°C with shaking. Three biological replicates' data were compared using unpaired two-tailed Student's *t*-test to the untreated control. Error bars represent the standard error of the means. **(D)** β-Galactosidase assays of the reporter strain EI011 culture in RPMI and B-medium showing Log_2FoldChange in MUG units comparing unstressed control vs MHQ-stressed cultures with the indicated concentrations (0.5 x MIC or 1 x MIC). The reporter strain grew in RPMI until OD_{600} = 1.25 ± 0.5. The reporter strain grew in B-medium until logarithmic phase and was diluted to OD_{600} = 0.5. MHQ was added to the indicated concentrations and further incubated, along with untreated control, at 37°C for two hours with shaking. The results are from four biological replicates except for RPMI + MHQ (30 µM), two biological replicates. Error bars represent the standard error of the means. Statistical analysis was carried out using one-way ANOVA and pairwise *t*-test with Bonferroni *p*-value adjustment; ns, not significant; *p < 0.05; **p < 0.01; ***p < 0.001; ****p < 0.0001. CHP, cumene hydroperoxide; FA, formaldehyde; Fosfo, fosfomycin; H_2O_2, hydrogen peroxide; MG, methylglyoxal; MHQ, methylhydroquinone; MIC, minimum inhibitory concentration; MUG, 4-methylumbelliferyl-

β-D-galactopyranoside; NaOCl, sodium hypochlorite; RCS, reactive chlorine species; RES, reactive electrophilic species; ROS, reactive oxygen species.

Growth kinetics of the different strains in the selected medium could affect the survival rate. Since p*ofrA* strain shows prolonged lag phase, as expected from strains bearing high-copy number plasmid, logarithmic phase cells were used in survival analysis due to growth behaviour similarities among JE2, Δ*ofrA*, and p*ofrA* strains (**Figure 5A**). To count for any possible differences in bacterial growth behaviour, the survived viable bacterial counts were normalized to the viable bacterial counts from split bacterial culture without any stressors (untreated control).

4.7 OfrA improves *S. aureus* survival in electrophilic, oxidative, and hypochlorite stress

S. aureus JE2, Δ*ofrA*, and p*ofrA* *in-vitro* survival were tested in RPMI medium against electrophilic, oxidative and hypochlorite stress. After three hours of exposure, Δ*ofrA* showed compromised survival in 0.5 mM MHQ and 2 mM methylglyoxal (**Figure 5B, 5C**). In quinone stress, JE2 and Δ*ofrA* survived 90% and 61%, respectively (**Figure 5B**). Similar survival defect phenotype is also seen in the toxic aldehyde methylglyoxal (**Figure 5C**). Genetic complementation (p*ofrA*) results in restoration of the wild-type survivability in both conditions (**Figure 5B, 5C**).

After one-hour exposure to 40 mM H_2O_2, Δ*ofrA* had decreased survival compared to the WT (**Figure 5D**). The complemented strain survival is similar to the WT phenotype (**Figure 5D**). Similar behaviour is seen in the *in-vitro* survival against hypochlorite stress.

S. aureus JE2 strain showed 70% survival rate after 30 minutes exposure to 1.5 mM NaOCl. However, Δ*ofrA* strain survived only 33% after the exposure to the same condition (**Figure 5E**). Though, the complemented strain survival (p*ofrA*) did not phenocopy the WT in NaOCl survival (**Figure 5E**). From the whole genome sequencing data, we can ensure the absence of secondary mutation that could cause non-*ofrA* related defective hypochlorite survival. Furthermore, the reporter strain EI011 showed *ofrA* induction in the presence of NaOCl condition (**Figure 4A, 4B**). Genetic complementation using high-copy number plasmid could overly consume the cellular resources making the cells less able to survive against the devastating killing by hypochlorite stress which damage cellular proteins, nucleic acids, and biomolecules (da Cruz Nizer et al., 2020).

In conclusion, OfrA enhances the survivability of *S. aureus* in *in-vitro* exposure to electrophilic (MHQ and methylglyoxal), oxidative (H_2O_2), and hypochlorite (NaOCl) stress.

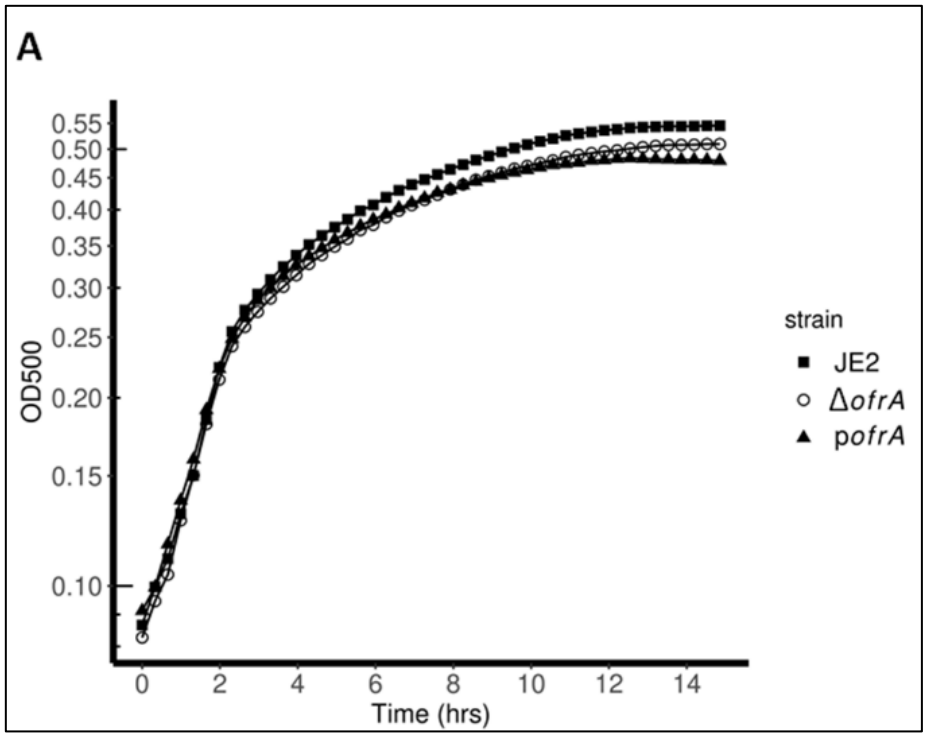
A
0.55
0.50
0.45
0.40
0.35
0.30
0.25
0.20
0.15
0.10
OD500
0
2
4
6
8
10
12
14
Time (hrs)
strain
JE2
ΔofrA
pofrA

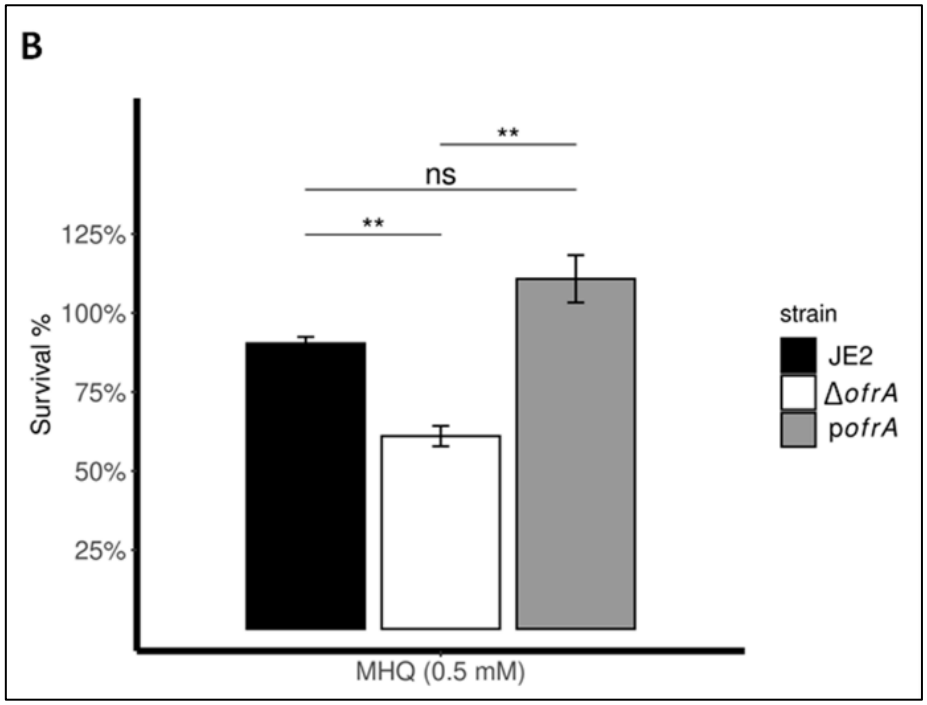
B
**
ns
**
125%
100%
75%
50%
25%
Survival %
MHQ (0.5 mM)
strain
JE2
ΔofrA
pofrA

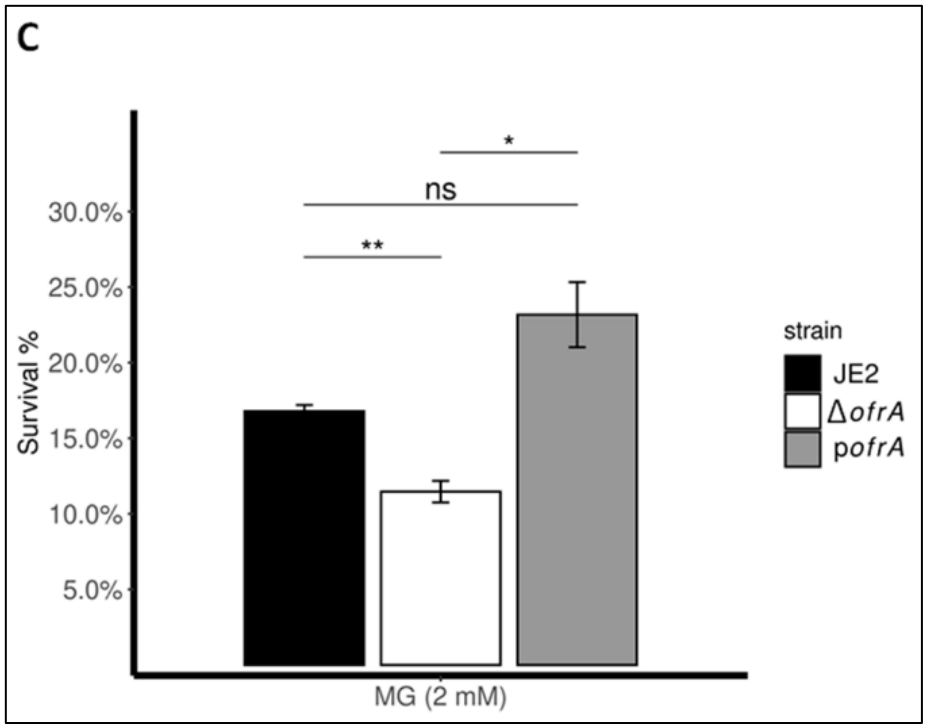
C
*
ns
**
30.0%
25.0%
20.0%
15.0%
10.0%
5.0%
Survival %
strain
JE2
ΔofrA
pofrA
MG (2 mM)

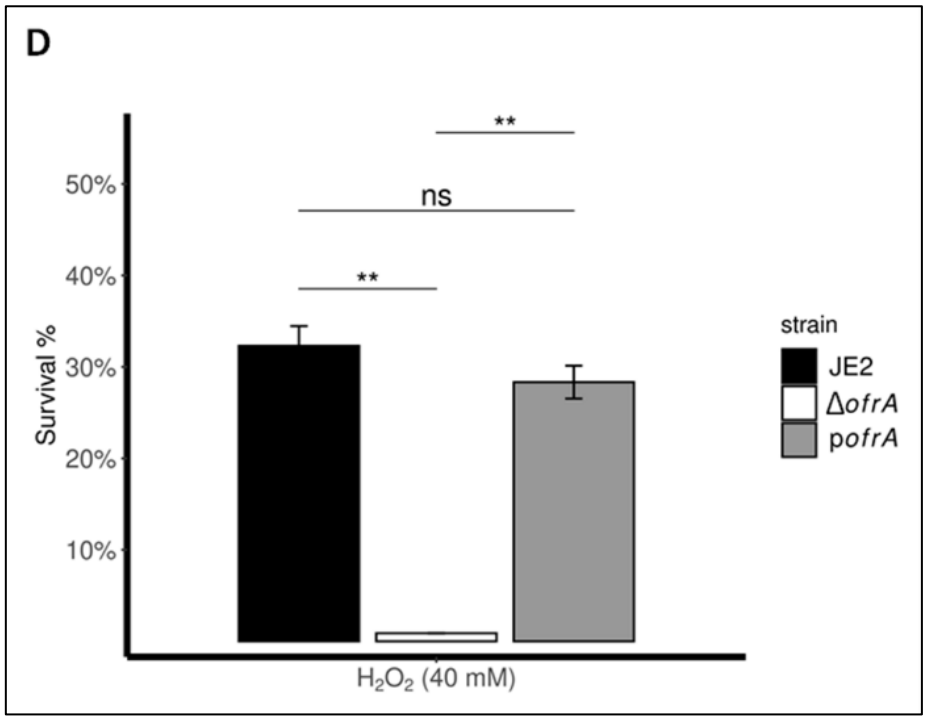
D
**
ns
**
50%
40%
30%
20%
10%
Survival %
strain
JE2
ΔofrA
pofrA
H2O2 (40 mM)

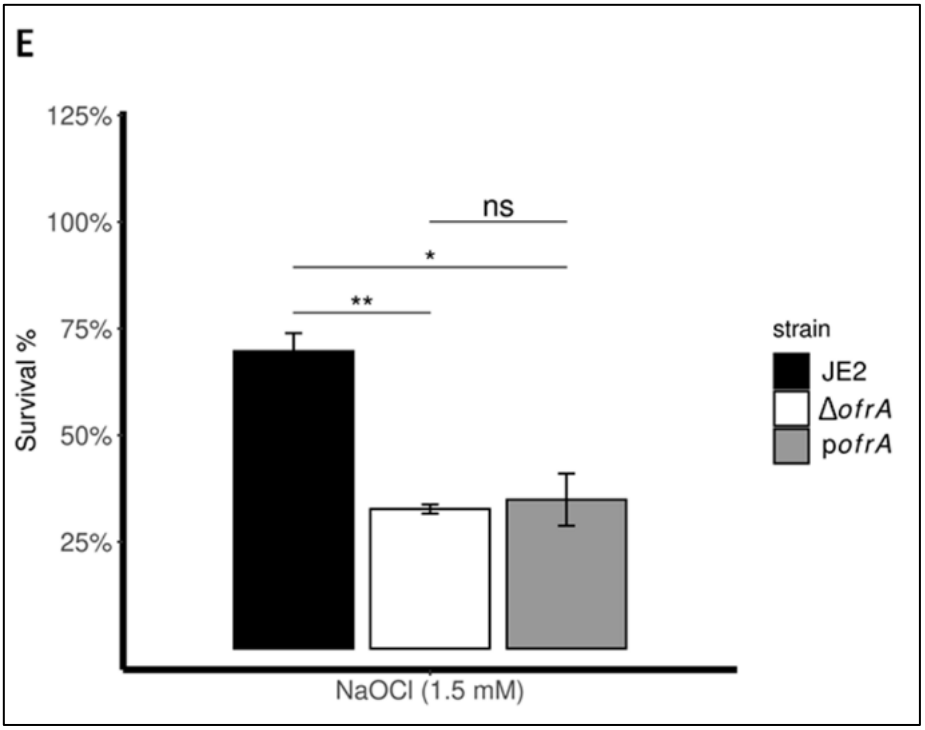

Figure 5 | OfrA protects *S. aureus* from quinone, toxic aldehyde, oxidative, and hypochlorite stresses. **(A)** Growth of unstressed logarithmic phase cells from *S. aureus* JE2, Δ*ofrA*, and p*ofrA* in RPMI at 37°C, measured with OD_{500} in microtiter plate reader, shows similar growth kinetics to be used in survival assays. Data represents average of three biological replicates. Survival analysis of *S. aureus* JE2, Δ*ofrA*, and p*ofrA*. Bacteria were allowed to grow in RPMI until logarithmic phase. Bacterial cells were collected with centrifugation then washed with sterile 1 x PBS and OD600 was adjusted to be 0.4 for each strain with fresh RPMI. Stressors were added as follows: **(B)** 0.5 mM MHQ for three hours, **(C)** 2 mM MG for three hours, **(D)** 40 mM H_2O_2 for one hour, or **(E)** 1.5 mM NaOCl for 30 minutes. Viable bacterial cells were assessed from the unstressed control (for normalization) or the stressed cultures with CFU determination on LB-agar. Four-five biological replicates were used for *in-vitro* survival analysis. Error bars represent the standard error of the means. Statistical analysis was carried out using one-way ANOVA and pairwise *t*-test with Bonferroni *p*-value adjustment; ns, not significant; $*p < 0.05$; $**p < 0.01$. H_2O_2, hydrogen peroxide; MG, methylglyoxal; MHQ, methylhydroquinone; NaOCl, sodium hypochlorite.

4.8 OfrA promotes *S. aureus* survival in RAW 264.7 macrophages and whole human blood

Inside macrophages, *S. aureus* has to cope the host-derived reactive electrophilic, oxygen, and chlorine species (Moldovan and Fraunholz, 2019). *S. aureus* USA300 LAC is capable of replication in RAW 264.7 murine macrophage cell line indicating the ability to overcome produced reactive species (Flannagan et al., 2018).

Since OfrA was proven an important staphylococcal factor for *in-vitro* survival in these conditions (**Figure 5**), the hypothesis was developed that *ofrA* mutation could affect *S. aureus* fitness in macrophages. Macrophage survival assays were conducted

and the survived bacteria were normalized to the viable intra-macrophages bacteria at four-hour post infection (p.i.) (**Figure 6A**). Indeed, at 24-hour p.i., *S. aureus* JE2, Δ*ofrA*, and p*ofrA* are able to replicate in RAW macrophages with statistical significance only noticed between Δ*ofrA* and p*ofrA* strains (**Figure 6B**). At 48-hour p.i., 50% difference between the normalized intra-macrophages viable JE2 and Δ*ofrA* was detected (**Figure 6B**). Likewise, p*ofrA* showed enhanced survival compared to the Δ*ofrA* (**Figure 6B**).

S. aureus survival in human blood determines a wide range of clinical outcomes, including the lethal bacteraemia. In human blood, *S. aureus* had to cope with many stress conditions including the neutrophils-derived reactive oxygen and chlorine species. Therefore, *S. aureus* JE2, Δ*ofrA*, and p*ofrA* survival was determined in the whole human blood. Whole human blood killing assay was optimized by Jessica Brock based on (van der Maten et al., 2017). Survival analysis in whole human blood, from multiple donors, for 60 minutes showed that JE2 strain survived 65% compared to only 23% in case of Δ*ofrA* (**Figure 6C**). Genetic complementation, in p*ofrA* strain, resulted in phenocopying the WT (**Figure 6C**).

Altogether, OfrA was concluded to be a factor enhancing *S. aureus* survivability inside RAW macrophages and in whole human blood. Therefore, I was interested to understand the mechanism by which Δ*ofrA* has a defective survival against the reactive species.

4.9 Whole transcriptomic analysis of JE2 and Δ*ofrA* indicates deregulation in redox- and stress-related genes

To know which mechanisms are affected by *ofrA* deletion from *S. aureus*, a transcriptomic approach was taken to compare Δ*ofrA vs* JE2 transcriptome in RPMI medium at mid-logarthmic phase (OD_{600} = 0.5). The analysis of the RNA sequencing results showed that there are 188 deregulated genes (**Figure 7A**). 93 genes were downregulated in Δ*ofrA* compared to the WT JE2 strain (**Figure 7B and Table 22**). On the other hands, 95 genes were upregulated in Δ*ofrA* compared to the WT JE2 strain (**Figure 7C and Table 23**). Some redox-related genes were deregulated such as (SAUSA300_0339, SAUSA300_0340, SAUSA300_0212, SAUSA300_0213, *ypdA*, and *cymR*. Furthermore, some stress-related genes were deregulated such as (*csbD*, *clpB*, *sigB*, and *rbsW*). Such a transcriptomic signature indicates unbalanced redox status which then results in deregulated level of stress in *S. aureus*.

Gene set enrichment analysis (GSEA) was conducted using the statistically significant deregulated genes. Two enriched gene sets are transcriptionally affected by *ofrA* mutation in *S. aureus* under normal conditions in RPMI medium: 1) one carbon pool metabolism and 2) carotenoid biosynthesis (**Table 24**).

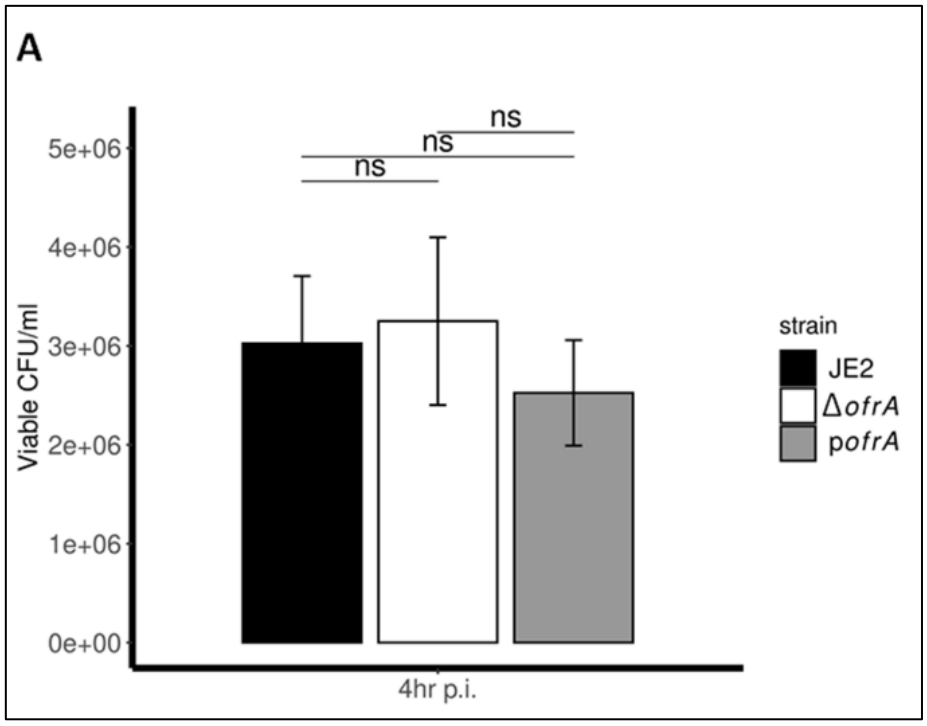
A
ns
ns
ns
5e+06
4e+06
3e+06
2e+06
1e+06
0e+00
Viable CFU/ml
4hr p.i.
strain
JE2
ΔofrA
pofrA

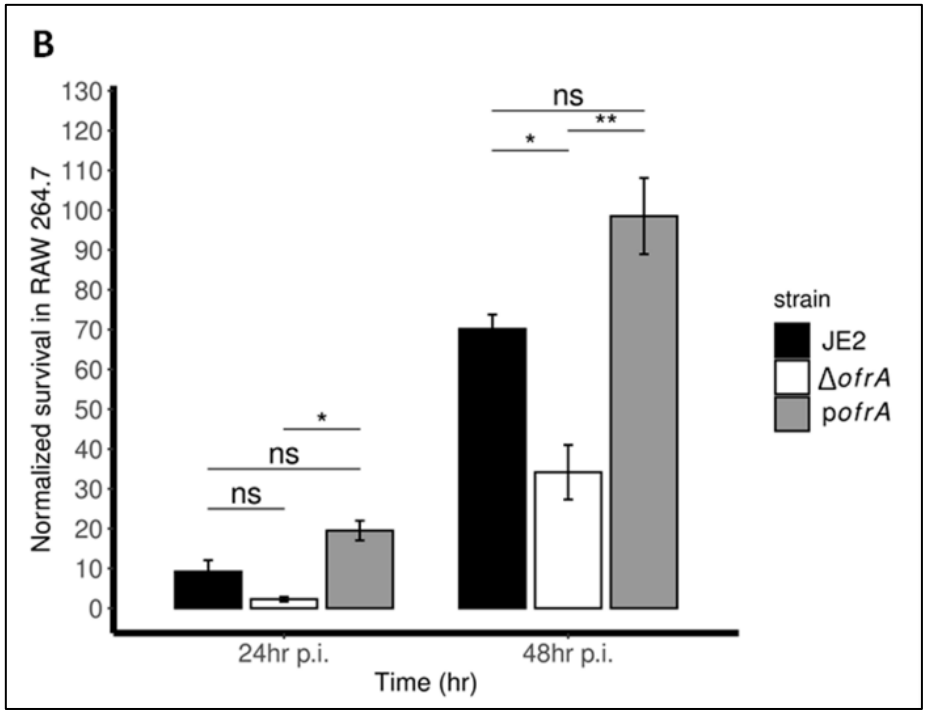
B
ns
**
*
*
ns
ns
130
120
110
100
90
80
70
60
50
40
30
20
10
0
Normalized survival in RAW 264.7
24hr p.i.
48hr p.i.
Time (hr)
strain
JE2
ΔofrA
pofrA

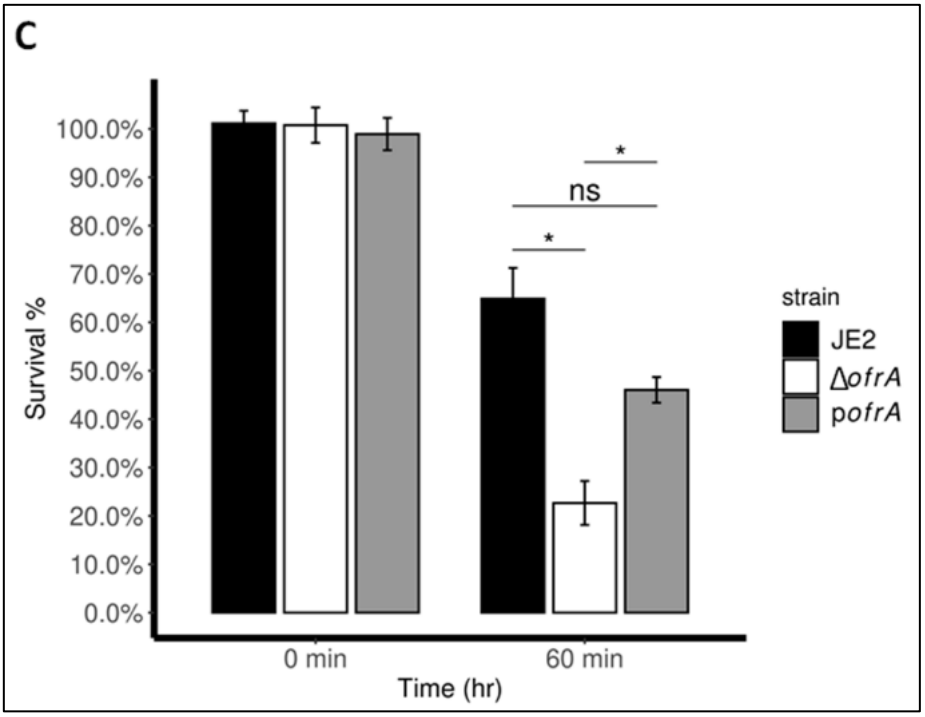

Figure 6 | OfrA enhances *S. aureus* fitness at the host-pathogen interface. **(A, B)** Macrophage survival assays show defective replication of Δ*ofrA* compared to JE2 and p*ofrA* in RAW 264.7 macrophage cell line at 48-hour post infection. Bacterial strains were added to RAW macrophages at 1:10 MOI in RPMI + 10% FCS for one hour. Extracellular bacteria were killed with addition of 150 µg/ml gentamicin for one hour. Fresh RPMI + 10% FCS was used to replace the old medium (*t* = 0). **(A)** At *t* = 4 hours, samples were taken for normalization of intracellular bacteria. Error bars indicate the standard deviation. **(B)** At *t* = 24 and 48 hours, samples were taken for viable intracellular bacterial CFU determination. Error bars indicate the standard error of the means. The whole assay was repeated three independent experiments. Here, I present data of five biological replicates from a representative experiment. **(C)** Whole human blood killing assays comparing the number of viable bacteria after exposure to whole human blood for 60 minutes. Data represent four biological replicates from a representative experiment out of four independent experiments performed by Jessica Brock. Error bars indicate the standard error of the means. Statistical analysis was carried out using one-way ANOVA and pairwise *t*-test with Bonferroni *p*-value adjustment; ns, not significant; *$p < 0.05$; **$p < 0.01$. hr, hour; p.i., post infection.

To validate the RNA-seq results, RT-qPCRs were performed for selected gene (*rocD*, *acuA*, and *crtM*). In agreement with RNA-seq analysis, RT-qPCRs validated the upregulation of *rocD*, and the downregulation of *acuA* and *crtM* (**Figure 7D**).

One carbon pool metabolism inhibition along with redox-related genes deregulation in Δ*ofrA* compared to JE2 indicate that there is unbalanced redox homeostasis. Moreover, downregulation of carotenoid biosynthesis indicates that there could be decreased staphyloxanthin (the carotenoid golden yellow pigment) production in Δ*ofrA* *vs* JE2. Staphyloxanthin (STX) is a staphylococcal virulence factor that enhance *S. aureus* survival in oxidative stress (Clauditz et al., 2006).

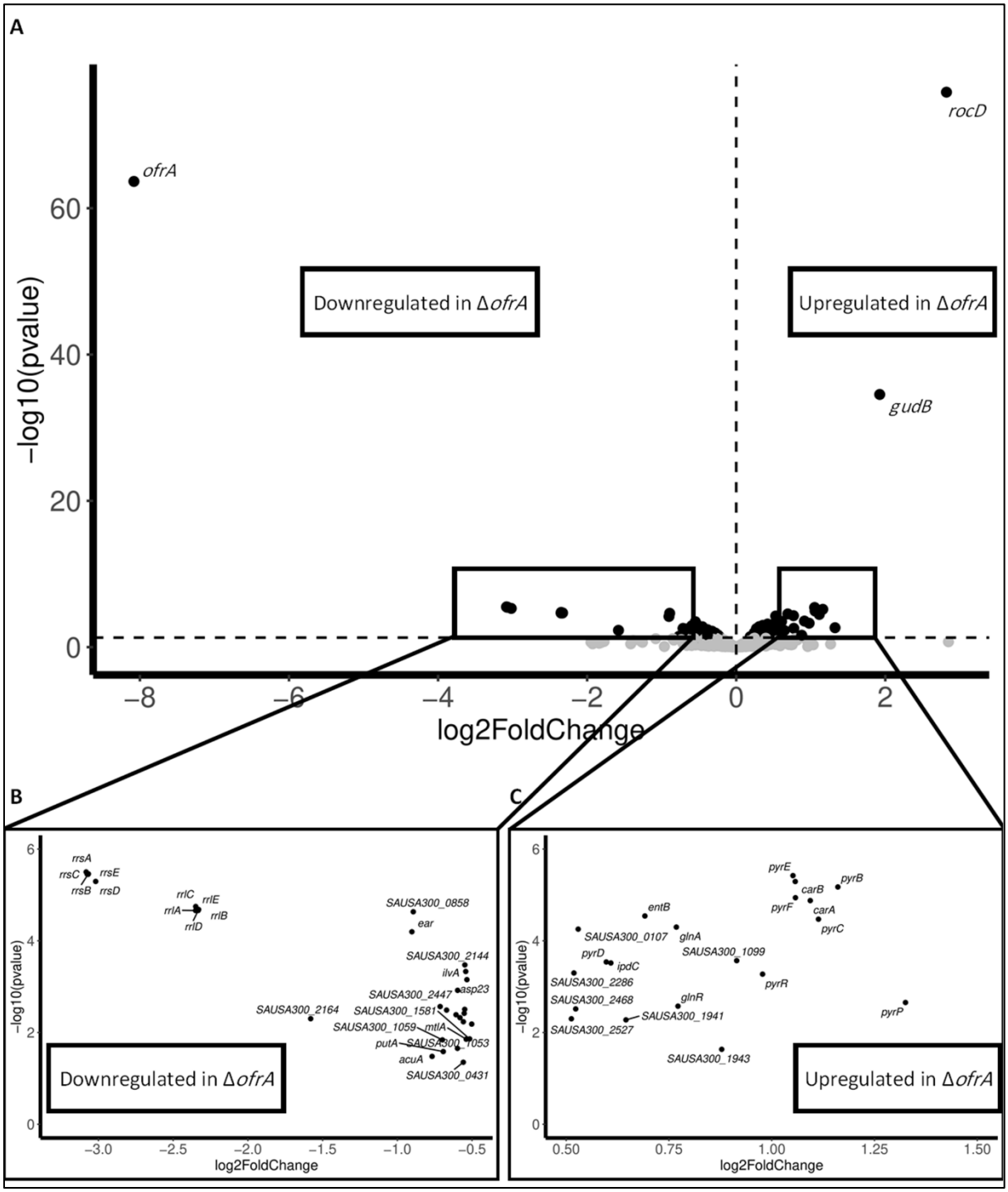
A
ofrA
rocD
gudB
Downregulated in ΔofrA
Upregulated in ΔofrA
−log10(pvalue)
log2FoldChange
B
C
rrsA
rrsC
rrsE
rrsB
rrsD
rrlC
rrlE
rrlA
rrlB
rrlD
SAUSA300_0858
ear
SAUSA300_2144
ilvA
asp23
SAUSA300_2447
SAUSA300_2164
SAUSA300_1581
SAUSA300_1059
mtlA
putA
SAUSA300_1053
acuA
SAUSA300_0431
pyrE
pyrB
carB
pyrF
carA
pyrC
entB
SAUSA300_0107
glnA
pyrD
SAUSA300_1099
ipdC
SAUSA300_2286
pyrR
SAUSA300_2468
glnR
SAUSA300_1941
pyrP
SAUSA300_2527
SAUSA300_1943

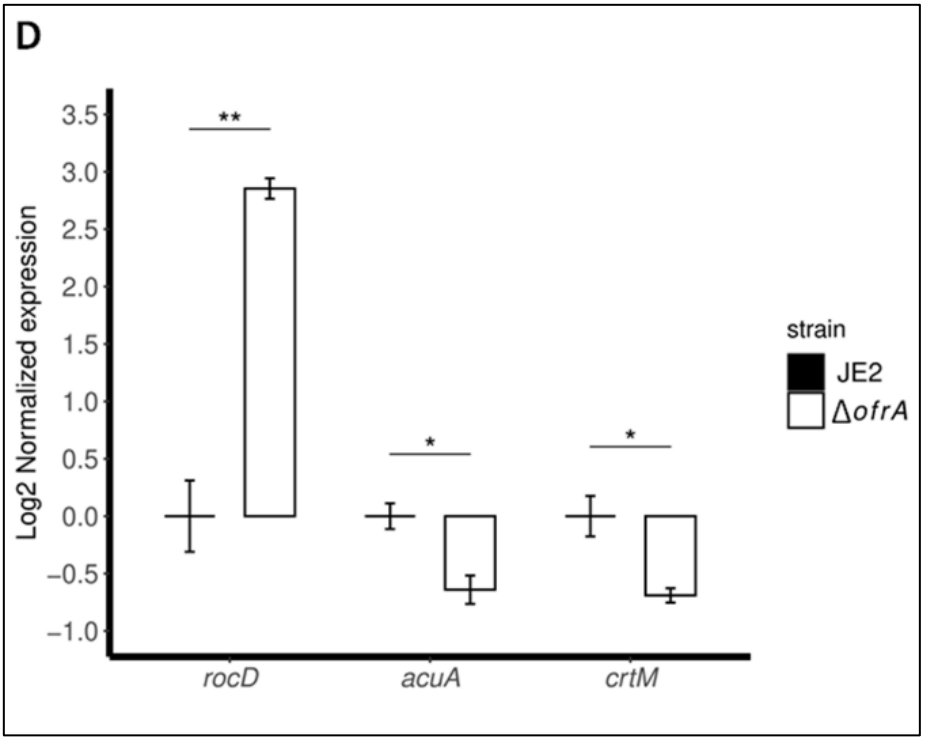

Figure 7 | Whole transcriptome analysis *via* RNA sequencing. **(A)** Differential gene expression comparing Δ*ofrA* vs JE2 transcriptome. Total RNA isolations were performed using RNeasy Mini Kit (Qiagen) from three biological replicates of JE2 and Δ*ofrA* that were grown in RPMI until mid-logarithmic phase (OD_{600} = 0.5) at 37°C with shaking. After DNase I digestion, rRNA depletion, cDNA library preparation, and next-generation sequencing, the trimmed reads were mapped to NC_007793.1 reference genome. Coverage calculations, gene quantification, and differential gene expression analysis were performed. The horizontal dashed line represents the statistical significance threshold *p*-value < 0.05 **(Table 22 and Table 23)**. Grey points act for statistically and biologically insignificant deregulation. Biologically and statistically significant **(B)** downregulated and **(C)** upregulated genes in Δ*ofrA* compared to JE2 strain are illustrated. **(D)** RT-qPCR assays of selected deregulated genes (*rocD*, *acuA*, and *crtM*) agree with the results of the RNA-seq analysis. Unpaired two-tailed Student's *t*-test was used for statistical significance inference; *$p < 0.05$; **$p < 0.01$.

Table 22: Downregulated genes in Δ*ofrA vs* JE2 with Log2FoldChange ≤ -0.5 and *P*-value < 0.05.

Locus	Gene	Description	Feature	Regulator	Log2FoldChange	*P*-value
SAUSA300_0859	*ofrA*	NADH-dependent flavin oxidoreductase	CDS		-8.080708	2.15E-64
SAUSA300_0455	*rrsA*	16S ribosomal RNA	rRNA		-3.081901	3.16E-06
SAUSA300_1841	*rrsD*	16S ribosomal RNA	rRNA		-3.075666	3.50E-06
SAUSA300_0499	*rrsB*	16S ribosomal RNA	rRNA		-3.068966	3.55E-06
SAUSA300_2124	*rrsF*	16S ribosomal RNA	rRNA		-3.066793	3.48E-06
SAUSA300_2017	*rrsE*	16S ribosomal RNA	rRNA		-3.018255	5.08E-06
SAUSA300_0456	*rrl1*	23S ribosomal RNA	rRNA		-2.349657	2.19E-05
SAUSA300_1838	*rrl3*	23S ribosomal RNA	rRNA		-2.348891	1.79E-05
SAUSA300_2123	*rrlF*	23S ribosomal RNA	rRNA		-2.335558	2.09E-05
SAUSA300_2016	*rrlE*	23S ribosomal RNA	rRNA		-2.332242	2.18E-05
SAUSA300_0501	*rrlB*	23S ribosomal RNA	rRNA		-2.329682	2.08E-05
SAUSA300_2164	-	hypothetical protein	CDS	SigB	-1.579792	5.00E-03

SAUSA300_0815	*ear*	Ear protein	CDS	SaeRS	-0.902575	6.36E-05
SAUSA300_0858	-	hypothetical protein	CDS		-0.893341	2.33E-05
SAUSA300_1680	*acuA*	acetoin utilization protein	CDS	CcpA	-0.767489	3.32E-02
SAUSA300_0372	-	hypothetical protein	CDS	SigB	-0.713585	2.71E-03
SAUSA300_1059	*ssl12*	superantigen-like protein	CDS		-0.698406	1.45E-02
SAUSA300_1711	*putA*	proline dehydrogenase	CDS	CcpA	-0.692700	2.60E-02
SAUSA300_2499	*crtM*	squalene desaturase	CDS	SigB	-0.670453	3.25E-03
SAUSA300_0221	*pflA*	pyruvate formate-lyase activating enzyme	CDS	Rex	-0.607220	4.10E-03
SAUSA300_1053	*flr*	formyl peptide receptor-like 1 inhibitory protein	CDS	MgrA	-0.597587	2.22E-02
SAUSA300_2447	-	hypothetical protein	CDS	SigB	-0.596698	1.20E-03
SAUSA300_2500	*crtQ*	glycosyl transferase	CDS	SigB	-0.580864	4.74E-03
SAUSA300_0431	-	hypothetical protein	CDS		-0.558496	4.45E-02
SAUSA300_2501	*crtP*	phytoene dehydrogenase	CDS	SigB	-0.558134	5.83E-03
SAUSA300_0340	-	NADH-dependent FMN reductase	CDS	QsrR	-0.552657	3.82E-03
SAUSA300_2106	*mtlR*	putative transcriptional regulator	CDS	MtlR	-0.549376	3.13E-03
SAUSA300_2144	*amaP*	hypothetical protein	CDS	SigB	-0.548346	3.36E-04
SAUSA300_1330	*ilvA1*	threonine dehydratase	CDS	CodY	-0.542518	4.67E-04
SAUSA300_2107	*mtlA*	PTS system, mannitol specific IIA component	CDS	MtlR	-0.539293	1.40E-02
SAUSA300_2142	*asp23*	alkaline shock protein 23	CDS	SigB	-0.534359	7.04E-04
SAUSA300_1581	-	hypothetical protein	CDS	SigB	-0.516195	1.38E-02
SAUSA300_0170	*aldA*	aldehyde dehydrogenase	CDS	CcpA	-0.502329	6.55E-03

Table 23: Upregulated genes in Δ*ofrA vs* JE2 with Log2FoldChange ≥ 0.5 and *P*-value < 0.05.

Locus	Gene	Description	Feature	Regulator	Log2FoldChange	*P*-value
SAUSA300_0860	*rocD*	ornithine--oxo-acid transaminase	CDS	CcpA	2.820476	1.35E-76
SAUSA300_0861	*gudB*	NAD-specific glutamate dehydrogenase	CDS	CcpA	1.924808	2.87E-35
SAUSA300_1092	*pyrP*	uracil permease	CDS	PyrR	1.325441	2.22E-03
SAUSA300_1093	*pyrB*	aspartate carbamoyltransferase catalytic subunit	CDS	PyrR	1.160946	6.71E-06
SAUSA300_1094	*pyrC*	dihydroorotase	CDS	PyrR	1.113761	3.38E-05
SAUSA300_1095	*carA*	carbamoyl phosphate synthase small subunit	CDS	PyrR	1.093776	1.33E-05
SAUSA300_1097	*pyrF*	orotidine 5'-phosphate decarboxylase	CDS	PyrR	1.057736	1.15E-05
SAUSA300_1096	*carB*	carbamoyl phosphate synthase large subunit	CDS	PyrR	1.057255	5.10E-06
SAUSA300_1098	*pyrE*	orotate phosphoribosyltransferase	CDS	PyrR	1.051715	3.79E-06
SAUSA300_1091	*pyrR*	bifunctional pyrimidine regulatory protein PyrR uracil phosphoribosyltransferase	CDS	TraP	0.977715	5.34E-04
SAUSA300_1099	-	hypothetical protein	CDS	PyrR	0.914792	2.71E-04
SAUSA300_1943	-	phi77 ORF040-like protein	CDS		0.878326	2.33E-02

SAUSA300_1200	*glnR*	glutamine synthetase repressor	CDS	GlnR	0.771931	2.66E-03
SAUSA300_1201	*glnA*	glutamine synthetase, type I	CDS	GlnR	0.767979	5.03E-05
SAUSA300_0189	-	isochorismatase	CDS		0.691455	2.88E-05
SAUSA300_1941	-	phi77 ORF003-like protein, phage terminase, large subunit	CDS		0.645374	5.30E-03
SAUSA300_0190	-	indole-3-pyruvate decarboxylase	CDS	CcpA	0.608584	3.05E-04
SAUSA300_2526	*pyrD*	dihydroorotate dehydrogenase 2	CDS		0.597480	2.89E-04
SAUSA300_0107	*nptA*	Na/Pi cotransporter family protein	CDS	GraRS	0.529171	5.57E-05
SAUSA300_2468	-	acetyltransferase	CDS		0.523080	3.06E-03
SAUSA300_2286	-	hypothetical protein	CDS		0.518715	5.04E-04
SAUSA300_2527	-	hypothetical protein	CDS		0.512625	5.02E-03

Table 24: Gene set enrichment analysis (GSEA) in Δ*ofrA vs* JE2.

Locus	Gene	Description	Enriched gene set	Log2FoldChange	*P*-value
SAUSA300_0358	*metF*	bifunctional homocysteine S-methyltransferase/5,10-methylenetetrahydrofolate reductase protein	One carbon pool by folate	-0.395075	3.40E-02
SAUSA300_0974	*purN*	phosphoribosylglycinamide formyltransferase		-0.378502	7.98E-03
SAUSA300_0975	*purH*	bifunctional phosphoribosylaminoimidazolecarboxamide formyltransferase/IMP cyclohydrolase		-0.386208	4.08E-03
SAUSA300_1678	*fhs*	formate--tetrahydrofolate ligase		-0.384792	1.61E-02
SAUSA300_2498	*crtN*	squalene synthase	Carotenoid biosynthesis	-0.463055	3.73E-03
SAUSA300_2499	*crtM*	squalene desaturase		-0.670453	3.25E-03
SAUSA300_2500	*crtQ*	glycosyl transferase		-0.580864	4.74E-03
SAUSA300_2501	*crtP*	phytoene dehydrogenase		-0.558134	5.83E-03

4.10 Supressed staphyloxanthin production in Δ*ofrA vs* JE2 *via* the upper mevalonate pathway

To test whether the STX production is supressed in Δ*ofrA vs* JE2, the stationary phase STX was quantified in *S. aureus* JE2, Δ*ofrA*, and p*ofrA*. The produced STX in Δ*ofrA* is 30% less than the produced in JE2 (**Figure 8A**). p*ofrA* produced STX more than both JE2 and Δ*ofrA*. Therefore, STX production is decreased in *ofrA* mutation.

In order to produce STX, *S. aureus* uses the available acetyl CoA, from cellular metabolism, to fuel the classical mevalonate pathway (MVA) which produces farnesyl pyrophosphate (FPP) (Reichert et al., 2018). FPP is then used to produce STX *via crtOPQMN* pathway (Pelz et al., 2005).

To test whether *ofrA* mutation affects STX production by changing the intracellular concentration of acetyl CoA, 0.5% glucose was supplemented to B-medium (growth medium

free from glycolytic substrates). When glucose is supplemented in the medium, the acetyl CoA is initially increased in *S. aureus*. The accumulated acetyl CoA is then secreted into the medium as acetate. Overall, the acetyl CoA levels decrease in case of glucose supplementation which than will decrease STX production (Tiwari et al., 2018a).

Addition of glucose results in the expected decrease in STX production from JE2 (**Figure 8B**). Moreover, a similar reduction is also seen from Δ*ofrA* (**Figure 8B**). Therefore, *ofrA* mutation does not affect STX production *via* changing the intracellular acetyl CoA concentration.

If *ofrA* has a role in STX production *via* the mevalonate pathway, then supplementing the metabolite in the medium should quench the *ofrA*-mediated phenotype. The classical mevalonate pathway can be divided into the upper (*mvaS* and *mvaA*) and the lower (*mvaK1*, *mvaK2*, and *mvaD*) pathways (Reichert et al., 2018). The output of the upper mevalonate is the mevalonate itself. When mevalonate was supplemented to the growth medium, the *ofrA*-mediated phenotype is quenched and the STX productions from JE2 and Δ*ofrA* are similar (**Figure 8C**).

In summary, *S. aureus*Δ*ofrA* has decreased STX production due to decreased activity of the upper mevalonate pathway.

4.11 Supressed staphyloxanthin cannot solely explain H_2O_2 hypersensitivity in *S. aureus*Δ*ofrA*

Since I was interested in understanding the mechanism by which Δ*ofrA* strain is more sensitive against H_2O_2 than JE2, decreased STX production in Δ*ofrA* could explain this hypersensitivity. To test the aforementioned hypothesis, *crtM* was deleted from both JE2 and Δ*ofrA* strains to abolish the STX biosynthesis (Clauditz et al., 2006).

After exposing 40 mM H_2O_2 to JE2, JE2Δ*ofrA*, JE2Δ*crtM* and JE2Δ*ofrA*Δ*crtM*, I observed a survival defect of JE2Δ*ofrA* and JE2Δ*crtM* as expected (**Figure 8D**). However, contrary to the tested hypothesis, JE2Δ*ofrA*Δ*crtM* is more sensitive to H_2O_2 stress compared to Δ*ofrA* or Δ*crtM* alone (**Figure 8D**). Furthermore, survival analysis of these four strains against 30 mM H_2O_2 confirmed the additive effect of the double deletion (**Figure 8E**). Therefore, *ofrA* and *crtM* are important staphylococcal defence factors against H_2O_2 but independently affect this phenotype. Thus, decreased STX production does not solely explain the H_2O_2 hypersensitivity of Δ*ofrA*.

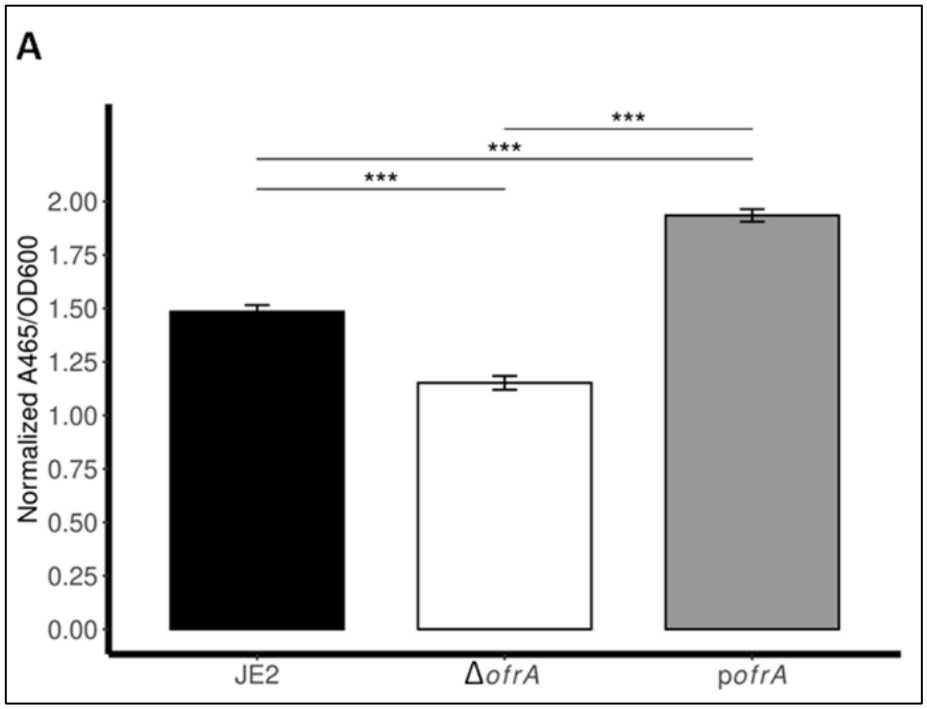
A
***
***
***
Normalized A465/OD600
2.00
1.75
1.50
1.25
1.00
0.75
0.50
0.25
0.00
JE2
ΔofrA
pofrA

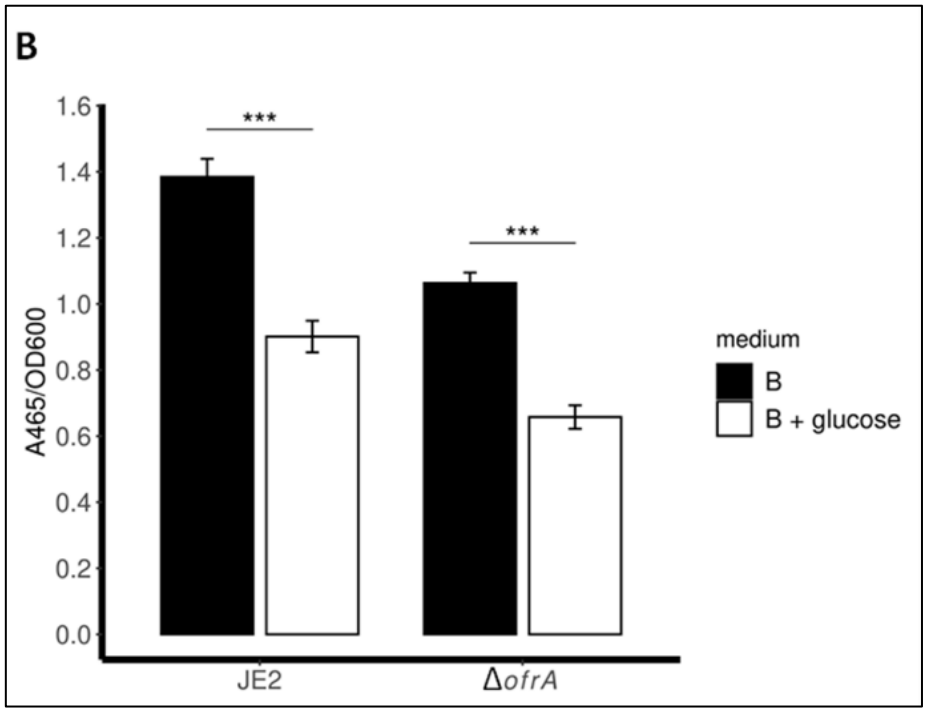
B
***
***
A465/OD600
1.6
1.4
1.2
1.0
0.8
0.6
0.4
0.2
0.0
JE2
ΔofrA
medium
B
B + glucose

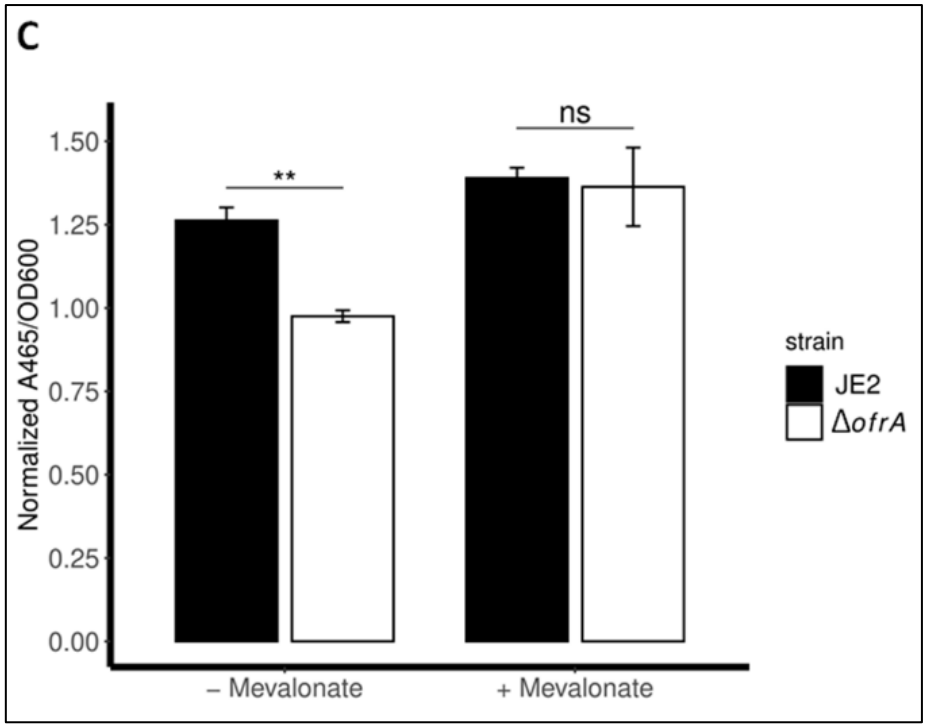
C
ns
**
1.50
1.25
1.00
0.75
0.50
0.25
0.00
Normalized A465/OD600
strain
JE2
ΔofrA
– Mevalonate
+ Mevalonate

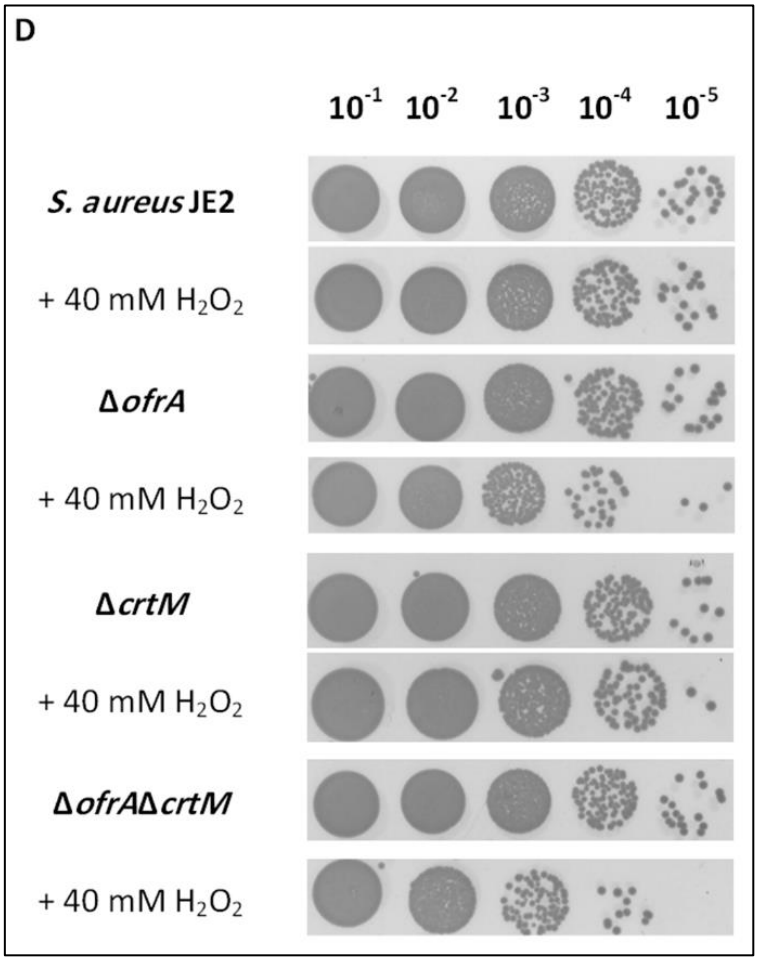
D
10-1 10-2 10-3 10-4 10-5
S. aureus JE2
+ 40 mM H2O2
ΔofrA
+ 40 mM H2O2
ΔcrtM
+ 40 mM H2O2
ΔofrAΔcrtM
+ 40 mM H2O2

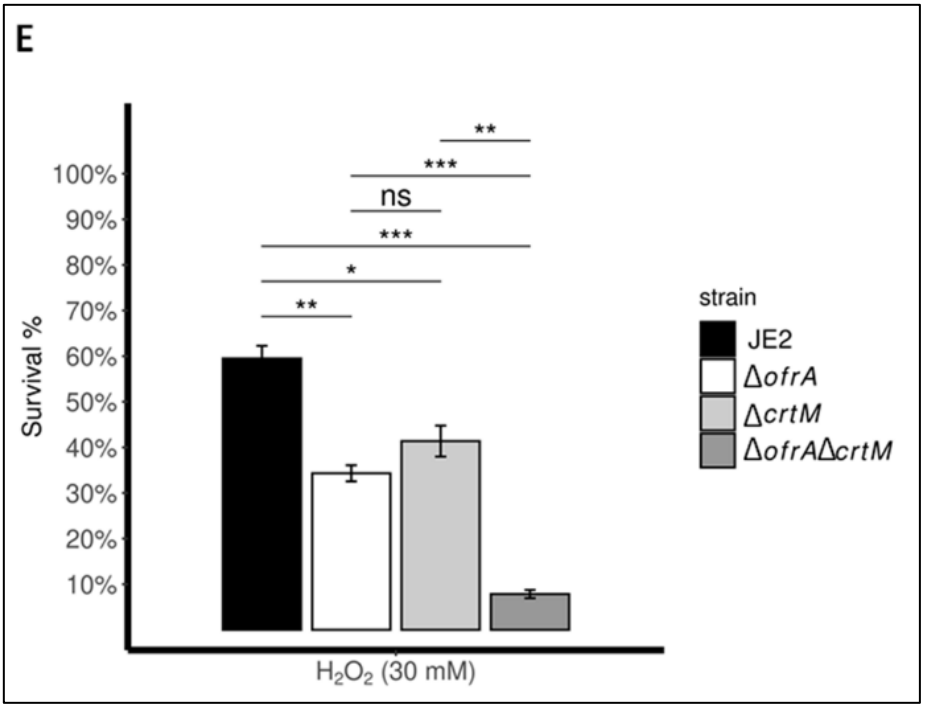

Figure 8 | Δ*ofrA* produces less STX than JE2. STX assay comparing the produced STX in TSB **(A)**, B-medium **(B)**, and RPMI **(C)**. Strains (JE2, Δ*ofrA*, and p*ofrA*) were allowed to grow in the respective medium without supplementation **(A-C)**, with 0.5% glucose **(B)**, or with 1 mM mevalonate **(C)**. After 24 hours of growth in 37°C with shaking, the bacterial pellets from 2-ml cultures were washed with sterilized water. OD_{600} was recorded for normalization. STX was extracted with methanol. A_{465} was used to quantify STX in the methanolic extract. **(D, E)** Bacterial survival analysis shows that *ofrA*-dependent H_2O_2 hypersensitivity phenotype is independent on *crtM*. JE2, Δ*ofrA*, Δ*crtM*, and Δ*ofrA*Δ*crtM* strains were grown in RPMI medium until mid-logarithmic phase. After washing the bacterial cells with sterile 1 x PBS, OD_{600} were adjusted to 0.4 with RPMI. Bacteria were challenged with 40 mM H_2O_2 **(D)** or as 30 mM H_2O_2 **(E)** for one hour. Viable cells were diluted in PBS after catalase treatment for removing residual H_2O_2. **(D)** 10 µl was spotted from different dilutions on LB agar. The shown data is a representative of two independent experiments. **(E)** Samples were taken from the unstressed controls (for normalization) or from the stressed cultures for CFU determination. Error bars represent the standard error of the means **(A, C, E)** or the standard deviation **(B)** of four biological replicates. Statistical analysis was carried out using one-way ANOVA and pairwise *t*-test with Bonferroni *p*-value adjustment **(A, E)** or unpaired two-tailed Student's *t*-test **(B, C)**; ns, not significant; *$p < 0.05$; **$p < 0.01$; ***$p < 0.001$. H_2O_2, hydrogen peroxide; STX, staphyloxanthin.

4.12 *ofrA* mutation does not result in increased production of reactive oxygen species

If decreased STX production cannot explain the H_2O_2 hypersensitivity phenotype in Δ*ofrA*, the next possibility is that Δ*ofrA* has increased production of reactive oxygen species. From the results of RNA-seq experiment, no deregulation could be detected in *sodA*, *sodM*, *katA*, peroxidases, or *hmp*. The aforementioned genes are upregulated in increased intracellular concentrations of superoxide anion and H_2O_2.

However, physiological concentration of H_2O_2 could result in more toxicities in case of increased intracellular iron concentration due to more generation of the lethal hydroxyl radical *via* Fenton reaction (Wang and Zhao, 2009). From RNA-seq analysis, iron homeostasis genes are not deregulated. In addition, growth inhibition experiment of both JE2 and Δ*ofrA* in different concentrations of streptonigrin, which requires intracellular iron for its antimicrobial activities (White and Yeowell, 1982; Duggan et al., 2020), suggests that intracellular levels of iron in both strains are similar (**Figure 9A-D**).

Altogether, the developed hypothesis is that H_2O_2 hypersensitivity phenotype in Δ*ofrA* is independent of increased levels of reactive oxygen species. To further validate this hypothesis, a survival analysis experiment was conducted comparing the survival of JE2 and Δ*ofrA* in presence of 40 mM H_2O_2 with or without 120 mM thiourea. Thiourea is quenching agent against reactive oxygen species, especially the highly toxic hydroxyl radical (Wasil et al., 1987). Indeed, 40 mM H_2O_2 causes more killing in Δ*ofrA* compared to JE2 (**Figure 9E**). As expected, 120 mM thiourea quenched the lethality of H_2O_2 against JE2 (**Figure 9E**). However, thiourea is able to quench H_2O_2 lethality against Δ*ofrA* up to similar level of JE2 (**Figure 9E**). The precedent results show that H_2O_2 hypersensitivity phenotype in Δ*ofrA* is independent of hydroxyl radical lethality.

4.13 *ofrA* supports thiol-dependent redox homeostasis in *S. aureus*

The only plausible explanation of the *ofrA*-mediated H_2O_2 hypersensitivity phenotype is that *ofrA* mutation results in compromised thiol-dependent redox homeostasis. To test this hypothesis, the survival of both JE2 and Δ*ofrA* in presence of 0.5 mM MHQ was analysed.

MHQ can act as an electrophile and as an oxidant (Fritsch et al., 2019). Therefore, 120 mM of thiourea was used to quench the oxidative-mediated MHQ toxicity *via* the secondarily produced reactive oxygen species. Addition of thiourea in MHQ survival assay protects neither JE2 nor Δ*ofrA* from MHQ toxicity under the experimental conditions (**Figure 10A**). This indicates that MHQ kills *S. aureus* through the electrophilic stress.

N-acetyl cysteine (NAC) can quench both the reactive oxygen and electrophilic species *via* enhancing the thiol-dependent redox homeostasis and repair (Pedre et al., 2021). Interestingly, when 1.25 mM NAC was added to the MHQ survival assay, it was able to quench the *ofrA*-mediated survival defect phenotype (**Figure 10B**). Therefore, OfrA enhances *S. aureus* survival *via* supporting the thiol-dependent redox homeostasis which

actively protects *S. aureus* against a wide range of reactive species including reactive oxygen, chlorine, and electrophilic species.

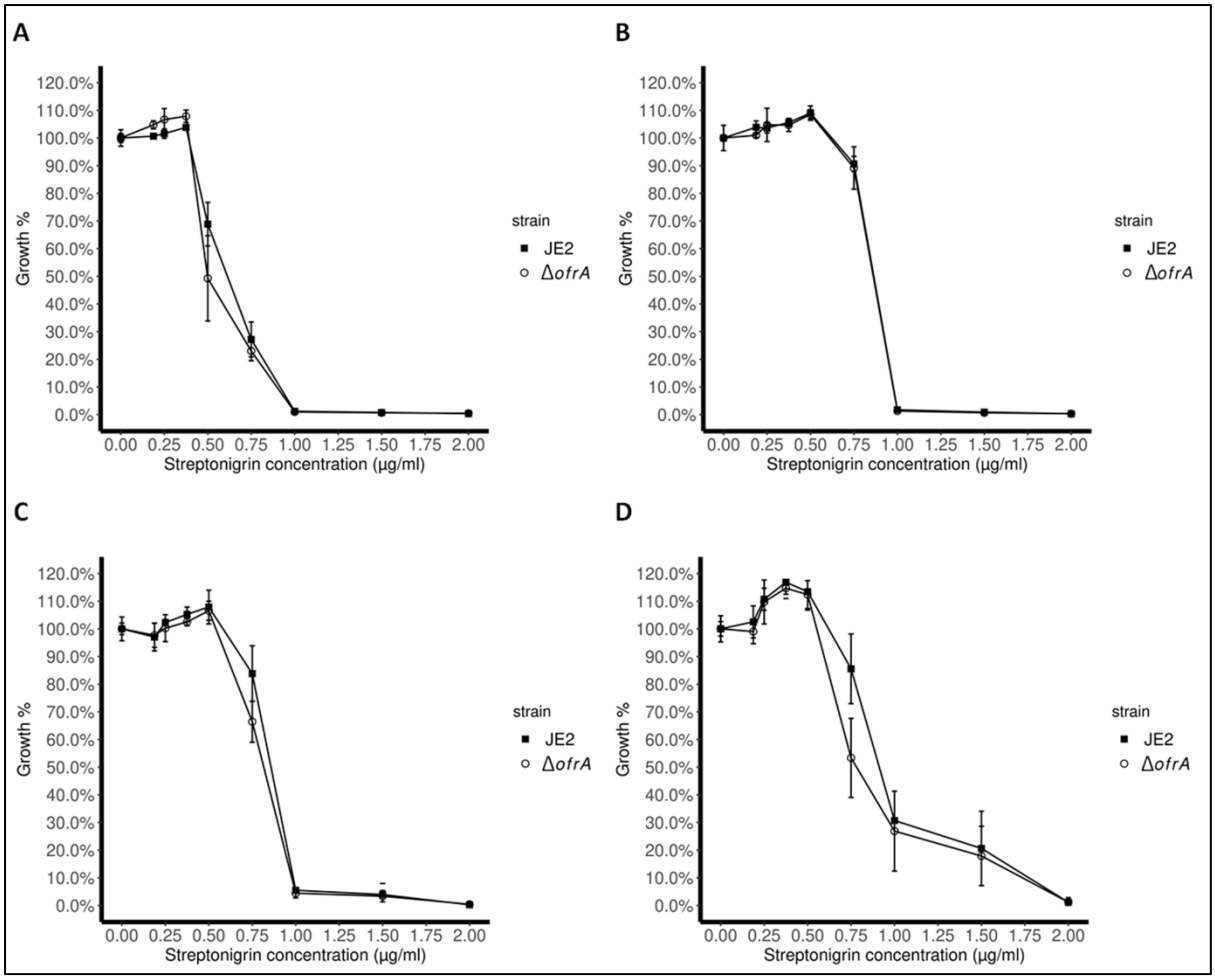

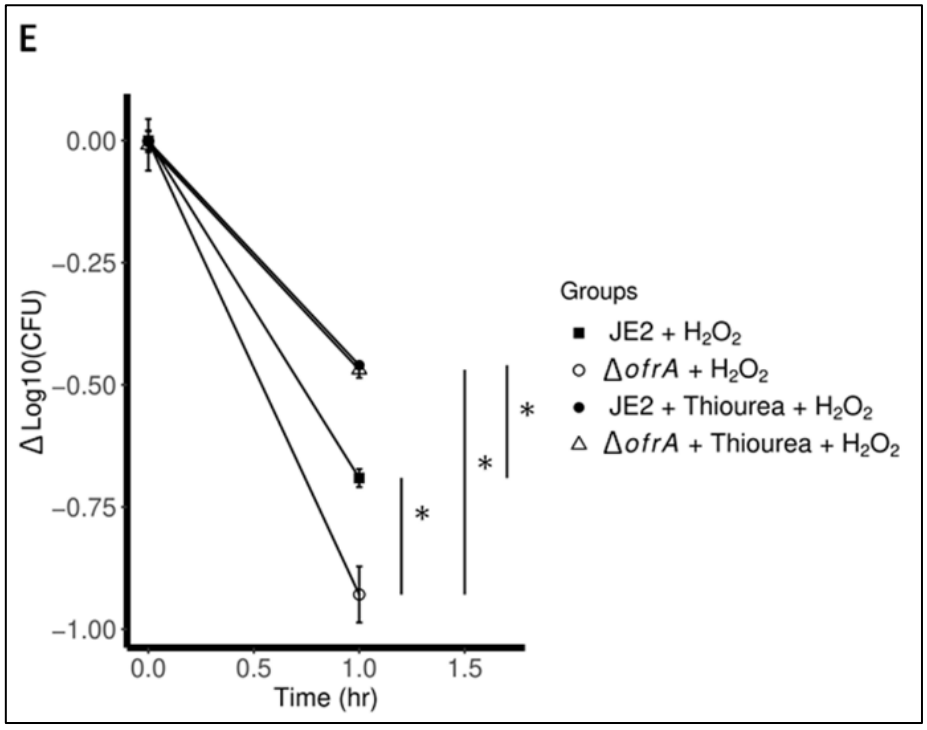

Figure 9 | JE2 and Δ*ofrA* have comparable levels of reactive oxygen species. **(A-D)** Growth inhibition assay shows insignificant difference between JE2 and Δ*ofrA*

in different concentrations of streptonigrin (related to intracellular iron levels) after 8 hr **(A)**, 12 hr **(B)**, 16 hr **(C)**, and 20 hr **(D)**. Data represent three biological replicates. Error bars represent the standard deviation. **(E)** Bacterial survival analysis in 40 mM H_2O_2 with or without 120 mM thiourea. Bacteria were allowed to grow to logarithmic phase, washed with sterilized 1 x PBS, and adjusted to OD_{600} = 0.4. Samples were taken for viability analysis before and after one hour exposure to 40 mM H_2O_2 ± 120 mM thiourea. Survived bacteria were normalized to the viable cells before stress. Error bars represent the standard error of the means of four biological replicates. Statistical analysis was carried out using one-way ANOVA and pairwise *t*-test with Bonferroni *p*-value; **p* < 0.05.

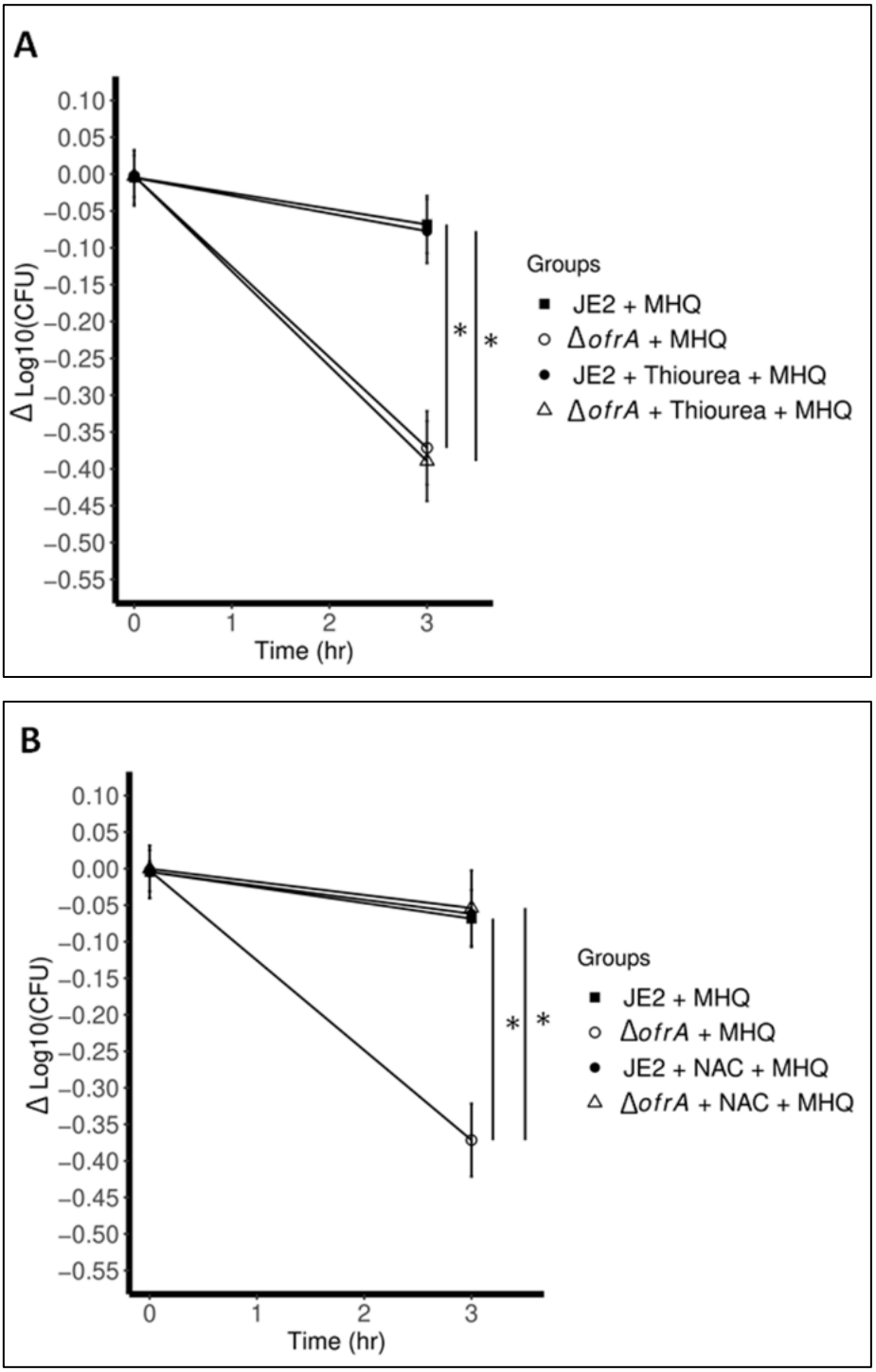

Figure 10 | OfrA supports the thiol-dependent redox homeostasis in *S. aureus*. **(A, B)** Bacterial survival analysis in 0.5 mM MHQ with or without 120 mM thiourea **(A)**

or 1.25 mM NAC **(B)**. Bacteria were allowed to grow to logarithmic phase, washed with sterilized 1 x PBS, and adjusted to OD_{600} = 0.4. Samples were taken for viability analysis before and after three-hour exposure to 0.5 mM MHQ ± 120 mM thiourea **(A)** or 0.5 mM MHQ ± 1.5 mM NAC **(B)**. Survived bacteria were normalized to the viable cells before stress. Error bars represent the standard error of the means of four biological replicates. Statistical analysis was carried out using one-way ANOVA and pairwise *t*-test with Bonferroni *p*-value; *$p < 0.05$. MHQ, methylhydroquinone; NAC, *N*-acetyl cysteine.

4.14 *ofrA* mRNA is independently transcribed from a SigA-dependent promoter

In *S. aureus*, transcription initiation, mediated *via* RNA polymerase, is either solely or in combination dependent on SigA, SigB, SigS, or SigH (Deora and Misra, 1995; Wu et al., 1996; Morikawa et al., 2003; Shaw et al., 2008). Since SigB affects the transcriptional initiation of many stress-mediating factors in *S. aureus* (Tuchscherr et al., 2015) and that *ofrA* is induced in electrophilic, oxidative, and hypochlorite stress (**Figure 4**); I wondered whether *ofrA* promoter activity is SigB-dependent.

A *sigB*::*ermB* mutation was transduced into EI011 creating EI011Δ*sigB*::*ermB* by Laura Cecchino (Lorenz et al., 2008). Since SigB regulon is known to be induced in stationary phase cells, I compared *ofrA* promoter activity in EI011 and EI011Δ*sigB* in mid-logarithmic, late-logarithmic, early-stationary, and late-stationary phase. After 4, 8, 12, and 24 hours of growth, both EI011 and EI011Δ*sigB* show similar *ofrA* transcriptional level (**Figure 11A**). Thus, I concluded that *ofrA* transcription initiation is SigB-independent.

In order to investigate the exact structure of *ofrA* promoter, 5' RACE was used to map the location of the transcriptional start site. The results indicated that the transcriptional start site is 25 bp upstreatm to the start codon (**Figure 11B**). Motif analysis was used to predict a conserved DNA motif in the pre-*ofrA* region in staphylococci. Motif analysis and transcriptional start site indicated that the -35 element (TTGGAGAA) and the -10 element (TATAGT) in *ofrA* promoter are SigA-dependent promoter elements.

4.15 *ofrA* is repressed in the presence of glycolytic substrates

Since methylglyoxal is a glycolysis by-product (Lee and Park, 2017), I wondered whether *ofrA* transcription is induced by glucose supplementation. To overcome the potential interference of pH drop due to increased sugar catabolism, B-medium buffered with 50 mM HEPES at pH=7.5 was used whenever sugar was supplemented in the medium (Seidl et al., 2009). Contrary to the aforementioned hypothesis, P_{ofrA} activity is actually suppressed after 2 hours incubation with 5, 10, or 20 mM glucose compared to the glucose-free B-HEPES medium (**Figure 12A**).

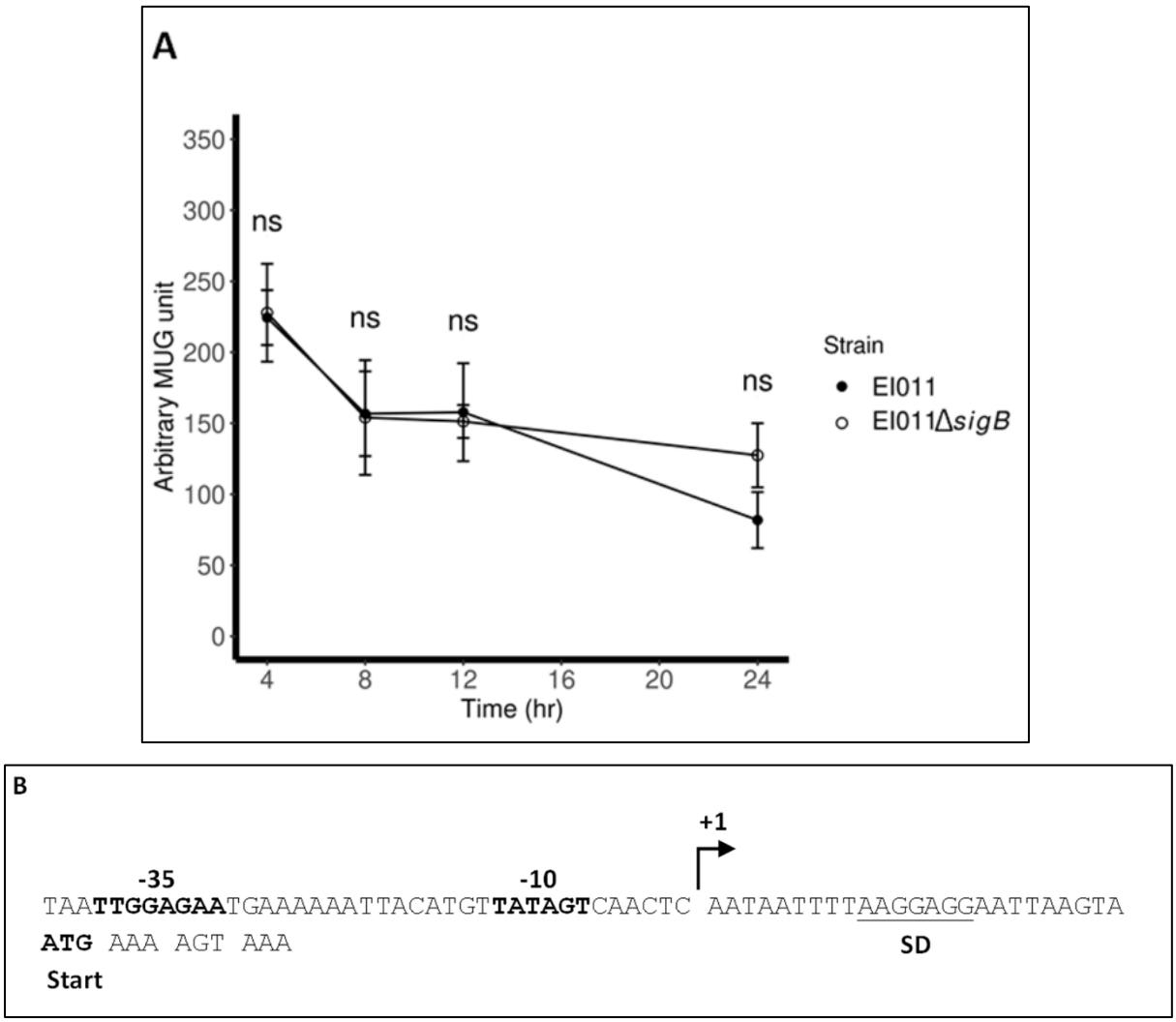

Figure 11 | *ofrA* is transcriped from SigA-dependent promoter. **(A)** Time-dependent *ofrA* transcription was quantified using promoter-less *lacZ*-transcriptional fusion in chromosomal reporter system in JE2 or JE2Δ*sigB* background in B-medium. Data is blotted with average ± standard error of the means of four biological replicates. Statistical analysis was carried out using unpaired two-tailed Student *t*-test. ns: not significant. **(B)** *ofrA* promoter structure showing canonical SigA-depedent transcriptional initiation. 5' Rapid Amplification cDNA Ends (5'RACE) was used to map the transcriptional start site (TSS) as indicated by (+1). Shine-Dalgarno (SD) sequence is underlined. The promoter structure (-35 and -10 elements) are indicated by bold sequences. MUG, 4-methylumbelliferyl-β-D-galactopyranoside.

To investigate whether *ofrA* repression is glucose-specific, P_{ofrA} activity is not repressed in other glycolytic substrates (fructose and glycerol) in *S. aureus* JE2 background (**Figure 12B**). To ensure that this phenotype is not strain-specific, Laura Cecchino transduced the chromosomal reporter system into *S. aureus* NewHG background (EI013). β-Galactosidase assays showed that P_{ofrA} activity is repressed in presence of 5-, 10-, or 20-mM glucose in B-HEPES medium (**Figure 12A**). However, *ofrA* was also repressed by the presence of 10 mM fructose and 20 mM glycerol (**Figure 12B**). Therefore, I analyzed the whole genome sequencing of both *S. aureus* JE2 strain and *S. aureus* NewHG strain compared

to the corresponding reference genomes NC_007793.1 and NC_009641.1, respectively. Although *S. aureus* NewHG did not show any relevant mutation regarding carbohydrate utilization machinery, *S. aureus* JE2 showed a frame shift mutation in *fruC* (encodes fructokinase). Therefore, I concluded that P_{ofrA} activity is repressed by increased glycolytic flux. To avoid the secondary effects from carbohydrate metabolism in JE2 and EI011 background, I utilized EI013 (*S. aureus* NewHG background).

Altogether, P_{ofrA} activity is 1) induced by the absence of glycolytic substrates or 2) repressed in the presence of glycolytic substrates.

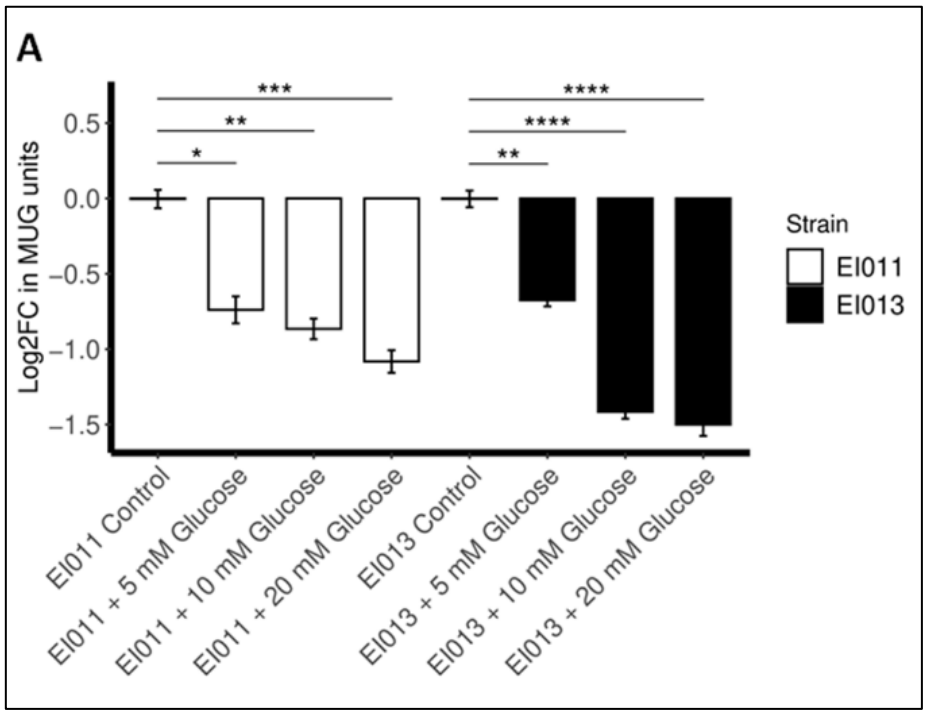

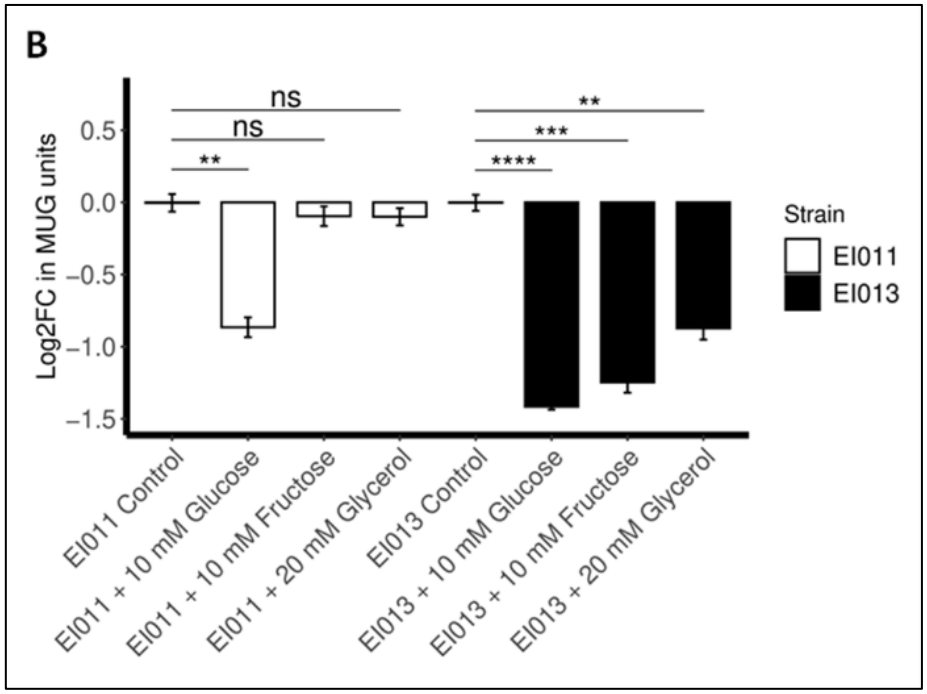

Figure 12 | Activated glycolytic flux represses *ofrA* transcription in *S. aureus*. **(A)** Dose-dependent repression of P_{ofrA} activity in B-medium buffered with 50 mM HEPES without (control) or with 5-, 10-, or 20-mM glucose after 2-hour incubation with logarithmic phase cells (OD_{600} = 0.5) of *S. aureus* JE2 (EI011) and NewHG (EI013) backgrounds. **(B)** P_{ofrA} activity in control, 10 mM glucose, 10 mM fructose, or 20 mM glycerol B-HEPES medium. Reporter strains in JE2 (EI011) and NewHG (EI013) backgrounds were incubated for 2 hours in the respective media after reaching the logarithmic phase (OD_{600} = 0.5). Error bars represent the standard error of the means of four biological replicates. Statistical analysis was carried out using unpaired two-tailed Student's *t*-test comparing the control measurement to the condition of question; ns, not significant; **p* < 0.05; ***p* < 0.01; ****p* < 0.001; *****p* < 0.0001. MUG, 4-methylumbelliferyl-β-D-galactopyranoside.

4.16 Transcriptional regulation of *ofrA* is linked to cellular metabolism independent to ArlR and CcpA

ArlR activity, from the ArlRS two component system, is reported to be increased in decreased glycolytic flux (Párraga Solórzano et al., 2019). Therefore, my hypothesis was that in the presence of glucose, ArlR activity is decreased which might inhibit P_{ofrA} activity. To test this hypothesis, *ofrA* transcription was measured using β-galactosidase assay in EI013 and EI013Δ*arlR*::*ermB* in absence of glucose. The reporter system showed that P_{ofrA} activity was not affected in B-medium by *arlR* mutation (**Figure 13A**). Hence, I concluded that ArlR does not mainly affect *ofrA* transcriptional regulation in glucose-free medium. In B-HEPES buffered medium, glycolytic substrates (glucose or fructose) repress *ofrA* transcription in EI013Δ*arlR* as well as in EI013 (**Figure 13B**). This phenotype cannot be noticed in addition of non-glycolytic substrate (xylose) (**Figure 13B**). Overall, ArlR cannot be a direct regulator in glycolytic flux-mediated repression of *ofrA*.

In glycolysis, fructose 1,6-bisphosphate is produced from glucose and fructose and causes CcpA activation (Richardson, 2019). Therefore, I hypothesized that CcpA could be a potential *ofrA* repressor specially that it represses *rocD-gudB* operon downstream to *ofrA*. Contrary to my hypothesis; in EI013Δ*ccpA*::*tetL*, P_{ofrA} activity is 1-log lower in Δ*ccpA* compared to the WT in B-medium (**Figure 13A**). Furthermore, analysis of pre-*ofrA* region showed a non-functional *cre*-box (TGTATG**T**GGATT**TG**) at -142 to the start codon, in which there are three critical mismatches to the canonical cre-site (TGNAAR**C**GNWWW**CA**) (Seidl et al., 2009).

After exposing EI013 and EI013Δ*ccpA* to 10 mM glucose in B-HEPES medium, a strong downregulation in P_{ofrA} activity was observed (**Figure 13C**). Therefore, glucose-mediated repression is independent of CcpA. However, CcpA mutation did decrease P_{ofrA} activity by causing a metabolic reconstruction in *S. aureus* indicating a close association between *ofrA* transcriptional regulation and *S. aureus* core metabolism.

In *S. aureus*, CcpA directly represses amino acids utilization genes to prevent wasting energy on a secondary carbon source (Seidl et al., 2009). *ccpA* mutation results in better suited metabolism to preferentially utilize amino acids (Seidl et al., 2009).

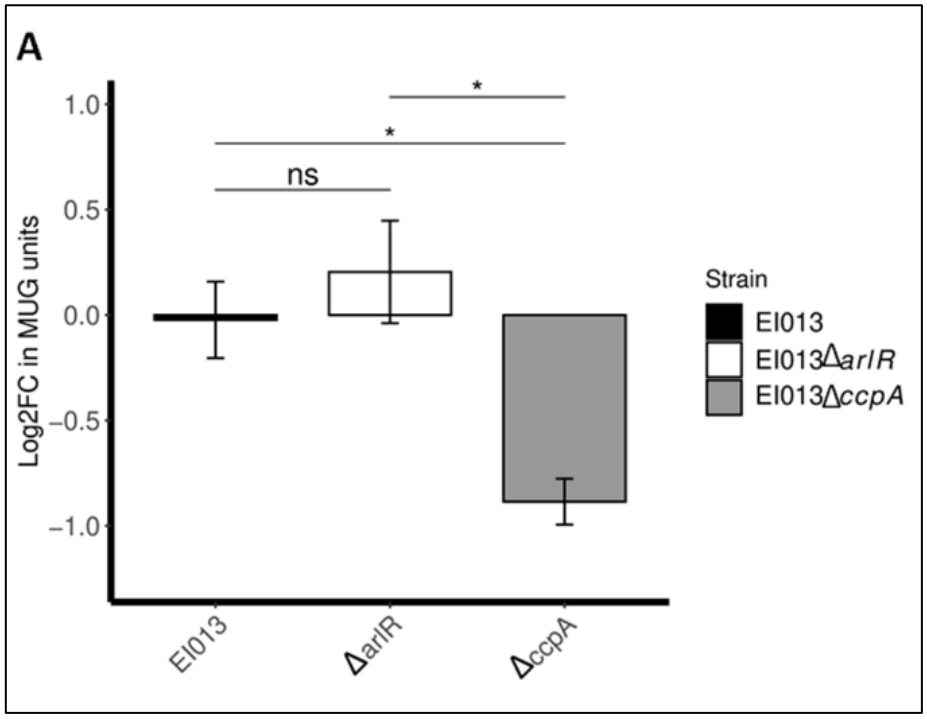

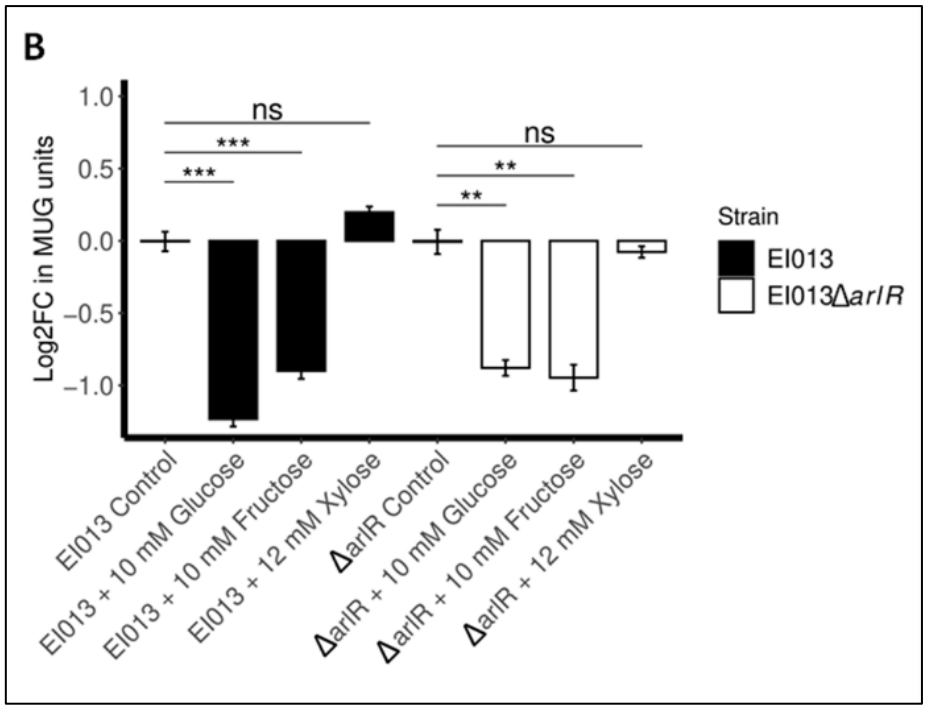

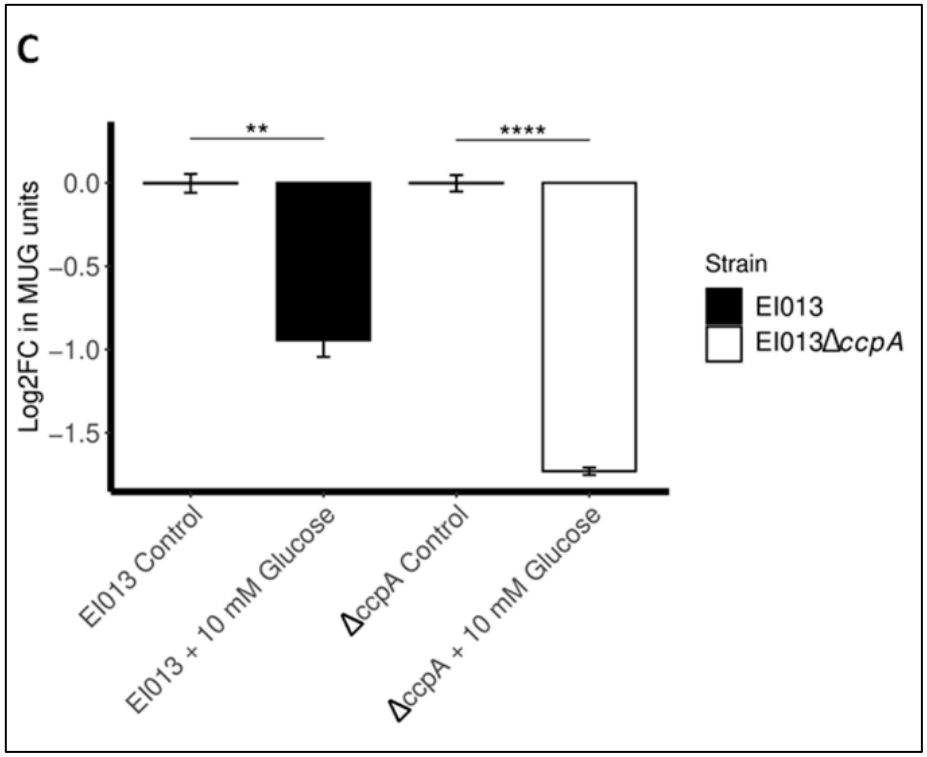

Figure 13 | Glucose-mediated repression of *ofrA* is independent of ArlR and CcpA. **(A)** P_{ofrA} activity is decreased in *ccpA* mutation but not in *arlR* mutation in the glucose-free B-medium. Bacteria were grown to logairthmic phase cells (OD_{600} = 0.5). **(B)** P_{ofrA} activity in control, 10 mM glucose, 10 mM fructose, or 12 mM xylose in B-HEPES medium. **(C)** P_{ofrA} activity in control or 10 mM glucose in B-HEPES medium. Reporter strains were incubated for 2 hours in the respective media after reaching the logarithmic phase (OD_{600} = 0.5). Error bars represent the standard error of the means of three **(A)** or four **(B and C)** biological replicates. Statistical analysis was carried out using unpaired two-tailed Student's *t*-test comparing the control measurement to the condition of question; ns, not significant; **p* < 0.05; ***p* < 0.01; ****p* < 0.001; *****p* < 0.0001. MUG, 4-methylumbelliferyl-β-D-galactopyranoside.

5 Discussion

In this study, I aimed at identifying the physiological role of the SAUSA300_0859 in *S. aureus*. A previous study showed that SAUSA300_0859 gene product has a nitroreductase activity and confers resistance against the novel DNA-binding antimicrobial MT02 (El-Hossary et al., 2018). Using bioinformatic analysis, I showed that SAUSA300_0859 gene product belongs to the widely distributed old yellow enzyme (**Figure 1A and 2**). Therefore, we named the gene into *ofrA.*

5.1 OfrA distribution

Oxidoreductases are mediators for electron(s) transfer through biomolecules. Depending on the nature of the reductant, the oxidant, and/or the localization of the reaction, oxidoreductases evolved to maintain certain functions in the cells. Since electron(s) transfer is a fundamental aspect of energy utilization in biological systems, oxidoreductases are vital for detoxification systems in many culturable and uncultured bacteria as revealed with metagenomic analyses (Bengtsson-Palme et al., 2014). Wide distribution of OYEs in bacteria, fungi, and plants is a sign for a common functionality of OYEs and unexplored role in the biological system.

Despite there is diversification in *S. aureus* strains, OfrA is well-maintained in the all-searched strains (**Figure 1C**). In addition, *ofrA* (SA0817) was ranked as 11th indicative gene for *S. aureus* strains typing due to its conservation and representative nucleotide sequence parameters (pairwise percentage nucleotide diversity, staphylococcal G+C percentage, codon adaptation, and d_S/d_N ratio) (Cooper and Feil, 2006).

Furthermore, OfrA represents a highly conserved staphylococcal OYE (**Figure 1F**). OfrA is more conserved compared to the metabolic classical mevalonate pathway (MvaA, hydroxymethylglutaryl-CoA reductase) and staphyloxanthin biosynthesis pathway (CrtM, dehydrosqualene synthase) (**Figure 1F**).

At the most distant clade of staphylococci (*S. felis*, *S. lutrae*, *S. pseudintermedius*, *S. hyicus*, *S. muscae*, and *S. agentis*), comparing OfrA orthologues to OfrA resulted in more than 56% amino acid identity (**Figure 1D**). The aforementioned result suggests that these staphylococci encode OYEs from the monophyletic group of OfrA.

OfrA distribution is still maintained in other Firmicutes. For example, despite the presence of OfrA orthologues in some *Lactobacillus* species normally found in human gastrointestinal tract (*L. oligofermentans*, *L. casei*, *L. salivarius*, and *L. ultunensis*), no OYEs are encoded

in the vaginal microbiota species (*L. gasseri*, *L. jensenii*, *L. crispatus*, and *L. iners*) (**Figure 2D**). One possibility of this distribution pattern is the need of some bacterial species to detoxify possible chemical compounds enriched in their specific niches.

5.2 Physiological function and regulation of an OYE is dependent on the phylogenetic class

Although OfrA and OfrB are two paralogous groups of OYEs in *S. aureus*, our lab only identified *ofrA* to be responsible for MT02 inactivation. Previous RNA-seq analysis showed that *ofrB* did not get deregulated in MT02 stress (El-Hossary et al., 2018).

In *E. coli*, *nemA* is regulated *via* the upstream NemR (Gray et al., 2013; Ozyamak et al., 2013). However, in *S. aureus* and *B. subtilis*, I could not detect a functional analogue of NemR. Therefore, I believe that the OYEs are regulated *via* different mechanisms among the different organisms (*E. coli* and *S. aureus*) or even in the same organism (*ofrA* and *ofrB*).

In agreement to the aforementioned observation, OYEs paralogues in *Saccharomyces cerevisiae* had different functional relevance (Nizam et al., 2015). Overexpression of both OYE2 and OYE3 protects *Saccharomyces cerevisiae* from the unsaturated aldehyde acrolein (Trotter et al., 2006). However, Δ*OYE2* not Δ*OYE3* showed defective survival against acrolein stress (Trotter et al., 2006).

From pfam, OfrA, OfrB, YqiG, YqjM, NemA, and XenB contain Oxidored_FMN domain which is relevant to OYEs functionality. Many proteins contain OYEs relevant protein domain as three major clusters based on protein length (cluster A, B, and C) (**Figure 14A**).

The shortest proteins' cluster (cluster A) has mode in protein length = 370 amino acids. Cluster-A contains monodomain proteins such as OfrA, OfrB, NemA, and XenB.

The intermediate proteins' cluster (cluster A) has mode in protein length = 673 amino acids. Cluster-B contains three major subgroups: bifunctional salicylyl-CoA 5-hydroxylase, and two distinct sub-groups of 2,4-dienoyl-CoA reductases. Bifunctional salicylyl-CoA 5-hydroxylase contains the additional FAD_binding_3 domain. 2,4-Dienoyl-CoA reductases contains an additional protein domain Pyr_redox_2. The proteins in cluster B are characterised by the presence of more cysteine residues, compared to cluster A and C, probably because they are attached to 4Fe-4S cluster as a part of added enzymatic activity (**Figure 14B**).

The longest proteins' cluster (cluster C) has mode in protein length = 925 amino acids. The proteins in cluster C are respiratory proteins due to the presence of (flavocytochrome c)

domain. One example of this cluster is a cytoplasmic fumarate reductase that was isolated from *Klebsiella pneumoniae* (Bertsova et al., 2020).

In the conservation analysis, OfrA is highly conserved in staphylococci compared to the less conserved OfrB. Altogether, we can speculate that *ofrA* and *ofrB* are not responsible for the same function in *S. aureus*.

5.3 OYEs act as a redox catalytic blueprint in bacteria

OYEs have the same enzymatic activity but the *in-vivo* enzymatic conditions are more relevant to the functional relevance. The presence of OYEs containing proteins is diverse in many medically important microbes (**Figure 15**). In some cases, the OYE domain was adapted to include a Fe-S cluster creating (DCR_FMN domain) for additional functionality. Moreover, some proteins contain an OYE or DCR_FMN domain fused to other protein domains. Therefore, some organisms have multiple versions of OYEs to count for different functions such as *S. aureus*, *B. subtilis*, and *Streptococcus pyogenes* that have two, two, and one version of OYEs encoded in their genomes, respectively. Contrary to many other bacterial species, *S. aureus*, *B. subtilis*, and *Streptococcus pyogenes* have OYEs as only monodomain proteins that are not fused to other protein domains.

In the intracellular pathogen *Listeria monocytogenes*, there are three proteins; one of them (lmo2471) is an OYE, the other two (lmo0489 and lmo2235) are fused to other protein domains for added functionality. In *Mycobacterium tuberculosis*, there are two proteins; one of them (Rv3359) is an OYE, the other (Rv1175c) is adapted to an Fe-S cluster (DCR_FMN domain) and fused to FadH2 protein domain.

Similarly, *E. coli* encodes the OYE NemA and FadH (DCR_FMN + FadH2 domains). However, *E. coli* O157:H7 str. Sakai contains an additional third OYE which is encoded by ECs_0331 (**Figure 16A**). ECs_0331 gene product belongs to OfrA-like sub-family (38% amino acid identity) and does not cluster with the usual NemA-like OYEs in *E. coli* K12 (**Figure 16B**).

Interestingly, *Pseudomonas aeruginosa* encodes for 10 homologues; PA0840, PA1334, PA2716, PA2932 (*morB*), PA4356 (*xenB*), and PA3723 are OYEs; PA5398 (*dgcA*) contains an OYE domain fused to FadH2 domain; PA3092 (*fadH1*), PA4814 (*fadH2*) contains an OYE domain fused to DCR_FMN domain; PA4986 is 648 amino acid protein that contains the OYE in addition to a Pyr_redox_2 domain.

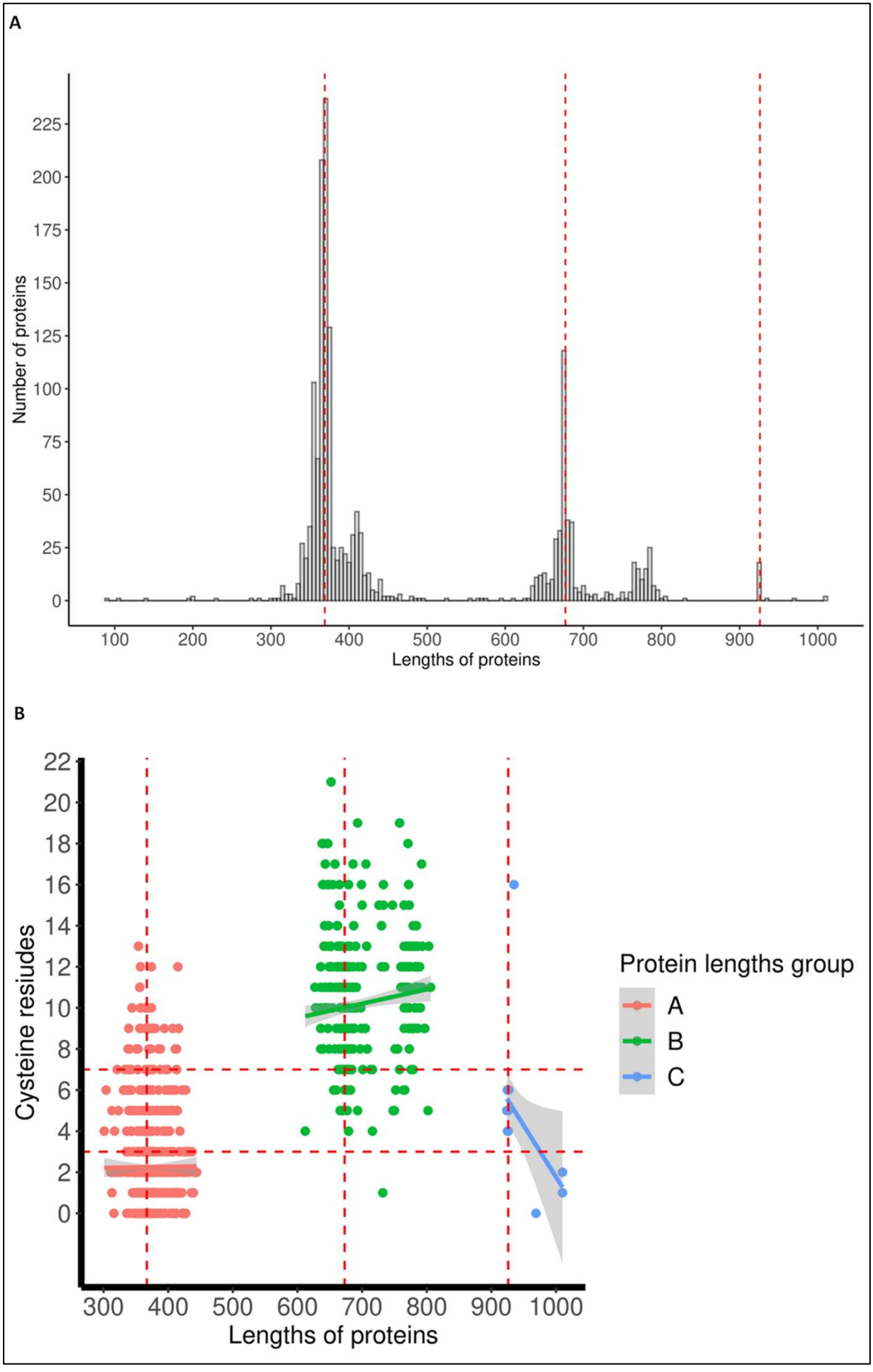
A
Number of proteins
225
200
175
150
125
100
75
50
25
0
100
200
300
400
500
600
700
800
900
1000
Lengths of proteins
B
Cysteine resiudes
22
20
18
16
14
12
10
8
6
4
2
0
300
400
500
600
700
800
900
1000
Lengths of proteins
Protein lengths group
A
B
C

Figure 14 | OYEs containing proteins in the microbial world. **(A)** Histogram shows the abundance of OYEs-relevant proteins based on the length of the protein. Three protein clusters can be showed. Dashed vertical lines represent the median of the proteins' lengths in each cluster. Bins' width equals 5 amino acids. **(B)** Scatter plot shows the number of cysteine residues in each protein as a function of the protein length. Dashed vertical lines represent the median of the length of the three proteins' clusters as in **Figure 15A**. Dashed horizontal lines categorize the protein into cysteine-poor (≤ 3), intermediate (4 - 7), or -rich (≥ 8). Criteria of categorizing proteins based on their cysteine residues were determined by cluster analysis and cysteine residues distribution in the OYEs containing proteins. OYE, old yellow enzyme.

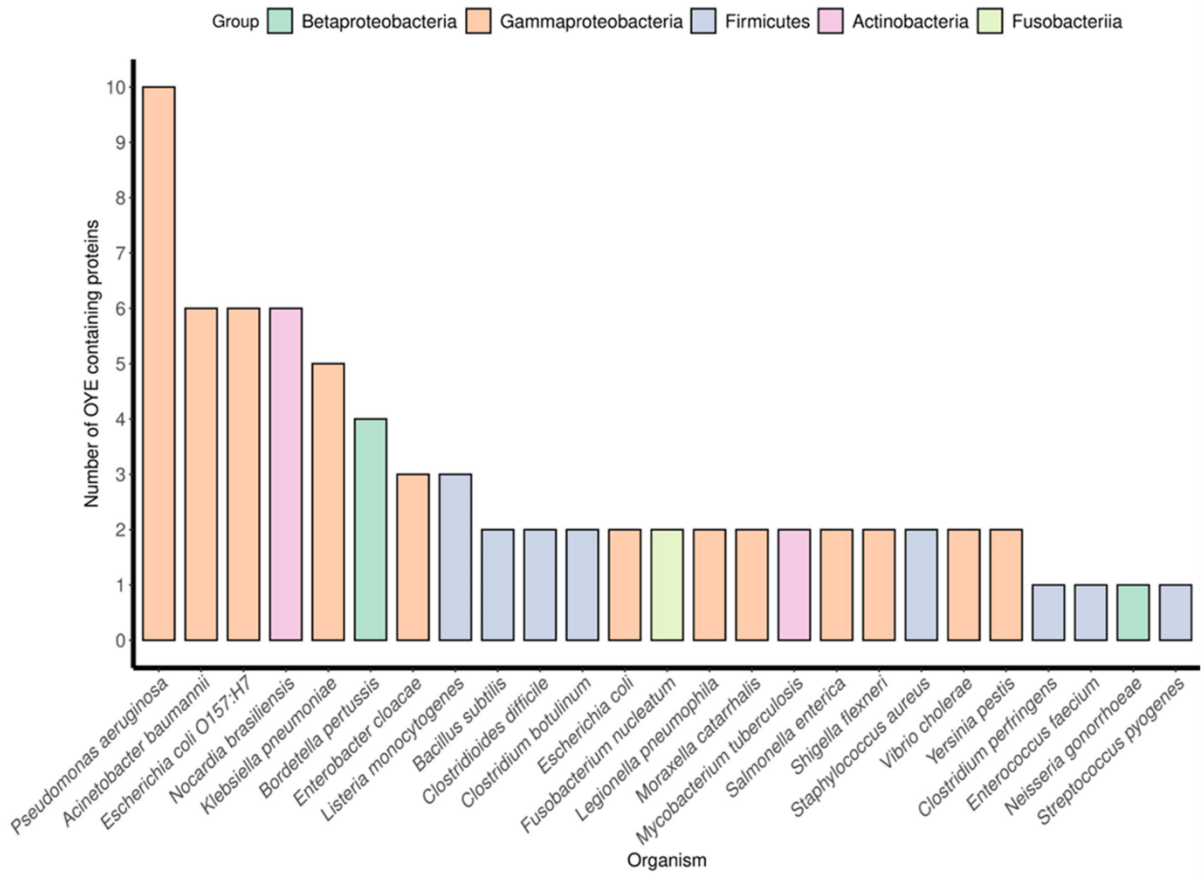

Figure 15| OYEs are widely spread in the bacterial kingdom. The numbers of OYEs containing proteins encoded in bacterial chromosomes that belong to different bacterial groups are plotted against the corresponding organism. *Vibrio cholerae*, for example, contains two chromosomes (each chromosome encodes one OYE containing protein, two in total). OYE, old yellow enzyme.

5.4 *ofrA* transcription in *S. aureus*

Since there were no linked phenotypes to OYEs in bacteria (except hypochlorite survival defect to Δ*nemA* in *E. coli*), regulation of *ofrA* in different conditions was used as a proxy to investigate the potential function (Gray et al., 2013) **(Figure 4)**. Second to that, reverse

genetics approach was used to assess the potential survival-relevant phenotypes *in-vitro* **(Figure 5)** and *ex-vivo* **(Figure 6)**.

This strategy revealed that *ofrA* is an important detoxification factor against reactive electrophilic, oxygen, and chlorine species. Additionally, OfrA enhances *S. aureus* survival in murine RAW 264.7 macrophages and whole human blood.

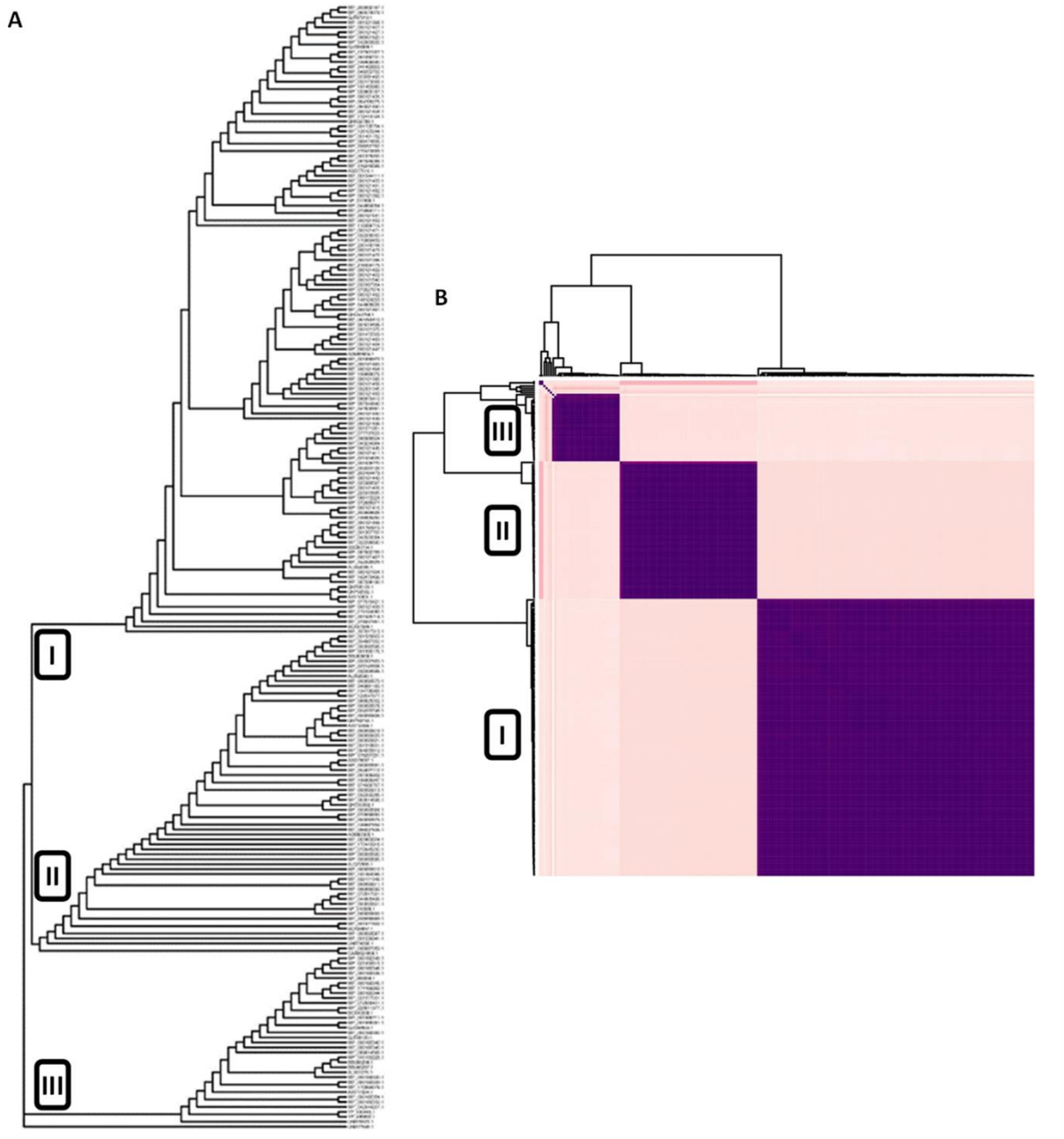

Figure 16| OfrA-like OYE is encoded in *E. coli* O157:H7 str. Sakai but not in *E. coli* MG1655 K12. Maximum likelihood tree **(A)** and cluster analysis **(B)** show three distinct clusters of OYEs containing proteins (I, II, and III) encoded in *E. coli* strains. Cluster I, OfrA-like OYEs; cluster II, NemA-like OYEs; cluster III, 2,4-dienoyl CoA reductase; OYE, old yellow enzyme.

First, *ofrA* induction conditions was shown to be dependent on the medium **(Figure 4D)**. Normal complex laboratory media (e.g. TSB, B, LB, MH, BHI) could affect stressors activities through direct interaction of the stressors with the medium components (Ashby et al., 2020) or indirectly supplementing *S. aureus* with nutrients to support the intracellular redox homeostasis (Lensmire et al., 2021). Here, RPMI 1640 was used as chemically defined medium for reporter system analysis and *in-vitro* survival assays.

Second, β-galactosidase assays, from the transcriptional reporter system **(Figure 3B)**, suggested that there is low transcriptional level of *ofrA* in *S. aureus*. This observation can be seen in the RT-qPCR results (average quantification cycle *ofrA* C_q = 28, *rpoB* C_q = 17, and *rho* C_q = 18.5 from the same dilution of cDNA as template).

In addition, our RNA-seq results showed low level of *ofrA* mRNA level in *S. aureus* JE2. Earlier RNA-seq result (El-Hossary et al., 2018) and *S. aureus* expression data browser (https://genome.jouy.inra.fr/cgi-bin/aeb/viewdetail.py?id=NA_856283_857410_1) showed similar low *ofrA* transcriptional level. However, these experiments were done in different strains of *S. aureus* and in different media.

One explanation for low *ofrA* transcription is that OYEs are highly promiscuous enzymes with wide substrate range (Sheng et al., 2016). Therefore, higher intracellular amounts of OfrA could be potentially toxic for the cells by over-shifting the redox potential in the cells towards reductive conditions and/or over-consuming the reducing equivalents NAD(P)H in the cells.

Although, overexpressing of OfrA and YqiG in *E. coli* did not result *in E. coli* toxicities (Sheng et al., 2016; El-Hossary et al., 2018), *ofrA* induction under xylose inducible promoter could not be successful in the presence of 0.5% xylose. Since the genetic complementation was only possible *via* the natural promoter, a possibility of strain and/or species-specific toxicity (from OfrA overexpression) could be further investigated.

5.5 *ofrA* reporter system in *S. aureus*

To report for *ofrA* transcription, a transcriptional fusion of *ofrA* promoter to a promoter-less *lacZ* was used **(Figure 3B and 4A)**. A chromosomal integration of P_{ofrA}::*lacZ* in *S. aureus* JE2 resulted in the creation of the reporter strain EI011. Chromosomal integration is advantageous to override the plasmid-copy number issues that could arise from plasmid-based reporter systems.

Although β-galactosidase is stable against proteolysis, heat, and degradation (Rohlfing and Crawford, 1966; Ohlsen et al., 1997), the β-galactosidase assay, using X-gal

as a substrate, is hindered by the presence of the golden pigment (staphyloxanthin) (Price et al., 2021). Therefore, the fluorescence-based β-galactosidase assay, converting the non-fluorescent MUG into the fluorescent MU, was used as more sensitive method to indirectly report for *ofrA* transcription (Vidal-Aroca et al., 2006).

Moreover, LacZ protein contains 16 cysteine residues (1.6% of the total amino acids). These cysteine residues could be targets for electrophilic, oxidative, and hypochlorite stressors.

The *lacZ* used in this study as a reporter is not codon-optimised for *S. aureus* (Ohlsen et al., 1997). Since one copy of *lacZ* was used to report for *ofrA* after the chromosomal integration **(Figure 3A)**, we could predict marginal effect(s) from the non-optimized *lacZ* expression in *S. aureus* especially from a low transcription derived from P_{ofrA} (see section 5.4). Recently, a codon-optimized *lacZ* (co*lacZ*) was established for *S. aureus* research. Using co*lacZ*, 16-fold higher activity was shown in β-galactosidase assay from the same promoter (Krute et al., 2017, 2021). With the recently developed co*lacZ*, higher sensitivities could be achieved from chromosomal co*lacZ* reporters.

To validate the results obtained from β-galactosidase assays, literature analysis, dose response, medium quenching, and RT-qPCRs were used **(Figure 4)**.

5.6 *ofrA* induction conditions

β-Galactosidase assays suggested that *ofrA* is induced in the presence of reactive electrophilic, oxygen, and chlorine species **(Figure 4A)**. Since H_2O_2 is metabolism *via* Catalase as well as peroxidases in *S. aureus*, cumene hydroperoxide (CHP) was used as catalase-resistant peroxide. Both hydrogen peroxide and the organic peroxide CHP were able to induce *ofrA* **(Figure 4A)**. In agreement with previous transcriptomic studies, MHQ (Fritsch et al., 2019), NaOCl (Loi et al., 2018b), and H_2O_2 (Chang et al., 2006) induce *ofrA* to significant levels in *S. aureus* at similar concentrations.

Additionally, previous proteomic analysis indicated that OfrA is over-represented to *S. aureus* exposed to diamide stress (Wolf et al., 2008). Increased *ofrA* promoter activity (measured with β-galactosidase assays) affected *ofrA* expression levels as measured with RT-qPCR **(Figure 4C)**.

The wide range of conditions (electrophilic, oxidative, and hypochlorite stress) in which *ofrA* is induced suggested that *ofrA* is induced in redox imbalance including substances like the surface coating antimicrobial AGXX (Loi et al., 2018a) **(Figure 4A and 4B)**. An additional

augmentation to the previous conclusion is that *ofrA* was found upregulated after *S. aureus* exposure to reactive sulfur species (Peng et al., 2017).

Not only in *S. aureus*, the *B. subtilis* orthologue (YqiG) was proven to be over-represented in the proteome of *B. subtilis* after formaldehyde and methylglyoxal stress (Huyen et al., 2009).

5.7 Sensing and transcriptional regulation

Sensing of the stress is key factor for survival. In RT-qPCR analysis, *S. aureus* was able to sense and upregulate *ofrA* after 15 minutes (0.25 x doubling time) of exposure to the stressors **(Figure 4C)**. In *S. aureus*, transcription is mediated *via* different sigma factors that interact with the promoter region to start DNA-dependent RNA polymerase activity.

Literature analysis concluded that *ofrA* is not a part of SigB, SigH, or SigS regulons (Wu et al., 1996; Morikawa et al., 2003; Pané-Farré et al., 2006; Shaw et al., 2008). SigA is the housekeeping sigma factor that is responsible for maintaining the transcription in the normal state. Since *ofrA* is induced under stressed conditions, transcription level must be modulated *via* a transcriptional regulator.

Since MHQ is the top inducing condition **(Figure 4A)**, MHQ stress must be sensed. However, MHQ causes both electrophilic and oxidative transcriptomic signatures in *S. aureus* (Fritsch et al., 2019). *In-vitro* survival analysis shows that MHQ survival defect phenotype of Δ*ofrA* is mainly due to electrophilic stress not oxidative stress **(Figure 10)**. Furthermore, neither H_2O_2 nor cumene hydroperoxide causes higher *ofrA* induction compared to MHQ, diamide, formaldehyde, or methylglyoxal. In RT-qPCR, the disulfide stress inducer formaldehyde causes even increased transcriptional induction after 15 minutes of exposure **(Figure 4C)**. Therefore, I believe that *ofrA* responds to the electrophilic not the oxidative stress caused by MHQ.

Two regulators were linked to the quinone stress; QsrR and MhqR. However, *ofrA* is not a part of QsrR or MhqR regulons (Ji et al., 2013; Fritsch et al., 2019). Interestingly, *B. subtilis* Δ*spx* showed downregulation in *yqiG*.

Spx is an unusual regulator which interacts with the C-terminal domain of the DNA-dependent RNA polymerase α-subunit and affects its promoter binding and hence the transcription levels (Rochat et al., 2012). Spx in *B. subtilis* and *S. aureus* has the ability to sense electrophilic stresses *via* its highly conserved CXXC motif (Nakano et al., 2004; Villanueva et al., 2016). Genome-wide profiling of Spx regulon in *S. aureus* is not adequate

since Spx is essential in *S. aureus* (Villanueva et al., 2016). Further studies should be done to test the hypothesis that *ofrA* could be under the regulation of Spx in *S. aureus*.

5.8 OfrA-mediated stress adaptability in *S. aureus*

In-vitro survival analysis showed that OfrA enhances *S. aureus* survival against quinone (MHQ), toxic aldehyde (methylglyoxal), oxidative (H_2O_2), and hypochlorite (NaOCl) stress **(Figure 5)**. *E. coli* Δ*nemA* showed compromised survival in hypochlorite stress not in electrophilic nor in oxidative stress (Gray et al., 2013; Lee et al., 2013; Ozyamak et al., 2013).

Extended functionality of the *S. aureus* OfrA compared tos the *E. coli* NemA could be due to the differences in redox maintenance machinery or in the OYE substrate specificities as a result of the differences in protein sequence **(Figure 1B)**. This supports our previous conclusion that OYEs do not share the same relevance towards the organismal physiology.

The defective survival against this wide range of stress conditions points toward the effect of *ofrA* mutation on redox homeostasis. Methylglyoxal detoxification in *S. aureus* could be mediated *via* thiol-dependent or independent mechanisms. Recently, it was shown that the thiol-dependent detoxification pathway is more profound in terms of *in-vitro* survivability (Imber et al., 2018).

Altogether, we can conclude that *ofrA* mutation resulted in defective common redox homeostasis; most probably the thiol-dependent redox homeostasis. Since OYEs are reported to utilize reducing equivalents NAD(P)H, this could imply OfrA function in regenerating thiol-dependent redox maintenance of so far unknown substrate(s).

5.9 OfrA enhances *S. aureus* survivability at the host-pathogen interface

In macrophages, *S. aureus* has to deal with the produced reactive species in early and late phagosomes and the phagolysosome (Moldovan and Fraunholz, 2019).
In RAW 264.7 macrophage cell line, the survival of Δ*ofrA* is defective compared to WT survival **(Figure 6B)**.

In our assays, the survival differences took 48 hours for statistical significance. A recent report showed that the stimulation of macrophage cell line (J774) increases the level of the produced reactive oxygen species (Rowe et al., 2020). Neutrophils are 60% of the leucocyte population in whole human blood and kill the invading bacteria *via* reactive oxygen species (de Jong et al., 2019). That could explain the quick survival defect (after 60 minutes) of Δ*ofrA* compared to WT in whole human blood **(Figure 6C)**.

Another difference is that, in whole human blood, *S. aureus* JE2 cannot replicate due to intense host factors response. However, *S. aureus* USA300 JE2 strain was able to replicate inside the RAW macrophages (Flannagan et al., 2018) indicating that the difference between WT and Δ*ofrA* is fitness- not survival-dependent **(Figure 6)**.

The macrophage survival defect phenotype was in line with *S. aureus* COL Δ*hypR* and Δ*mhqR* survival defect in J774A.1 macrophage cell line due to compromised *S. aureus* response to hypochlorite and quinone stress, respectively (Loi et al., 2018b; Fritsch et al., 2019). However, strain differences account for the measured phenotype; fitness or survivability of USA300 JE2 and COL strains, respectively.

Δ*ofrA* showed decreased survival compared to WT strain in whole human blood **(Figure 6C)**. In agreement with our result, a transcriptomic approach reported that *ofrA* (SAR0918) was at least two-fold upregulated in two *S. aureus* isolates exposed to 30, 60, and 90 minutes (den Reijer et al., 2013).

Dual RNA-seq experiments comparing *S. aureus* SH1000 strain in kidneys of the resistant C57BL/6 and the susceptible A/J mice highlighted the staphylococcal factors enable proper survivability in the resistant compared to susceptible host (Thänert et al., 2017). Interestingly, *ofrA* (SAOUHSC_00893) is upregulated in *S. aureus* infecting the resistant C57BL/6 mice compared to *S. aureus* infecting the susceptible A/J mice (Thänert et al., 2017). This result demonstrates the importance of *ofrA* as a staphylococcal survival factor in increased encountered host resistance.

A recent report showed that a transposon mutant (inactivating *ofrA*) caused a decreased damage to human microvascular endothelial cells (HMEC-1) (roughly 13%) compared to *S. aureus* JE2 (roughly 50%) (Xiao et al., 2022). Our results supported by the aforementioned result illustrate the imperative role of *ofrA* for *S. aureus* at the host-pathogen interface.

NTR2 gene encodes for an orthologue of OfrA in the parasite *Leishmania*. Intriguingly, a knockout of NTR2 gene in *Leishmania* results in reduced replication within macrophages (Wyllie et al., 2016). This could be explained by a conserved functionality of OfrA-class OYEs to enhance the survivability of the organism (prokaryote or eukaryote) by a universal anti-stress mechanism with chromosomal evolution for better fitting the organismal niche.

5.10 Transcriptomic approach in studying the effect of *ofrA* mutation in *S. aureus*

We took transcriptomic approach to study the effect of *ofrA* mutation. In this regard, mid-logarithmic phase cells (from WT and Δ*ofrA*) were used to avoid the accumulating stress

in the stationary phase. Furthermore, we compared the unstressed cells to avoid additional gene deregulation from a stressor and to reflect the role of *ofrA* in unstressed condition.

From RNA-seq analysis, we observed 188 deregulated genes **(Figure 7)**. Despite the large number of statistically significant transcriptionally-affected genes, only 24% (22/93) and 19% (18/95) of the downregulated and upregulated genes are equal to or more than 1.5-fold deregulated, respectively **(Table 22 and Table 23)**.

At the logarithmic phase of unstressed cells, *ofrA* mutation affects 40 genes at least at the transcriptional level (> 1.5-fold). This result indicates that *ofrA* could be more important at protein and/or metabolite-level. This observation is in-line with the conclusion that *ofrA* supports the thiol-dependent redox homeostasis to maintain a healthy proteome.

Although only 21 genes are more than two-fold transcriptionally deregulated in unstressed cells, *ofrA* mutant showed a quickly (one hour and less) compromised survivability in H_2O_2, NaOCl, and whole human blood **(Figure 5D, 5E, and 6C)**. This supports our conception that OfrA protects *S. aureus via* direct degradation of stressor(s) and/or protecting the already made staphylococcal proteins.

In this regard, *ofrA* had to be promptly upregulated as a response of an impulse exposure (15 minutes or less) as indicated in the RT-qPCR experiment **(Figure 4C)**. In *E. coli*, *nemA* was shown to be transcriptionally upregulated for as quick as only five minutes of exposure to hypochlorite stress (Gray et al., 2013).

5.11 One carbon metabolism in Δ*ofrA*

Our RNA-seq analysis revealed that one carbon (1C) metabolism is inhibited in Δ*ofrA* **(Table 24)**. 1C metabolism is composed of intercalating metabolic pathways (e.g., methionine and folate cycles) to provide methyl groups (a.k.a. one carbon unit) for DNA, amino acids, … etc biosynthesis (Clare et al., 2019). 1C metabolism activity is partly dependent on the availability of the reducing equivalents (NADPH and NADH) that are required for multiple steps in the folate metabolism (Shetty and Varshney, 2021).

Interestingly, 1C metabolism is one of three pathways (thiol-, ribulose monophosphate-, and pterin-dependent) *via* which *S. aureus* detoxifies the toxic aldehyde formaldehyde (Chen et al., 2016). Formaldehyde toxicity mediation is decisive for *S. aureus* survival at the host-pathogen interface as formaldehyde is produced as a by-product from heme degradation in iron acquisition *via* IsdG and IsdI (Matsui et al., 2013).

In 1C metabolism, the carbon atom of formaldehyde (HCHO) is loaded on the pterin moiety of tetrahydrofolate resulting in the formation of N^5,N^{10}-methylene-tetrahydrofolate

(Chen et al., 2016). Indeed, formaldehyde can upregulate *ofrA* mRNA up to 38-fold after 15 minutes of exposure **(Figure 4C)**. Additionally, our *in-vitro* survival analysis shows Δ*ofrA* survival defect (9%) compared to WT strain (23%) after one-hour exposure of 0.5 mM formaldehyde in RPMI medium.

Accordingly, we could speculate that OfrA affects the NAD(P)H/NAD(P)$^+$ ratio which in turn activates 1C metabolism. This activation could protect *S. aureus* against formaldehyde stress.

Another hypothesis is that thiol-dependent toxicity of formaldehyde could account for the observed *ofrA* induction in WT strain and Δ*ofrA* survival defect (Chen et al., 2016). Further studies will be needed to support one or both of these hypotheses.

5.12 Staphyloxanthin biosynthesis in Δ*ofrA*

Staphyloxanthin biosynthesis *via crtOPQMN* operon is inhibited in Δ*ofrA* **(Table 24, Figure 7D and 8A)**. *crtOPQMN* operon is activated in stationary phase due to the accumulated stress which increases SigB-dependent transcriptional activity (Götz, 2005).

Interestingly, our RNA-sequencing showed that SigB-encoding *rpoF* is downregulated (log_2FoldChange = - 0.25) in Δ*ofrA*. Although this change is only 20% difference to the WT, regarding the mRNA levels, in logarithmic phase, multiple genes, that belong to SigB-regulon, are transcriptionally downregulated in Δ*ofrA* **(Table 22 and 24)**.

It was expected that Δ*ofrA* might accumulate stress and activate SigB-regulon. Contrary to this hypothesis, SigB-regulon is downregulated including *crtOPQMN* operon for staphyloxanthin biosynthesis. Therefore, I predict that OfrA is important in case of stressed conditions. In-line with this observation, logarithmic phase cells of WT, Δ*ofrA*, and p*ofrA* have similar growth kinetics in RPMI medium **(Figure 5A)**.

Additionally, the reason for *crtM* downregulation in Δ*ofrA* was due to metabolic effects of *ofrA* mutation in the upper classical mevalonate pathway **(Figure 8B and 8C)**. In the upper mevalonate pathway, HMG-CoA reductase utilizes the NAD(P)H as reducing equivalents for mevalonate biosynthesis (Wilding et al., 2000). This redox reaction is the rate limiting step in the mevalonate biosynthesis (Matsumoto et al., 2016). Consequently, OfrA could affect the NAD(P)H/NAD(P)$^+$ ratio which could affect the mevalonate biosynthesis rate. These results link the role of OfrA in energy metabolism with the central metabolic pathways (1C metabolism and mevalonate pathway) in *S. aureus* **(Table 24)**.

Although the observed downregulation of downregulated SigB-controlled genes (such as *crtM*) could affect the survivability of Δ*ofrA* in stress condition (such as H_2O_2),

I showed that *crtM*-mediated survival defect against H_2O_2 is independent of *ofrA* **(Figure 8D)**. In fact, both *crtM* and *ofrA* mutations have additive survival defect in the double mutation against H_2O_2 **(Figure 8E)**.

5.13 OfrA supports thiol-dependent redox homeostasis

As discussed in section 5.12, Δ*ofrA* does not accumulate stress. However, OYEs are well-known for their promiscuity which makes them ideal for industrial applications (Lee et al., 2013). Moreover, OfrA could exhibit nitroreductase activity (El-Hossary et al., 2018). Thus, we cannot exclude the possibility that OfrA directly degrade different stressors.

Utilization of *in-vitro* enzyme assays to detect direct substrates will be hindered by the fact that *in-vivo* reaction kinetics have additional complexity in stress conditions; when energy is the critical factor for bacterial survival. Hence, bacterial survival assays were used as a readout to shed the light on the survival relevant mechanism(s) **(Figure 9 and 10)**.

Another possibility is that OfrA acts as a functional redundant enzyme for detoxification systems already present in *S. aureus*. If this is true, Δ*ofrA* will not have defective survival in a wide range of stress conditions (electrophilic, oxidative, and hypochlorite) **(Figure 5)**. In addition, functional redundancy hypothesis is against the fact that OfrA is conserved with high degree of amino acid identities in all strains of *S. aureus* and in all staphylococci **(Figure 1C-F)** and that *ofrA* mutation results in compromised fitness and survival in RAW macrophages and human blood, respectively **(Figure 6)**.

5.14 Beyond thiol-dependent redox homeostasis

In summary of the previous results, the current knowledge about *S. aureus ofrA* is presented as follows (**Figure 17**). *ofrA* is upregulated in oxidative, electrophilic, and hypochlorite stress. Conversly, *ofrA* is downregulated by activated glycolytic flux independent of both ArlR and CcpA. In fact, *ccpA* mutation downregulates P_{ofrA} activity, most probably through metabolic reconstruction. OfrA enhances *S. aureus* survival in whole human blood and murine macrophage cell line RAW 264.7. *ofrA* mutation results in decreased production of the virulence agent staphyloxanthin. Decreased staphyloxanthin alone cannot explain Δ*ofrA* increased sensitivity towards H_2O_2.

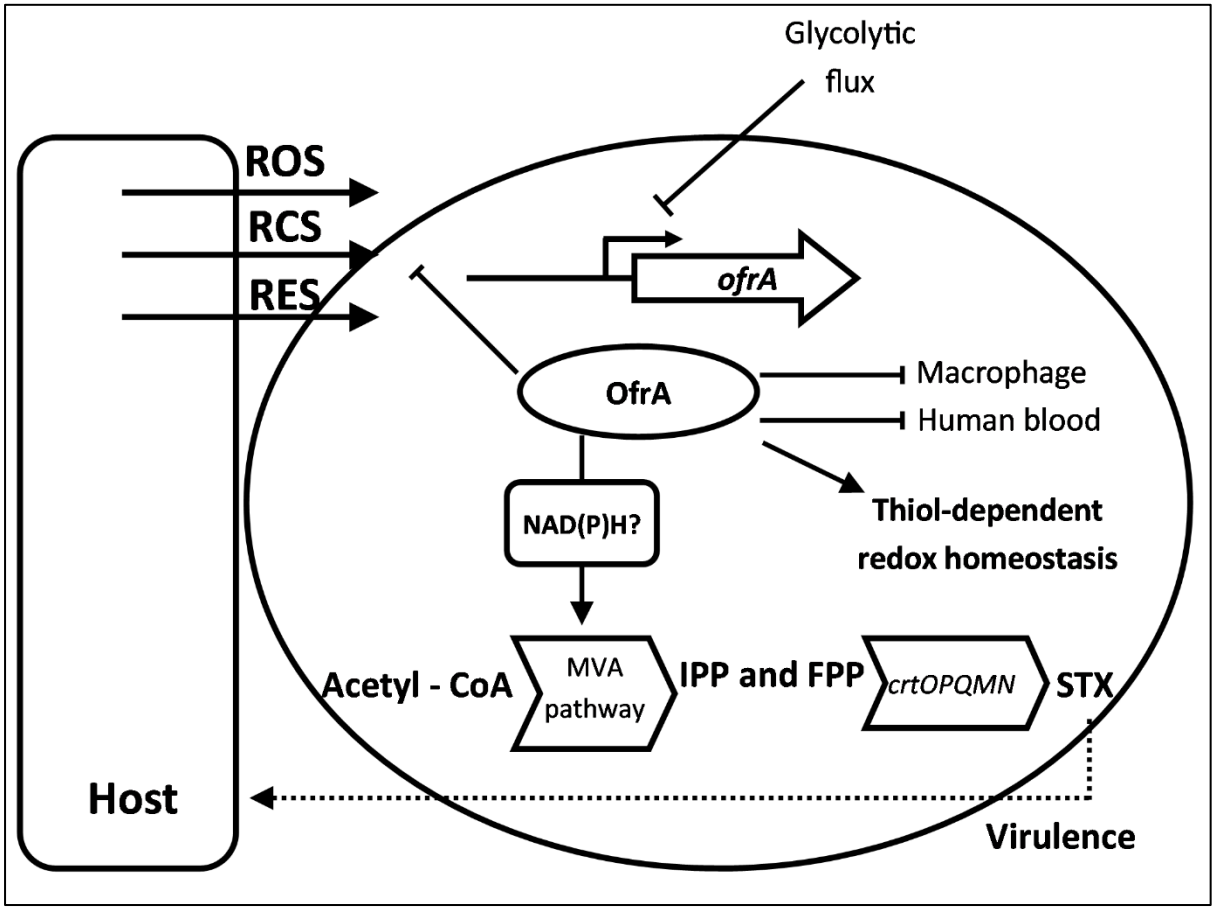

Figure 17| Summarizing model of the current knowledge of *ofrA* function and regulation in *S. aureus*. OfrA enhances *S. aureus* survival in RAW246.7 macrophage cell line, in human blood, and against reactive oxygen, chlorine, and electrophilic stresses. In Δ*ofrA*, staphyloxanthin production is decreased as a result of decreased mevalonate production from the upper mevalonate pathway. OfrA supports thiol-dependent redox homeostasis. *ofrA* is induced in oxidative, hypochlorite, and electrophilic stresses but repressed in activated glycolytic flux. FPP, farnesyl pyrophosphate; IPP, isopentenyl pyrophosphate; MVA, mevalonate; RCS, reactive hypochlorite species; RES, reactive electrophilic species; ROS, reactive oxygen species; STX, staphyloxanthin.

OYEs utilize NAD(P)H to regenerate their FMN prosthetic group and eventually reduce a substrate (Williams and Bruce, 2002). Although, except for *pflA* downregulation, we could not spot significant changes in Rex-regulon (involved in energy homeostasis) in our RNA-seq results analysing logarithmic phase cells, *ofrA* mutation is linked to cellular energy metabolism such as 1C metabolism and mevalonate pathway (see section 5.12).

ofrA mutation might result in imbalanced NAD(P)H/NAD(P)$^+$ and/or reduced/oxidized ratio of OfrA *in-vivo* substrate(s). Interestingly, the available NADPH supports the thiol-dependent redox homoeostasis as used by the different reductases to regenerate the free thiol such as AhpF (Jönsson et al., 2007) and YpdA (Mikheyeva et al., 2019) regenerating AhpC and bacillithiol, respectively.

The role of OfrA in staphylococcal energy metabolism has not been discussed yet. In addition to this study, a follow-up experiment using the reporter strain EI011 in glucose rich and glucose-free medium suggested that *ofrA* could be downregulated in the presence of glucose. We can speculate that *ofrA* could be under metabolic regulation not to cause reducing equivalents over-consumption.

Surprisingly, OfrA was found to be enriched in UV-mediated crosslinked protein-RNA complexes compared to non-crosslinked samples in *S. aureus* (Chu et al., 2022). Further studies are needed to investigate the role of OfrA as an RNA binding protein.

OfrB is enriched in a pull-down assay using GST-tagged GcvH-L as bait in *S. aureus* (Rack et al., 2015). In addition, OfrB accompanies a staphylococcal sirtuin system (which includes GcvH-L) for protein ADP-ribosylation modulation in *S. aureus* and *Streptococcus pyogenes* (Rack et al., 2015).

5.15 Conclusion

Microbial physiology is an important research niche to understand the microbe-microbe and host-microbe interaction. Many bacterial factors at the host-pathogen interface are still understudied. One of these factors is a widely found protein family in the bacterial kingdom name as the OYEs family. Here I found that OYEs are encoded in two independent paralogues (OfrA and OfrB). I studied the role of OfrA as a highly conserved staphylococcal factor. *ofrA* is induced in electrophilic, oxidative, and hypochlorite stress. Δ*ofrA* exhibits compromised survival in the aforementioned conditions. At the host-pathogen interface, OfrA enhances *S. aureus* survival in macrophages and whole human blood.

In unstressed conditions, Δ*ofrA* showed inhibited upper mevalonate pathway, as well as, one carbon metabolism compared to the WT. We can speculate that *ofrA* mutation affects the energy metabolism in *S. aureus* due to deregulation of NAD(P)H/NAD(P)$^+$ ratio. However, decreased staphyloxanthin production cannot solely explain the survival defect in H_2O_2. In stressed conditions, OfrA supports thiol-dependent redox homeostasis which is critical for staphylococcal survival in electrophilic, oxidative, and hypochlorite stress.

In conclusion, further studies are needed to investigate whether the survival defect phenotype of Δ*ofrA* is caused by imbalanced NAD(P)H/NAD(P)$^+$, *in-vivo* reduced/oxidized substate, or both. I believe that multiple layers of complexity are still to be added to OYEs functions in biological system. These layers are as follows: 1) OfrA role in the thiol-dependent homeostasis and the energy metabolism of *S. aureus*, 2) OYEs implications for the bacterial physiology *via* interaction with RNA and/or proteins, and 3) exploitation of such mechanisms to enhance antibiotic therapy and/or design novel antimicrobials against pathogens.

6 References

Amato, E. D., and Stewart, J. D. (2015). Applications of protein engineering to members of the old yellow enzyme family. *Biotechnol. Adv.* 33, 624–631. doi:10.1016/j.biotechadv.2015.04.011.

Anjum, M. F., Marco-Jimenez, F., Duncan, D., Marín, C., Smith, R. P., and Evans, S. J. (2019). Livestock-Associated Methicillin-Resistant Staphylococcus aureus From Animals and Animal Products in the UK. *Front. Microbiol.* 10. doi:10.3389/fmicb.2019.02136.

Arbeit, R. D., Maki, D., Tally, F. P., Campanaro, E., and Eisenstein, B. I. (2004). The Safety and Efficacy of Daptomycin for the Treatment of Complicated Skin and Skin-Structure Infections. *Clin. Infect. Dis.* 38, 1673–1681. doi:10.1086/420818.

Arora, S., Gordon, J., and Hook, M. (2021). Collagen Binding Proteins of Gram-Positive Pathogens. *Front. Microbiol.* 12, 90. doi:10.3389/fmicb.2021.628798.

Ashby, L. V., Springer, R., Hampton, M. B., Kettle, A. J., and Winterbourn, C. C. (2020). Evaluating the bactericidal action of hypochlorous acid in culture media. *Free Radic. Biol. Med.* 159, 119–124. doi:10.1016/j.freeradbiomed.2020.07.033.

Bae, T., and Schneewind, O. (2006). Allelic replacement in Staphylococcus aureus with inducible counter-selection. *Plasmid* 55, 58–63. doi:10.1016/j.plasmid.2005.05.005.

Bengtsson-Palme, J., Alm Rosenblad, M., Molin, M., and Blomberg, A. (2014). Metagenomics reveals that detoxification systems are underrepresented in marine bacterial communities. *BMC Genomics* 15, 749. doi:10.1186/1471-2164-15-749.

Benson, M. A., Lilo, S., Nygaard, T., Voyich, J. M., and Torres, V. J. (2012). Rot and SaeRS Cooperate To Activate Expression of the Staphylococcal Superantigen-Like Exoproteins. *J. Bacteriol.* 194, 4355–4365. doi:10.1128/JB.00706-12.

Berends, E. T. M., Horswill, A. R., Haste, N. M., Monestier, M., Nizet, V., and von Köckritz-Blickwede, M. (2010). Nuclease Expression by Staphylococcus aureus Facilitates Escape from Neutrophil Extracellular Traps. *J. Innate Immun.* 2, 576–586. doi:10.1159/000319909.

Bertsova, Y. V., Oleynikov, I. P., and Bogachev, A. V. (2020). A new water-soluble bacterial NADH: fumarate oxidoreductase. *FEMS Microbiol. Lett.* 367, 175. doi:10.1093/femsle/fnaa175.

Bigger, J. W. (1944). TREATMENT OF STAPHYLOCOCCAL INFECTIONS WITH PENICILLIN BY INTERMITTENT STERILISATION. *Lancet* 244, 497–500. doi:10.1016/S0140-6736(00)74210-3.

Bogdan, C. (2015). Nitric oxide synthase in innate and adaptive immunity: an update. *Trends Immunol.* 36, 161–178. doi:10.1016/j.it.2015.01.003.

BOKAREWA, M., JIN, T., and TARKOWSKI, A. (2006). Staphylococcus aureus: Staphylokinase. *Int. J. Biochem. Cell Biol.* 38, 504–509. doi:10.1016/j.biocel.2005.07.005.

Bonamore, A., and Boffi, A. (2008). Flavohemoglobin: Structure and reactivity. *IUBMB Life* 60, 19–28. doi:10.1002/IUB.9.

Brauner, A., Fridman, O., Gefen, O., and Balaban, N. Q. (2016). Distinguishing between resistance, tolerance and persistence to antibiotic treatment. *Nat. Rev. Microbiol.* 14, 320–330. doi:10.1038/nrmicro.2016.34.

Brynildsen, M. P., Winkler, J. A., Spina, C. S., MacDonald, I. C., and Collins, J. J. (2013). Potentiating antibacterial activity by predictably enhancing endogenous microbial ROS production. *Nat. Biotechnol.* 31, 160–165. doi:10.1038/nbt.2458.

Bukharie, H. (2010). A review of community-acquired methicillin-resistant Staphylococcus aureus for primary care physicians. *J. Fam. Community Med.* 17, 117. doi:10.4103/1319-1683.74320.

Bukowski, M., Wladyka, B., and Dubin, G. (2010). Exfoliative Toxins of Staphylococcus aureus. *Toxins (Basel).* 2, 1148. doi:10.3390/TOXINS2051148.

Campbell, E. A., Korzheva, N., Mustaev, A., Murakami, K., Nair, S., Goldfarb, A., et al. (2001). Structural Mechanism for Rifampicin Inhibition of Bacterial RNA Polymerase. *Cell* 104, 901–912. doi:10.1016/S0092-8674(01)00286-0.

Chakraborty, S., Karmakar, K., and Chakravortty, D. (2014). Cells producing their own nemesis: Understanding methylglyoxal metabolism. *IUBMB Life* 66, 667–678. doi:10.1002/iub.1324.

Chandrangsu, P., Loi, V. Van, Antelmann, H., and Helmann, J. D. (2018). The Role of Bacillithiol in Gram-Positive Firmicutes. Mary Ann Liebert Inc. doi:10.1089/ars.2017.7057.

Chang, W., Small, D. A., Toghrol, F., and Bentley, W. E. (2006). Global Transcriptome Analysis of

Staphylococcus aureus Response to Hydrogen Peroxide. *J. Bacteriol.* 188, 1648–1659. doi:10.1128/jb.188.4.1648-1659.2006.

Chapman, A. L. P., Hampton, M. B., Senthilmohan, R., Winterbourn, C. C., and Kettle, A. J. (2002). Chlorination of Bacterial and Neutrophil Proteins during Phagocytosis and Killing of Staphylococcus aureus. *J. Biol. Chem.* 277, 9757–9762. doi:10.1074/jbc.M106134200.

Chen, N. H., Djoko, K. Y., Veyrier, F. J., and McEwan, A. G. (2016). Formaldehyde Stress Responses in Bacterial Pathogens. *Front. Microbiol.* 7, 257. doi:10.3389/fmicb.2016.00257.

Cheung, G. Y. C., Wang, R., Khan, B. A., Sturdevant, D. E., and Otto, M. (2011). Role of the Accessory Gene Regulator agr in Community-Associated Methicillin-Resistant Staphylococcus aureus Pathogenesis. *Infect. Immun.* 79, 1927–1935. doi:10.1128/IAI.00046-11.

Cho, H., Jeong, D.-W., Liu, Q., Yeo, W.-S., Vogl, T., Skaar, E. P., et al. (2015). Calprotectin Increases the Activity of the SaeRS Two Component System and Murine Mortality during Staphylococcus aureus Infections. *PLOS Pathog.* 11, e1005026. doi:10.1371/journal.ppat.1005026.

Chouchani, E. T., James, A. M., Fearnley, I. M., Lilley, K. S., and Murphy, M. P. (2011). Proteomic approaches to the characterization of protein thiol modification. *Curr. Opin. Chem. Biol.* 15, 120–128. doi:10.1016/j.cbpa.2010.11.003.

Christodoulou, D., Link, H., Fuhrer, T., Kochanowski, K., Gerosa, L., and Sauer, U. (2018). Reserve Flux Capacity in the Pentose Phosphate Pathway Enables Escherichia coli's Rapid Response to Oxidative Stress. *Cell Syst.* 6, 569-578.e7. doi:10.1016/j.cels.2018.04.009.

Chu, L.-C., Arede, P., Li, W., Urdaneta, E. C., Ivanova, I., McKellar, S. W., et al. (2022). The RNA-bound proteome of MRSA reveals post-transcriptional roles for helix-turn-helix DNA-binding and Rossmann-fold proteins. *Nat. Commun.* 13, 2883. doi:10.1038/s41467-022-30553-8.

Clare, C. E., Brassington, A. H., Kwong, W. Y., and Sinclair, K. D. (2019). One-Carbon Metabolism: Linking Nutritional Biochemistry to Epigenetic Programming of Long-Term Development. *Annu. Rev. Anim. Biosci.* 7, 263–287. doi:10.1146/annurev-animal-020518-115206.

Clarke, R. S., Ha, K. P., and Edwards, A. M. (2021). RexAB Promotes the Survival of Staphylococcus aureus Exposed to Multiple Classes of Antibiotics. *Antimicrob. Agents Chemother.* 65. doi:10.1128/AAC.00594-21.

Clauditz, A., Resch, A., Wieland, K.-P., Peschel, A., and Götz, F. (2006). Staphyloxanthin Plays a Role in the Fitness of Staphylococcus aureus and Its Ability To Cope with Oxidative Stress. *Infect. Immun.* 74, 4950–4953. doi:10.1128/IAI.00204-06.

Clements, M. O., Watson, S. P., and Foster, S. J. (1999). Characterization of the Major Superoxide Dismutase of Staphylococcus aureus and Its Role in Starvation Survival, Stress Resistance, and Pathogenicity. *J. Bacteriol.* 181, 3898–3903. doi:10.1128/JB.181.13.3898-3903.1999.

Coady, A., Xu, M., Phung, Q., Cheung, T. K., Bakalarski, C., Alexander, M. K., et al. (2015). The Staphylococcus aureus ABC-Type Manganese Transporter MntABC Is Critical for Reinitiation of Bacterial Replication Following Exposure to Phagocytic Oxidative Burst. *PLoS One* 10, e0138350. doi:10.1371/journal.pone.0138350.

Coates-Brown, R., Moran, J., Pongchaikul, P., Darby, A., and Horsburgh, M. J. (2018). Comparative Genomics of Staphylococcus Reveals Determinants of Speciation and Diversification of Antimicrobial Defense. *bioRxiv*, 277400. doi:10.1101/277400.

Cooper, J. E., and Feil, E. J. (2006). The phylogeny of Staphylococcus aureus – which genes make the best intra-species markers? *Microbiology* 152, 1297–1305. doi:10.1099/mic.0.28620-0.

Cosgrove, K., Coutts, G., Jonsson, I.-M. M., Tarkowski, A., Kokai-Kun, J. F., Mond, J. J., et al. (2007). Catalase (KatA) and alkyl hydroperoxide reductase (AhpC) have compensatory roles in peroxide stress resistance and are required for survival, persistence, and nasal colonization in Staphylococcus aureus. *J. Bacteriol.* 189, 1025–1035. doi:10.1128/JB.01524-06.

Cosgrove, S. E., Sakoulas, G., Perencevich, E. N., Schwaber, M. J., Karchmer, A. W., and Carmeli, Y. (2003). Comparison of Mortality Associated with Methicillin-Resistant and Methicillin-Susceptible Staphylococcus aureus Bacteremia: A Meta-analysis. *Clin. Infect. Dis.* 36, 53–59. doi:10.1086/345476.

Crosby, H. A., Schlievert, P. M., Merriman, J. A., King, J. M., Salgado-Pabón, W., and Horswill, A. R. (2016). The Staphylococcus aureus Global Regulator MgrA Modulates Clumping and Virulence by Controlling Surface Protein Expression. *PLOS Pathog.* 12, e1005604.

doi:10.1371/journal.ppat.1005604.
da Cruz Nizer, W. S., Inkovskiy, V., and Overhage, J. (2020). Surviving Reactive Chlorine Stress: Responses of Gram-Negative Bacteria to Hypochlorous Acid. *Microorganisms* 8, 1220. doi:10.3390/microorganisms8081220.
Dahl, J.-U., Gray, M. J., and Jakob, U. (2015). Protein Quality Control under Oxidative Stress Conditions. *J. Mol. Biol.* 427, 1549–1563. doi:10.1016/j.jmb.2015.02.014.
Davis, B. D., Chen, L. L., and Tai, P. C. (1986). Misread protein creates membrane channels: an essential step in the bactericidal action of aminoglycosides. *Proc. Natl. Acad. Sci.* 83, 6164–6168. doi:10.1073/pnas.83.16.6164.
de Jong, N. W. M., van Kessel, K. P. M., and van Strijp, J. A. G. (2019). Immune Evasion by Staphylococcus aureus. *Microbiol. Spectr.* 7. doi:10.1128/microbiolspec.GPP3-0061-2019.
DelCardayré, S. B., and Davies, J. E. (1998). Staphylococcus aureus Coenzyme A Disulfide Reductase, a New Subfamily of Pyridine Nucleotide-Disulfide Oxidoreductase: SEQUENCE, EXPRESSION, AND ANALYSIS OF cdr *. *J. Biol. Chem.* 273, 5752–5757. doi:10.1074/JBC.273.10.5752.
Delmastro-Greenwood, M., Freeman, B. A., and Wendell, S. G. (2014). Redox-Dependent Anti-Inflammatory Signaling Actions of Unsaturated Fatty Acids. *Annu. Rev. Physiol.* 76, 79–105. doi:10.1146/annurev-physiol-021113-170341.
den Reijer, P. M., Lemmens-den Toom, N., Kant, S., Snijders, S. V., Boelens, H., Tavakol, M., et al. (2013). Characterization of the Humoral Immune Response during Staphylococcus aureus Bacteremia and Global Gene Expression by Staphylococcus aureus in Human Blood. *PLoS One* 8, e53391. doi:10.1371/JOURNAL.PONE.0053391.
Deora, R., and Misra, T. K. (1995). Purification and Characterization of DNA-Dependent RNA Polymerase from Staphylococcus aureus. *Biochem. Biophys. Res. Commun.* 208, 610–616. doi:10.1006/bbrc.1995.1382.
Dickerhof, N., Paton, L., and Kettle, A. J. (2020). Oxidation of bacillithiol by myeloperoxidase-derived oxidants. *Free Radic. Biol. Med.* 158, 74–83. doi:10.1016/j.freeradbiomed.2020.06.009.
Dolan, S. K., and Welch, M. (2018). The Glyoxylate Shunt, 60 Years On. *Annu. Rev. Microbiol.* 72, 309–330. doi:10.1146/annurev-micro-090817-062257.
Duggan, S., Laabei, M., Alnahari, A. A., O'Brien, E. C., Lacey, K. A., Bacon, L., et al. (2020). A small membrane stabilizing protein critical to the pathogenicity of staphylococcus aureus. *Infect. Immun.* 88. doi:10.1128/IAI.00162-20.
Dunman, P. M., Murphy, E., Haney, S., Palacios, D., Tucker-Kellogg, G., Wu, S., et al. (2001). Transcription Profiling-Based Identification of Staphylococcus aureus Genes Regulated by the agr and/or sarA Loci. *J. Bacteriol.* 183, 7341–7353. doi:10.1128/JB.183.24.7341-7353.2001.
Duran-Reynals, F. (1933). STUDIES ON A CERTAIN SPREADING FACTOR EXISTING IN BACTERIA AND ITS SIGNIFICANCE FOR BACTERIAL INVASIVENESS. *J. Exp. Med.* 58, 161–181. doi:10.1084/jem.58.2.161.
El-Halfawy, O. M., and Valvano, M. A. (2015). Antimicrobial Heteroresistance: an Emerging Field in Need of Clarity. *Clin. Microbiol. Rev.* 28, 191–207. doi:10.1128/CMR.00058-14.
El-Hossary, E. M., Förstner, K. U., François, P., Baud, D., Streker, K., Schrenzel, J., et al. (2018). A Novel Mechanism of Inactivating Antibacterial Nitro Compounds in the Human Pathogen Staphylococcus aureus by Overexpression of a NADH-Dependent Flavin Nitroreductase. *Antimicrob. Agents Chemother.* 62, e01510-17. doi:10.1128/AAC.01510-17.
Ezraty, B., Gennaris, A., Barras, F., and Collet, J.-F. (2017). Oxidative stress, protein damage and repair in bacteria. *Nat. Rev. Microbiol.* 15, 385–396. doi:10.1038/nrmicro.2017.26.
Farmer, E. E., and Davoine, C. (2007). Reactive electrophile species. *Curr. Opin. Plant Biol.* 10, 380–386. doi:10.1016/J.PBI.2007.04.019.
Fernandes, P. (2016). Fusidic Acid: A Bacterial Elongation Factor Inhibitor for the Oral Treatment of Acute and Chronic Staphylococcal Infections. *Cold Spring Harb. Perspect. Med.* 6, a025437. doi:10.1101/cshperspect.a025437.
Fey, P. D., Endres, J. L., Yajjala, K., Widhelm, T. J., Boissy, R. J., Bose, J. L., et al. (2013). A Genetic Resource for Rapid and Comprehensive Phenotype Screening of Nonessential Staphylococcus aureus Genes. *MBio* 4, e00537-12-e00537-12. doi:10.1128/mBio.00537-12.
Fischbach, M. A., and Walsh, C. T. (2009). Antibiotics for Emerging Pathogens. *Science (80-.).* 325,

1089–1093. doi:10.1126/science.1176667.

Fitzpatrick, T. B., Amrhein, N., and Macheroux, P. (2003). Characterization of YqjM, an Old Yellow Enzyme Homolog from Bacillus subtilis Involved in the Oxidative Stress Response. *J. Biol. Chem.* 278, 19891–19897. doi:10.1074/jbc.M211778200.

Flannagan, R. S., Kuiack, R. C., McGavin, M. J., and Heinrichs, D. E. (2018). Staphylococcus aureus uses the GraXRS regulatory system to sense and adapt to the acidified phagolysosome in macrophages. *MBio* 9. doi:10.1128/mBio.01143-18.

Flint, D. H., Tuminello, J. F., and Emptage, M. H. (1993). The inactivation of Fe-S cluster containing hydro-lyases by superoxide. *J. Biol. Chem.* 268, 22369–22376. doi:10.1016/S0021-9258(18)41538-4.

Förstner, K. U., Vogel, J., and Sharma, C. M. (2014). READemption—a tool for the computational analysis of deep-sequencing–based transcriptome data. *Bioinformatics* 30, 3421–3423. doi:10.1093/BIOINFORMATICS/BTU533.

Foster, M. W., McMahon, T. J., and Stamler, J. S. (2003). S-nitrosylation in health and disease. *Trends Mol. Med.* 9, 160–168. doi:10.1016/S1471-4914(03)00028-5.

Foster, T. J. (2017). Antibiotic resistance in Staphylococcus aureus. Current status and future prospects. *FEMS Microbiol. Rev.* 41, 430–449. doi:10.1093/femsre/fux007.

Foster, T. J. (2019). The MSCRAMM Family of Cell-Wall-Anchored Surface Proteins of Gram-Positive Cocci. *Trends Microbiol.* 27, 927–941. doi:10.1016/j.tim.2019.06.007.

Fournier, B., Klier, A., and Rapoport, G. (2001). The two-component system ArlS-ArlR is a regulator of virulence gene expression in Staphylococcus aureus. *Mol. Microbiol.* 41, 247–261. doi:10.1046/j.1365-2958.2001.02515.x.

Fritsch, V. N., Loi, V. Van, Busche, T., Sommer, A., Tedin, K., Nürnberg, D. J., et al. (2019). The MarR-Type Repressor MhqR Confers Quinone and Antimicrobial Resistance in Staphylococcus aureus. *Antioxid. Redox Signal.* 31, 1235–1252. doi:10.1089/ars.2019.7750.

Gaballa, A., Newton, G. L., Antelmann, H., Parsonage, D., Upton, H., Rawat, M., et al. (2010). Biosynthesis and functions of bacillithiol, a major low-molecular-weight thiol in Bacilli. *Proc. Natl. Acad. Sci.* 107, 6482–6486. doi:10.1073/pnas.1000928107.

García-Nafría, J., Watson, J. F., and Greger, I. H. (2016). IVA cloning: A single-tube universal cloning system exploiting bacterial In Vivo Assembly. *Sci. Rep.* 6, 27459. doi:10.1038/srep27459.

Gaupp, R., Ledala, N., and Somerville, G. A. (2012). Staphylococcal response to oxidative stress. *Front. Cell. Infect. Microbiol.* 2, 33. doi:10.3389/fcimb.2012.00033.

Geiger, T., Francois, P., Liebeke, M., Fraunholz, M., Goerke, C., Krismer, B., et al. (2012). The Stringent Response of Staphylococcus aureus and Its Impact on Survival after Phagocytosis through the Induction of Intracellular PSMs Expression. *PLoS Pathog.* 8, e1003016. doi:10.1371/journal.ppat.1003016.

Giles, G. I., and Jacob, C. (2002). Reactive Sulfur Species: An Emerging Concept in Oxidative Stress. *Biol. Chem.* 383, 375–388. doi:10.1515/BC.2002.042.

Giraudo, A. T., Calzolari, A., Cataldi, A. A., Bogni, C., and Nagel, R. (1999). The sae locus of Staphylococcus aureus encodes a two-component regulatory system. *FEMS Microbiol. Lett.* 177, 15–22. doi:10.1111/j.1574-6968.1999.tb13707.x.

Götz, F. (2005). Genetic and Biochemical Analysis of the Biosynthesis of the Orange Carotenoid Staphyloxanthin of Staphylococcus aureus. *Microb. Fundam. Biotechnol.*, 284–294. doi:10.1002/3527602720.CH17.

Gray, M. J., Wholey, W. Y., Parker, B. W., Kim, M., and Jakob, U. (2013). NemR is a bleach-sensing transcription factor. *J. Biol. Chem.* 288, 13789–13798. doi:10.1074/jbc.M113.454421.

Groitl, B., and Jakob, U. (2014). Thiol-based redox switches. *Biochim. Biophys. Acta - Proteins Proteomics* 1844, 1335–1343. doi:10.1016/j.bbapap.2014.03.007.

Grumann, D., Nübel, U., and Bröker, B. M. (2014). Staphylococcus aureus toxins - Their functions and genetics. *Infect. Genet. Evol.* 21, 583–592. doi:10.1016/j.meegid.2013.03.013.

Grunenwald, C. M., Choby, J. E., Juttukonda, L. J., Beavers, W. N., Weiss, A., Torres, V. J., et al. (2019). Manganese Detoxification by MntE Is Critical for Resistance to Oxidative Stress and Virulence of Staphylococcus aureus. *MBio* 10. Available at: https://journals.asm.org/doi/abs/10.1128/mBio.02915-18 [Accessed December 14, 2021].

Guerra, F. E., Borgogna, T. R., Patel, D. M., Sward, E. W., and Voyich, J. M. (2017). Epic Immune Battles of History: Neutrophils vs. Staphylococcus aureus. *Front. Cell. Infect. Microbiol.* 7, 286. doi:10.3389/fcimb.2017.00286.

Guo, Y., Song, G., Sun, M., Wang, J., and Wang, Y. (2020). Prevalence and Therapies of Antibiotic-Resistance in Staphylococcus aureus. *Front. Cell. Infect. Microbiol.* 10, 107. doi:10.3389/fcimb.2020.00107.

Hazen, S. L., D'Avignon, A., Anderson, M. M., Hsu, F. F., and Heinecke, J. W. (1998). Human Neutrophils Employ the Myeloperoxidase-Hydrogen Peroxide-Chloride System to Oxidize α-Amino Acids to a Family of Reactive Aldehydes. *J. Biol. Chem.* 273, 4997–5005. doi:10.1074/jbc.273.9.4997.

Hooper, D. C. (2002). Fluoroquinolone resistance among Gram-positive cocci. *Lancet Infect. Dis.* 2, 530–538. doi:10.1016/S1473-3099(02)00369-9.

Horvatek, P., Salzer, A., Hanna, A. M. F., Gratani, F. L., Keinhörster, D., Korn, N., et al. (2020). Inducible expression of (pp)pGpp synthetases in Staphylococcus aureus is associated with activation of stress response genes. *PLOS Genet.* 16, e1009282. doi:10.1371/journal.pgen.1009282.

Hu, C., Xiong, N., Zhang, Y., Rayner, S., and Chen, S. (2012). Functional characterization of lipase in the pathogenesis of Staphylococcus aureus. *Biochem. Biophys. Res. Commun.* 419, 617–620. doi:10.1016/J.BBRC.2012.02.057.

Hung, D. T., and Helmann, J. D. (2013). How antibiotics kill bacteria: new models needed? *Nat. Med.* 19, 544–545. doi:10.1038/nm.3198.

Huyen, N. T. T., Eiamphungporn, W., Mäder, U., Liebeke, M., Lalk, M., Hecker, M., et al. (2009). Genome-wide responses to carbonyl electrophiles in Bacillus subtilis : control of the thiol-dependent formaldehyde dehydrogenase AdhA and cysteine proteinase YraA by the MerR-family regulator YraB (AdhR). *Mol. Microbiol.* 71, 876–894. doi:10.1111/j.1365-2958.2008.06568.x.

Ibberson, C. B., Jones, C. L., Singh, S., Wise, M. C., Hart, M. E., Zurawski, D. V., et al. (2014). Staphylococcus aureus hyaluronidase is a CodY-regulated virulence factor. *Infect. Immun.* 82, 4253–4264. doi:10.1128/IAI.01710-14.

Ibrahim, E. S., Kashef, M. T., Essam, T. M., and Ramadan, M. A. (2017). A Degradome-Based Polymerase Chain Reaction to Resolve the Potential of Environmental Samples for 2,4-Dichlorophenol Biodegradation. *Curr. Microbiol.* 74, 1365–1372. doi:10.1007/s00284-017-1327-6.

Imber, M., Loi, V. Van, Reznikov, S., Fritsch, V. N., Pietrzyk-Brzezinska, A. J., Prehn, J., et al. (2018). The aldehyde dehydrogenase AldA contributes to the hypochlorite defense and is redox-controlled by protein S-bacillithiolation in Staphylococcus aureus. *Redox Biol.* 15, 557–568. doi:10.1016/j.redox.2018.02.001.

Imlay, J. A. (2013). The molecular mechanisms and physiological consequences of oxidative stress: lessons from a model bacterium. *Nat. Rev. Microbiol. 2013 117* 11, 443–454. doi:10.1038/nrmicro3032.

Imlay, J. A. (2019). Where in the world do bacteria experience oxidative stress? *Environ. Microbiol.* 21, 521–530. doi:10.1111/1462-2920.14445.

Imsande, J. (1978). Genetic regulation of penicillinase synthesis in Gram-positive bacteria. *Microbiol. Rev.* 42, 67–83. doi:10.1128/MMBR.42.1.67-83.1978.

Jang, S., and Imlay, J. A. (2007). Micromolar Intracellular Hydrogen Peroxide Disrupts Metabolism by Damaging Iron-Sulfur Enzymes. *J. Biol. Chem.* 282, 929–937. doi:10.1074/jbc.M607646200.

Jenul, C., and Horswill, A. R. (2019). Regulation of Staphylococcus aureus Virulence. *Microbiol. Spectr.* 7. doi:10.1128/microbiolspec.GPP3-0031-2018.

Jeong, W., Cha, M.-K., and Kim, I.-H. (2000). Thioredoxin-dependent Hydroperoxide Peroxidase Activity of Bacterioferritin Comigratory Protein (BCP) as a New Member of the Thiol-specific Antioxidant Protein (TSA)/Alkyl Hydroperoxide Peroxidase C (AhpC) Family. *J. Biol. Chem.* 275, 2924–2930. doi:10.1074/jbc.275.4.2924.

Ji, Q., Zhang, L., Jones, M. B., Sun, F., Deng, X., Liang, H., et al. (2013). Molecular mechanism of quinone signaling mediated through S-quinonization of a YodB family repressor QsrR. *Proc.*

Natl. Acad. Sci. 110, 5010–5015. doi:10.1073/pnas.1219446110.

Johnson, P. J. T., and Levin, B. R. (2013). Pharmacodynamics, Population Dynamics, and the Evolution of Persistence in Staphylococcus aureus. *PLoS Genet.* 9, e1003123. doi:10.1371/journal.pgen.1003123.

Jönsson, T. J., Ellis, H. R., and Poole, L. B. (2007). Cysteine Reactivity and Thiol−Disulfide Interchange Pathways in AhpF and AhpC of the Bacterial Alkyl Hydroperoxide Reductase System. *Biochemistry* 46, 5709–5721. doi:10.1021/bi7001218.

Kaplan, S. L. (2005). Treatment of Community-Associated Methicillin-Resistant Staphylococcus aureus Infections. *Pediatr. Infect. Dis. J.* 24, 457–458. doi:10.1097/01.inf.0000164162.00163.9d.

Kayser, F. H., Benner, E. J., and Hoeprich, P. D. (1970). Acquired and Native Resistance of Staphylococcus aureus to Cephalexin and Other β-Lactam Antibiotics. *Appl. Microbiol.* 20, 1–5. doi:10.1128/am.20.1.1-5.1970.

Keyer, K., and Imlay, J. A. (1996). Superoxide accelerates DNA damage by elevating free-iron levels. *Proc. Natl. Acad. Sci.* 93, 13635–13640. doi:10.1073/pnas.93.24.13635.

Kinkel, T. L., Roux, C. M., Dunman, P. M., and Fang, F. C. (2013). The Staphylococcus aureus SrrAB two-component system promotes resistance to nitrosative stress and hypoxia. *MBio* 4, 1–9. doi:10.1128/mBio.00696-13.

Kitzing, K., Fitzpatrick, T. B., Wilken, C., Sawa, J., Bourenkov, G. P., Macheroux, P., et al. (2005). The 1.3 Å crystal structure of the flavoprotein YqjM reveals a novel class of old yellow enzymes. *J. Biol. Chem.* 280, 27904–27913. doi:10.1074/jbc.M502587200.

Klebanoff, S. J., Kettle, A. J., Rosen, H., Winterbourn, C. C., and Nauseef, W. M. (2013). Myeloperoxidase: a front-line defender against phagocytosed microorganisms. *J. Leukoc. Biol.* 93, 185. doi:10.1189/JLB.0712349.

Klevens, R. M., Morrison, M. A., Nadle, J., Petit, S., Gershman, K., Ray, S., et al. (2007). Invasive Methicillin-Resistant Staphylococcus aureus Infections in the United States. *JAMA* 298, 1763–1771. doi:10.1001/JAMA.298.15.1763.

Kohanski, M. A., Dwyer, D. J., Hayete, B., Lawrence, C. A., and Collins, J. J. (2007). A Common Mechanism of Cellular Death Induced by Bactericidal Antibiotics. *Cell* 130, 797–810. doi:10.1016/j.cell.2007.06.049.

Krismer, B., Weidenmaier, C., Zipperer, A., and Peschel, A. (2017). The commensal lifestyle of Staphylococcus aureus and its interactions with the nasal microbiota. *Nat. Rev. Microbiol.* 15, 675–687. doi:10.1038/nrmicro.2017.104.

Krute, C. N., Rice, K. C., and Bose, J. L. (2017). VfrB is a key activator of the staphylococcus aureus SaeRS two- component system. *J. Bacteriol.* 199. doi:10.1128/JB.00828-16/FORMAT/EPUB.

Krute, C. N., Seawell, N. A., and Bose, J. L. (2021). "Measuring Staphylococcal Promoter Activities Using a Codon-Optimized β-Galactosidase Reporter," in *Methods in molecular biology (Clifton, N.J.)* (NIH Public Access), 37–44. doi:10.1007/978-1-0716-1550-8_6.

Kuehl, R., Morata, L., Meylan, S., Mensa, J., and Soriano, A. (2020). When antibiotics fail: a clinical and microbiological perspective on antibiotic tolerance and persistence of Staphylococcus aureus. *J. Antimicrob. Chemother.* 75, 1071–1086. doi:10.1093/jac/dkz559.

Kuipers, A., Stapels, D. A. C., Weerwind, L. T., Ko, Y.-P., Ruyken, M., Lee, J. C., et al. (2016). The Staphylococcus aureus polysaccharide capsule and Efb-dependent fibrinogen shield act in concert to protect against phagocytosis. *Microbiology* 162, 1185–1194. doi:10.1099/mic.0.000293.

Lacey, K. A., Geoghegan, J. A., and McLoughlin, R. M. (2016). The Role of Staphylococcus aureus Virulence Factors in Skin Infection and Their Potential as Vaccine Antigens. *Pathogens* 5. doi:10.3390/PATHOGENS5010022.

Lee, C., and Park, C. (2017). Bacterial Responses to Glyoxal and Methylglyoxal: Reactive Electrophilic Species. *Int. J. Mol. Sci.* 18, 169. doi:10.3390/ijms18010169.

Lee, C., Shin, J., and Park, C. (2013). Novel regulatory system nemRA - gloA for electrophile reduction in Escherichia coli K-12. *Mol. Microbiol.* 88, 395–412. doi:10.1111/mmi.12192.

Lee, M. C., Rios, A. M., Aten, M. F., Mejias, A., Cavuoti, D., McCracken, G. H., et al. (2004). Management and outcome of children with skin and soft tissue abscesses caused by

community-acquired methicillin-resistant. *Pediatr. Res.* 23, 123–127. doi:10.1097/01.inf.0000109288.06912.21.

Lensmire, J. M., Wischer, M. R., Sosinski, L. M., Ensink, E., Dodson, J. P., Shook, J. C., et al. (2021). The glutathione import system satisfies the Staphylococcus aureus nutrient sulfur requirement and promotes interspecies competition. *bioRxiv*, 2021.10.26.465763. doi:10.1101/2021.10.26.465763.

Leonardi, R., Chohnan, S., Zhang, Y.-M., Virga, K. G., Lee, R. E., Rock, C. O., et al. (2005). A Pantothenate Kinase from Staphylococcus aureus Refractory to Feedback Regulation by Coenzyme A. *J. Biol. Chem.* 280, 3314–3322. doi:10.1074/jbc.M411608200.

Levin-Reisman, I., Brauner, A., Ronin, I., and Balaban, N. Q. (2019). Epistasis between antibiotic tolerance, persistence, and resistance mutations. *Proc. Natl. Acad. Sci.* 116, 14734–14739. doi:10.1073/pnas.1906169116.

Li, H., Zhou, X., Huang, Y., Liao, B., Cheng, L., and Ren, B. (2021). Reactive Oxygen Species in Pathogen Clearance: The Killing Mechanisms, the Adaption Response, and the Side Effects. *Front. Microbiol.* 11, 3610. doi:10.3389/fmicb.2020.622534.

Lindsay, J. A. (2013). Hospital-associated MRSA and antibiotic resistance—What have we learned from genomics? *Int. J. Med. Microbiol.* 303, 318–323. doi:10.1016/j.ijmm.2013.02.005.

Linzner, N., Loi, V. Van, Fritsch, V. N., and Antelmann, H. (2020). Thiol-based redox switches in the major pathogen Staphylococcus aureus. *Biol. Chem.* 0, 333–361. doi:10.1515/hsz-2020-0272.

Linzner, N., Loi, V. Van, Fritsch, V. N., Tung, Q. N., Stenzel, S., Wirtz, M., et al. (2019). Staphylococcus aureus Uses the Bacilliredoxin (BrxAB)/Bacillithiol Disulfide Reductase (YpdA) Redox Pathway to Defend Against Oxidative Stress Under Infections. *Front. Microbiol.* 10, 1355. doi:10.3389/fmicb.2019.01355.

Liu, J., Chen, D., Peters, B. M., Li, L., Li, B., Xu, Z., et al. (2016). Staphylococcal chromosomal cassettes mec (SCCmec): A mobile genetic element in methicillin-resistant Staphylococcus aureus. *Microb. Pathog.* 101, 56–67. doi:10.1016/j.micpath.2016.10.028.

Liu, Y., Manna, A. C., Pan, C.-H., Kriksunov, I. A., Thiel, D. J., Cheung, A. L., et al. (2006). Structural and function analyses of the global regulatory protein SarA from Staphylococcus aureus. *Proc. Natl. Acad. Sci.* 103, 2392–2397. doi:10.1073/pnas.0510439103.

Loi, V. Van, Busche, T., Preuß, T., Kalinowski, J., Bernhardt, J., and Antelmann, H. (2018a). The AGXX® Antimicrobial Coating Causes a Thiol-Specific Oxidative Stress Response and Protein S-bacillithiolation in Staphylococcus aureus. *Front. Microbiol.* 9, 3037. doi:10.3389/fmicb.2018.03037.

Loi, V. Van, Busche, T., Tedin, K., Bernhardt, J., Wollenhaupt, J., Huyen, N. T. T., et al. (2018b). Redox-Sensing Under Hypochlorite Stress and Infection Conditions by the Rrf2-Family Repressor HypR in Staphylococcus aureus. *Antioxidants Redox Signal.* 29, 615–636. doi:10.1089/ars.2017.7354.

Lorenz, U., Hüttinger, C., Schäfer, T., Ziebuhr, W., Thiede, A., Hacker, J., et al. (2008). The alternative sigma factor sigma B of Staphylococcus aureus modulates virulence in experimental central venous catheter-related infections. *Microbes Infect.* 10, 217–223. doi:10.1016/j.micinf.2007.11.006.

Luong, T. T., Newell, S. W., and Lee, C. Y. (2003). mgr , a Novel Global Regulator in Staphylococcus aureus. *J. Bacteriol.* 185, 3703–3710. doi:10.1128/JB.185.13.3703-3710.2003.

Macheroux, P., Kappes, B., and Ealick, S. E. (2011). Flavogenomics - a genomic and structural view of flavin-dependent proteins. *FEBS J.* 278, 2625–2634. doi:10.1111/j.1742-4658.2011.08202.x.

Mainiero, M., Goerke, C., Geiger, T., Gonser, C., Herbert, S., and Wolz, C. (2010). Differential Target Gene Activation by the Staphylococcus aureus Two-Component System saeRS. *J. Bacteriol.* 192, 613–623. doi:10.1128/JB.01242-09.

Manna, A. C., and Ray, B. (2007). Regulation and characterization of rot transcription in Staphylococcus aureus. *Microbiology* 153, 1538–1545. doi:10.1099/mic.0.2006/004309-0.

Marchler-Bauer, A., Bo, Y., Han, L., He, J., Lanczycki, C. J., Lu, S., et al. (2017). CDD/SPARCLE: functional classification of proteins via subfamily domain architectures. *Nucleic Acids Res.* 45, D200–D203. doi:10.1093/nar/gkw1129.

Marincola, G., Schäfer, T., Behler, J., Bernhardt, J., Ohlsen, K., Goerke, C., et al. (2012). RNase Y of Staphylococcus aureus and its role in the activation of virulence genes. *Mol. Microbiol.* 85, 817–

832. doi:10.1111/j.1365-2958.2012.08144.x.
Marnett, L. J., Riggins, J. N., and West, J. D. (2003). Endogenous generation of reactive oxidants and electrophiles and their reactions with DNA and protein. *J. Clin. Invest.* 111, 583–593. doi:10.1172/JCI18022.
Martin, M. (2011). Cutadapt removes adapter sequences from high-throughput sequencing reads. *EMBnet.journal* 17, 10. doi:10.14806/ej.17.1.200.
Matsui, T., Nambu, S., Ono, Y., Goulding, C. W., Tsumoto, K., and Ikeda-Saito, M. (2013). Heme Degradation by Staphylococcus aureus IsdG and IsdI Liberates Formaldehyde Rather Than Carbon Monoxide. *Biochemistry* 52, 3025–3027. doi:10.1021/bi400382p.
Matsumoto, Y., Yasukawa, J., Ishii, M., Hayashi, Y., Miyazaki, S., and Sekimizu, K. (2016). A critical role of mevalonate for peptidoglycan synthesis in Staphylococcus aureus. *Sci. Rep.* 6, 22894. doi:10.1038/srep22894.
Matthews, R. G., and Massey, V. (1969). Isolation of Old Yellow Enzyme in Free and Complexed Forms. *J. Biol. Chem.* 244, 1779–1786. doi:10.1016/S0021-9258(18)91750-3.
McAdow, M., Missiakas, D. M., and Schneewind, O. (2012). Staphylococcus aureus secretes coagulase and von willebrand factor binding protein to modify the coagulation cascade and establish host infections. *J. Innate Immun.* 4, 141–148. doi:10.1159/000333447.
Meerwein, M., Tarnutzer, A., Böni, M., Van Bambeke, F., Hombach, M., and Zinkernagel, A. S. (2020). Increased Azithromycin Susceptibility of Multidrug-Resistant Gram-Negative Bacteria on RPMI-1640 Agar Assessed by Disk Diffusion Testing. *Antibiotics* 9, 218. doi:10.3390/antibiotics9050218.
Memmi, G., Nair, D. R., and Cheung, A. (2012). Role of ArlRS in Autolysis in Methicillin-Sensitive and Methicillin-Resistant Staphylococcus aureus Strains. *J. Bacteriol.* 194, 759–767. doi:10.1128/JB.06261-11.
Mikheyeva, I. V., Thomas, J. M., Kolar, S. L., Corvaglia, A., Gaïa, N., Leo, S., et al. (2019). YpdA, a putative bacillithiol disulfide reductase, contributes to cellular redox homeostasis and virulence in Staphylococcus aureus. *Mol. Microbiol.* 111, 1039–1056. doi:10.1111/mmi.14207.
Moldovan, A., and Fraunholz, M. J. (2019). In or out: Phagosomal escape of Staphylococcus aureus. *Cell. Microbiol.* 21, e12997. doi:10.1111/cmi.12997.
Monk, I. R., Tree, J. J., Howden, B. P., Stinear, T. P., and Foster, T. J. (2015). Complete Bypass of Restriction Systems for Major Staphylococcus aureus Lineages. *MBio* 6, 1–12. doi:10.1128/mBio.00308-15.
Morikawa, K., Inose, Y., Okamura, H., Maruyama, A., Hayashi, H., Takeyasu, K., et al. (2003). A new staphylococcal sigma factor in the conserved gene cassette: functional significance and implication for the evolutionary processes. *Genes to Cells* 8, 699–712. doi:10.1046/j.1365-2443.2003.00668.x.
Morikawa, K., Ohniwa, R. L., Kim, J., Maruyama, A., Ohta, T., and Takeyasu, K. (2006). Bacterial nucleoid dynamics: oxidative stress response in Staphylococcus aureus. *Genes to Cells* 11, 409–423. doi:10.1111/j.1365-2443.2006.00949.x.
Morikawa, K., Ushijima, Y., Ohniwa, R. L., Miyakoshi, M., and Takeyasu, K. (2019). What Happens in the Staphylococcal Nucleoid under Oxidative Stress? *Microorganisms* 7, 631. doi:10.3390/microorganisms7120631.
Morrison, J. (2012). The staphylococcal accessory regulator, SarA, is an RNA-binding protein that modulates the mRNA turnover properties of late-exponential and stationary phase Staphylococcus aureus cells. *Front. Cell. Infect. Microbiol.* 2, 26. doi:10.3389/fcimb.2012.00026.
Moskovitz, J., Singh, V. K., Requena, J., Wilkinson, B. J., Jayaswal, R. K., and Stadtman, E. R. (2002). Purification and Characterization of Methionine Sulfoxide Reductases from Mouse and Staphylococcus aureus and Their Substrate Stereospecificity. *Biochem. Biophys. Res. Commun.* 290, 62–65. doi:10.1006/bbrc.2001.6171.
Naimi, T. S., LeDell, K. H., Como-Sabetti, K., Borchardt, S. M., Boxrud, D. J., Etienne, J., et al. (2003). Comparison of Community- and Health Care - Associated Methicillin-Resistant Staphylococcus aureus Infection. *J. Am. Med. Assoc.* 290, 2976–2984. doi:10.1001/jama.290.22.2976.
Nakano, S., Erwin, K. N., Ralle, M., and Zuber, P. (2004). Redox-sensitive transcriptional control by a thiol/disulphide switch in the global regulator, Spx. *Mol. Microbiol.* 55, 498–510.

doi:10.1111/j.1365-2958.2004.04395.x.

Nguyen, D., Joshi-Datar, A., Lepine, F., Bauerle, E., Olakanmi, O., Beer, K., et al. (2011). Active Starvation Responses Mediate Antibiotic Tolerance in Biofilms and Nutrient-Limited Bacteria. *Science (80-.).* 334, 982–986. doi:10.1126/science.1211037.

Nicoloff, H., Hjort, K., Levin, B. R., and Andersson, D. I. (2019). The high prevalence of antibiotic heteroresistance in pathogenic bacteria is mainly caused by gene amplification. *Nat. Microbiol.* 4, 504–514. doi:10.1038/s41564-018-0342-0.

Nizam, S., Verma, S., Borah, N. N., Gazara, R. K., and Verma, P. K. (2015). Comprehensive genome-wide analysis reveals different classes of enigmatic old yellow enzyme in fungi. *Sci. Rep.* 4, 4013. doi:10.1038/srep04013.

Oefner, C., Bandera, M., Haldimann, A., Laue, H., Schulz, H., Mukhija, S., et al. (2009). Increased hydrophobic interactions of iclaprim with Staphylococcus aureus dihydrofolate reductase are responsible for the increase in affinity and antibacterial activity. *J. Antimicrob. Chemother.* 63, 687–698. doi:10.1093/jac/dkp024.

Ohlsen, K., Koller, K. P., and Hacker, J. (1997). Analysis of expression of the alpha-toxin gene (hla) of Staphylococcus aureus by using a chromosomally encoded hla::lacZ gene fusion. *Infect. Immun.* 65, 3606–3614. doi:10.1128/iai.65.9.3606-3614.1997.

Oliveira, D., Borges, A., and Simões, M. (2018). Staphylococcus aureus Toxins and Their Molecular Activity in Infectious Diseases. *Toxins (Basel).* 10, 252. doi:10.3390/toxins10060252.

Otto, M. (2013). Community-associated MRSA: What makes them special? *Int. J. Med. Microbiol.* 303, 324–330. doi:10.1016/j.ijmm.2013.02.007.

Overton, T. W., Justino, M. C., Li, Y., Baptista, J. M., Melo, A. M. P., Cole, J. A., et al. (2008). Widespread Distribution in Pathogenic Bacteria of Di-Iron Proteins That Repair Oxidative and Nitrosative Damage to Iron-Sulfur Centers. *J. Bacteriol.* 190, 2004–2013. doi:10.1128/JB.01733-07.

Ozyamak, E., Almeida, C., Moura, A. P. S., Miller, S., and Booth, I. R. (2013). Integrated stress response of E scherichia coli to methylglyoxal: transcriptional readthrough from the nemRA operon enhances protection through increased expression of glyoxalase I. *Mol. Microbiol.* 88, 936–950. doi:10.1111/mmi.12234.

Pané-Farré, J., Jonas, B., Förstner, K., Engelmann, S., and Hecker, M. (2006). The σB regulon in Staphylococcus aureus and its regulation. *Int. J. Med. Microbiol.* 296, 237–258. doi:10.1016/j.ijmm.2005.11.011.

Párraga Solórzano, P. K., Yao, J., Rock, C. O., and Kehl-Fie, T. E. (2019). Disruption of Glycolysis by Nutritional Immunity Activates a Two-Component System That Coordinates a Metabolic and Antihost Response by Staphylococcus aureus. *MBio* 10. doi:10.1128/mBio.01321-19.

Peacock, S. J., and Paterson, G. K. (2015). Mechanisms of Methicillin Resistance in Staphylococcus aureus. *Annu. Rev. Biochem.* 84, 577–601. doi:10.1146/annurev-biochem-060614-034516.

Pedre, B., Barayeu, U., Ezeriņa, D., and Dick, T. P. (2021). The mechanism of action of N-acetylcysteine (NAC): The emerging role of H2S and sulfane sulfur species. *Pharmacol. Ther.* 228, 107916. doi:10.1016/J.PHARMTHERA.2021.107916.

Pelz, A., Wieland, K.-P., Putzbach, K., Hentschel, P., Albert, K., and Götz, F. (2005). Structure and Biosynthesis of Staphyloxanthin from Staphylococcus aureus. *J. Biol. Chem.* 280, 32493–32498. doi:10.1074/jbc.M505070200.

Penewit, K., Holmes, E. A., McLean, K., Ren, M., Waalkes, A., and Salipante, S. J. (2018). Efficient and Scalable Precision Genome Editing in Staphylococcus aureus through Conditional Recombineering and CRISPR/Cas9-Mediated Counterselection. *MBio* 9, 1–14. doi:10.1128/mBio.00067-18.

Peng, H., Shen, J., Edmonds, K. A., Luebke, J. L., Hickey, A. K., Palmer, L. D., et al. (2017). Sulfide Homeostasis and Nitroxyl Intersect via Formation of Reactive Sulfur Species in Staphylococcus aureus. *mSphere* 2. doi:10.1128/mSphere.00082-17.

Peng, H., Zhang, Y., Trinidad, J. C., and Giedroc, D. P. (2018). Thioredoxin profiling of multiple thioredoxin-like proteins in staphylococcus aureus. *Front. Microbiol.* 9, 1–13. doi:10.3389/fmicb.2018.02385.

Pidwill, G. R., Gibson, J. F., Cole, J., Renshaw, S. A., and Foster, S. J. (2021). The Role of Macrophages

in Staphylococcus aureus Infection. *Front. Immunol.*, 3506. Available at: https://www.frontiersin.org/articles/10.3389/fimmu.2020.620339/full [Accessed July 21, 2021].

Poole, L. B. (2005). Bacterial defenses against oxidants: mechanistic features of cysteine-based peroxidases and their flavoprotein reductases. *Arch. Biochem. Biophys.* 433, 240–254. doi:10.1016/j.abb.2004.09.006.

Portolés, M., Kiser, K. B., Bhasin, N., Chan, K. H. N., and Lee, J. C. (2001). Staphylococcus aureus Cap5O Has UDP-ManNAc Dehydrogenase Activity and Is Essential for Capsule Expression. *Infect. Immun.* 69, 917–923. doi:10.1128/IAI.69.2.917-923.2001.

Powell, III, R. W., Buteler, M. P., Lenka, S., Crotti, M., Santangelo, S., Burg, M. J., et al. (2018). Investigating Saccharomyces cerevisiae alkene reductase OYE 3 by substrate profiling, X-ray crystallography and computational methods. *Catal. Sci. Technol.* 8, 5003–5016. doi:10.1039/C8CY00440D.

Price, E. E., Rudra, P., Norambuena, J., Román-Rodríguez, F., and Boyd, J. M. (2021). Tools, Strains, and Strategies To Effectively Conduct Anaerobic and Aerobic Transcriptional Reporter Screens and Assays in Staphylococcus aureus. *Appl. Environ. Microbiol.* 87, e0110821. doi:10.1128/AEM.01108-21.

Prinz, W. A., Åslund, F., Holmgren, A., and Beckwith, J. (1997). The role of the thioredoxin and glutaredoxin pathways in reducing protein disulfide bonds in the Escherichia coli cytoplasm. *J. Biol. Chem.* 272, 15661–15667. doi:10.1074/jbc.272.25.15661.

Rack, J. G. M., Morra, R., Barkauskaite, E., Kraehenbuehl, R., Ariza, A., Qu, Y., et al. (2015). Identification of a Class of Protein ADP-Ribosylating Sirtuins in Microbial Pathogens. *Mol. Cell* 59, 309–320. doi:10.1016/j.molcel.2015.06.013.

Rausch, M., Deisinger, J. P., Ulm, H., Müller, A., Li, W., Hardt, P., et al. (2019). Coordination of capsule assembly and cell wall biosynthesis in Staphylococcus aureus. *Nat. Commun.* 10, 1404. doi:10.1038/s41467-019-09356-x.

Ray, A., Edmonds, K. A., Palmer, L. D., Skaar, E. P., and Giedroc, D. P. (2020). Staphylococcus aureus Glucose-Induced Biofilm Accessory Protein A (GbaA) Is a Monothiol-Dependent Electrophile Sensor. *Biochemistry* 59, 2882–2895. doi:10.1021/acs.biochem.0c00347.

Reichert, S., Ebner, P., Bonetti, E.-J. J., Luqman, A., Nega, M., Schrenzel, J., et al. (2018). Genetic Adaptation of a Mevalonate Pathway Deficient Mutant in Staphylococcus aureus. *Front. Microbiol.* 0, 1539. doi:10.3389/FMICB.2018.01539.

Reichmann, D., Voth, W., and Jakob, U. (2018). Maintaining a Healthy Proteome during Oxidative Stress. *Mol. Cell* 69, 203–213. doi:10.1016/j.molcel.2017.12.021.

Renner, L. D., Zan, J., Hu, L. I., Martinez, M., Resto, P. J., Siegel, A. C., et al. (2017). Detection of ESKAPE Bacterial Pathogens at the Point of Care Using Isothermal DNA-Based Assays in a Portable Degas-Actuated Microfluidic Diagnostic Assay Platform. *Appl. Environ. Microbiol.* 83. doi:10.1128/AEM.02449-16.

Richardson, A. R. (2019). Virulence and Metabolism. *Microbiol. Spectr.* 7. doi:10.1128/MICROBIOLSPEC.GPP3-0011-2018/FORMAT/EPUB.

Richardson, A. R., Libby, S. J., and Fang, F. C. (2008). A Nitric Oxide–Inducible Lactate Dehydrogenase Enables Staphylococcus aureus to Resist Innate Immunity. *Science (80-.).* 319, 1672–1676. doi:10.1126/science.1155207.

Richardson, A. R., Payne, E. C., Younger, N., Karlinsey, J. E., Thomas, V. C., Becker, L. A., et al. (2011). Multiple Targets of Nitric Oxide in the Tricarboxylic Acid Cycle of Salmonella enterica Serovar Typhimurium. *Cell Host Microbe* 10, 33–43. doi:10.1016/j.chom.2011.06.004.

Roberts, C. A., Al-Tameemi, H. M., Mashruwala, A. A., Rosario-Cruz, Z., Chauhan, U., Sause, W. E., et al. (2017). The Suf Iron-Sulfur Cluster Biosynthetic System Is Essential in Staphylococcus aureus, and Decreased Suf Function Results in Global Metabolic Defects and Reduced Survival in Human Neutrophils. *Infect. Immun.* 85. doi:10.1128/IAI.00100-17.

Rochat, T., Nicolas, P., Delumeau, O., Rabatinová, A., Korelusová, J., Leduc, A., et al. (2012). Genome-wide identification of genes directly regulated by the pleiotropic transcription factor Spx in Bacillus subtilis. *Nucleic Acids Res.* 40, 9571–9583. doi:10.1093/nar/gks755.

Rohlfing, S. R., and Crawford, I. P. (1966). Purification and Characterization of the β-Galactosidase of

Aeromonas formicans. *J. Bacteriol.* 91, 1085–1097. doi:10.1128/jb.91.3.1085-1097.1966.

Rosdahl, V. T. (2009). Localisation of the Penicillinase Gene in Naturally Occurring Staphylococcus Aureus Strains. *Acta Pathol. Microbiol. Scand. Ser. B Microbiol.* 93B, 383–388. doi:10.1111/j.1699-0463.1985.tb02906.x.

Rowe, S. E., Wagner, N. J., Li, L., Beam, J. E., Wilkinson, A. D., Radlinski, L. C., et al. (2020). Reactive oxygen species induce antibiotic tolerance during systemic Staphylococcus aureus infection. *Nat. Microbiol.* 5, 282–290. doi:10.1038/s41564-019-0627-y.

Salamzade, R., Cheong, J. Z. A., Sandstrom, S., Swaney, M. H., Starr, N. L., Singh, A. M., et al. (2022). lsaBGC provides a comprehensive framework for evolutionary analysis of biosynthetic gene clusters within focal taxa. *bioRxiv*, 2022.04.20.488953. doi:10.1101/2022.04.20.488953.

Sanz, R., Marín, I., Ruiz-Santa-Quiteria, J. A., Orden, J. A., Cid, D., Diez, R. M., et al. (2000). Catalase deficiency in Staphylococcus aureus subsp. anaerobius is associated with natural loss-of-function mutations within the structural gene The GenBank accession numbers for the sequences reported in this paper are AJ000472 (S. aureus ATCC 12600 katA). *Microbiology* 146, 465–475. doi:10.1099/00221287-146-2-465.

Sato, A., Yamaguchi, T., Hamada, M., Ono, D., Sonoda, S., Oshiro, T., et al. (2019). Morphological and Biological Characteristics of Staphylococcus aureus Biofilm Formed in the Presence of Plasma. *Microb. Drug Resist.* 25, 668–676. doi:10.1089/mdr.2019.0068.

Scholtissek, A., Tischler, D., Westphal, A., van Berkel, W., and Paul, C. (2017). Old Yellow Enzyme-Catalysed Asymmetric Hydrogenation: Linking Family Roots with Improved Catalysis. *Catalysts* 7, 130. doi:10.3390/catal7050130.

Seaver, L. C., and Imlay, J. A. (2004). Are Respiratory Enzymes the Primary Sources of Intracellular Hydrogen Peroxide? *J. Biol. Chem.* 279, 48742–48750. doi:10.1074/jbc.M408754200.

Seidl, K., Müller, S., François, P., Kriebitzsch, C., Schrenzel, J., Engelmann, S., et al. (2009). Effect of a glucose impulse on the CcpA regulon in Staphylococcus aureus. *BMC Microbiol.* 9, 95. doi:10.1186/1471-2180-9-95.

Shatalin, K., Shatalina, E., Mironov, A., and Nudler, E. (2011). H2S: A universal defense against antibiotics in bacteria. *Science (80-.).* 334, 986–990. doi:10.1126/science.1209855.

Shaw, L. N., Lindholm, C., Prajsnar, T. K., Miller, H. K., Brown, M. C., Golonka, E., et al. (2008). Identification and Characterization of σS, a Novel Component of the Staphylococcus aureus Stress and Virulence Responses. *PLoS One* 3, e3844. doi:10.1371/journal.pone.0003844.

Sheng, X., Yan, M., Xu, L., and Wei, M. (2016). Identification and characterization of a novel Old Yellow Enzyme from Bacillus subtilis str.168. *J. Mol. Catal. B Enzym.* 130, 18–24. doi:10.1016/j.molcatb.2016.04.011.

Shetty, S., and Varshney, U. (2021). Regulation of translation by one-carbon metabolism in bacteria and eukaryotic organelles. *J. Biol. Chem.* 296, 100088. doi:10.1074/JBC.REV120.011985.

Shi, Q., Wang, H., Liu, J., Li, S., Guo, J., Li, H., et al. (2020). Old yellow enzymes: structures and structure-guided engineering for stereocomplementary bioreduction. *Appl. Microbiol. Biotechnol.* 104, 8155–8170. doi:10.1007/s00253-020-10845-z.

Sihto, H.-M., Tasara, T., Stephan, R., and Johler, S. (2014). Validation of reference genes for normalization of qPCR mRNA expression levels in Staphylococcus aureus exposed to osmotic and lactic acid stress conditions encountered during food production and preservation. *FEMS Microbiol. Lett.* 356, 134–140. doi:10.1111/1574-6968.12491.

Singh, V. K., Vaish, M., Johansson, T. R., Baum, K. R., Ring, R. P., Singh, S., et al. (2015). Significance of Four Methionine Sulfoxide Reductases in Staphylococcus aureus. *PLoS One* 10, e0117594. doi:10.1371/journal.pone.0117594.

Singh, V. K., Xiong, A., Usgaard, T. R., Chakrabarti, S., Deora, R., Misra, T. K., et al. (1999). ZntR is an autoregulatory protein and negatively regulates the chromosomal zinc resistance operon znt of Staphylococcus aureus. *Mol. Microbiol.* 33, 200–207. doi:10.1046/j.1365-2958.1999.01466.x.

Smith, D. S., Siggins, M. K., Gierula, M., Pichon, B., Turner, C. E., Lynskey, N. N., et al. (2016). Identification of commonly expressed exoproteins and proteolytic cleavage events by proteomic mining of clinically relevant UK isolates of Staphylococcus aureus. *Microb. Genomics* 2, 1–12. doi:10.1099/mgen.0.000049.

Soutourina, O., Poupel, O., Coppée, J.-Y. Y., Danchin, A., Msadek, T., and Martin-Verstraete, I. (2009).

CymR, the master regulator of cysteine metabolism in Staphylococcus aureus, controls host sulphur source utilization and plays a role in biofilm formation. *Mol. Microbiol.* 73, 194–211. doi:10.1111/j.1365-2958.2009.06760.x.

Speziale, P., and Pietrocola, G. (2020). The Multivalent Role of Fibronectin-Binding Proteins A and B (FnBPA and FnBPB) of Staphylococcus aureus in Host Infections. *Front. Microbiol.* 11, 2054. doi:10.3389/fmicb.2020.02054.

Stamatakis, A. (2014). RAxML version 8: A tool for phylogenetic analysis and post-analysis of large phylogenies. *Bioinformatics* 30, 1312–1313. doi:10.1093/bioinformatics/btu033.

Sullivan, L. E., and Rice, K. C. (2021). "Measurement of Pigmentation by Methanol Extraction," in *Methods in Molecular Biology* (Humana, New York, NY), 1–7. doi:10.1007/978-1-0716-1550-8_1.

Sun, F., Ji, Q., Jones, M. B., Deng, X., Liang, H., Frank, B., et al. (2012). AirSR, a [2Fe-2S] Cluster-Containing Two-Component System, Mediates Global Oxygen Sensing and Redox Signaling in Staphylococcus aureus. *J. Am. Chem. Soc.* 134, 305–314. doi:10.1021/ja2071835.

Thammavongsa, V., Kim, H. K., Missiakas, D., and Schneewind, O. (2015). Staphylococcal manipulation of host immune responses. *Nat. Rev. Microbiol.* 13, 529–543. doi:10.1038/nrmicro3521.

Thänert, R., Goldmann, O., Beineke, A., and Medina, E. (2017). Host-inherent variability influences the transcriptional response of Staphylococcus aureus during in vivo infection. *Nat. Commun.* 8, 14268. doi:10.1038/ncomms14268.

Tharmalingam, S., Alhasawi, A., Appanna, V. P., Lemire, J., and Appanna, V. D. (2017). Reactive Nitrogen Species (RNS)-resistant microbes: Adaptation and medical implications. *Biol. Chem.* 398, 1193–1208. doi:10.1515/HSZ-2017-0152/MACHINEREADABLECITATION/RIS.

Thomas, C. M., Hothersall, J., Willis, C. L., and Simpson, T. J. (2010). Resistance to and synthesis of the antibiotic mupirocin. *Nat. Rev. Microbiol.* 8, 281–289. doi:10.1038/nrmicro2278.

Thomas, P., Sekhar, A. C., Upreti, R., Mujawar, M. M., and Pasha, S. S. (2015). Optimization of single plate-serial dilution spotting (SP-SDS) with sample anchoring as an assured method for bacterial and yeast cfu enumeration and single colony isolation from diverse samples. *Biotechnol. Reports* 8, 45–55. doi:10.1016/j.btre.2015.08.003.

Throup, J. P., Zappacosta, F., Lunsford, R. D., Annan, R. S., Carr, S. A., Lonsdale, J. T., et al. (2001). The srhSR Gene Pair from Staphylococcus aureus : Genomic and Proteomic Approaches to the Identification and Characterization of Gene Function. *Biochemistry* 40, 10392–10401. doi:10.1021/bi0102959.

Tiwari, K., Gatto, C., and Wilkinson, B. (2018a). Interrelationships between Fatty Acid Composition, Staphyloxanthin Content, Fluidity, and Carbon Flow in the Staphylococcus aureus Membrane. *Molecules* 23, 1201. doi:10.3390/molecules23051201.

Tiwari, S., Rajak, S., Mondal, D. P., and Biswas, D. (2018b). Sodium hypochlorite is more effective than 70% ethanol against biofilms of clinical isolates of Staphylococcus aureus. *Am. J. Infect. Control* 46, e37–e42. doi:10.1016/j.ajic.2017.12.015.

Toliver-Kinsky, T., Cui, W., Törö, G., Lee, S.-J., Shatalin, K., Nudler, E., et al. (2019). H 2 S, a Bacterial Defense Mechanism against the Host Immune Response. *Infect. Immun.* 87, 272–290. doi:10.1128/IAI.00272-18.

Tong, S. Y. C., Davis, J. S., Eichenberger, E., Holland, T. L., and Fowler, V. G. (2015). Staphylococcus aureus Infections: Epidemiology, Pathophysiology, Clinical Manifestations, and Management. *Clin. Microbiol. Rev.* 28, 603–661. doi:10.1128/CMR.00134-14.

Toogood, H. S., Gardiner, J. M., and Scrutton, N. S. (2010). Biocatalytic Reductions and Chemical Versatility of the Old Yellow Enzyme Family of Flavoprotein Oxidoreductases. *ChemCatChem* 2, 892–914. doi:10.1002/CCTC.201000094.

Trotter, E. W., Collinson, E. J., Dawes, I. W., and Grant, C. M. (2006). Old Yellow Enzymes Protect against Acrolein Toxicity in the Yeast Saccharomyces cerevisiae. *Appl. Environ. Microbiol.* 72, 4885–4892. doi:10.1128/AEM.00526-06.

Tsuchiya, Y., Zhyvoloup, A., Baković, J., Thomas, N., Yu, B. Y. K., Das, S., et al. (2018). Protein CoAlation and antioxidant function of coenzyme A in prokaryotic cells. *Biochem. J.* 475, 1909–1937. doi:10.1042/BCJ20180043.

Tuchscherr, L., Bischoff, M., Lattar, S. M., Noto Llana, M., Pförtner, H., Niemann, S., et al. (2015). Sigma Factor SigB Is Crucial to Mediate Staphylococcus aureus Adaptation during Chronic Infections. *PLOS Pathog.* 11, e1004870. doi:10.1371/journal.ppat.1004870.

Ulrich, M., Bastian, M., Cramton, S. E., Ziegler, K., Pragman, A. A., Bragonzi, A., et al. (2007). The staphylococcal respiratory response regulator SrrAB induces ica gene transcription and polysaccharide intercellular adhesin expression, protecting Staphylococcus aureus from neutrophil killing under anaerobic growth conditions. *Mol. Microbiol.* 65, 1276–1287. doi:10.1111/j.1365-2958.2007.05863.x.

Valderas, M. W., and Hart, M. E. (2001). Identification and Characterization of a Second Superoxide Dismutase Gene (sodM) from Staphylococcus aureus. *J. Bacteriol.* 183, 3399–3407. doi:10.1128/JB.183.11.3399-3407.2001.

van der Maten, E., de Jonge, M. I., de Groot, R., van der Flier, M., and Langereis, J. D. (2017). A versatile assay to determine bacterial and host factors contributing to opsonophagocytotic killing in hirudin-anticoagulated whole blood. *Sci. Rep.* 7, 1–10. doi:10.1038/srep42137.

Van Loi, V., Busche, T., Fritsch, V. N., Weise, C., Gruhlke, M. C. H., Slusarenko, A. J., et al. (2021). The two-Cys-type TetR repressor GbaA confers resistance under disulfide and electrophile stress in Staphylococcus aureus. *Free Radic. Biol. Med.* 177, 120–131. Available at: https://linkinghub.elsevier.com/retrieve/pii/S0891584921007759 [Accessed November 10, 2021].

Van Loi, V., Rossius, M., Antelmann, H., Loi, V. Van, Rossius, M., and Antelmann, H. (2015). Redox regulation by reversible protein S-thiolation in bacteria. Frontiers Media S.A. doi:10.3389/fmicb.2015.00187.

Vashist, S., Urena, L., and Goodfellow, I. (2012). Development of a strand specific real-time RT-qPCR assay for the detection and quantitation of murine norovirus RNA. *J. Virol. Methods* 184, 69–76. doi:10.1016/j.jviromet.2012.05.012.

Vidal-Aroca, F., Giannattasio, M., Brunelli, E., Vezzoli, A., Plevani, P., Muzi-Falconi, M., et al. (2006). One-step high-throughput assay for quantitative detection of β-galactosidase activity in intact Gram-negative bacteria, yeast, and mammalian cells. *Biotechniques* 40, 433–440. doi:10.2144/000112145.

Villanueva, M., Jousselin, A., Baek, K. T., Prados, J., Andrey, D. O., Renzoni, A., et al. (2016). Rifampin Resistance rpoB Alleles or Multicopy Thioredoxin/Thioredoxin Reductase Suppresses the Lethality of Disruption of the Global Stress Regulator spx in Staphylococcus aureus. *J. Bacteriol.* 198, 2719–2731. doi:10.1128/JB.00261-16.

Votintseva, A. A., Fung, R., Miller, R. R., Knox, K., Godwin, H., Wyllie, D. H., et al. (2014). Prevalence of Staphylococcus aureus protein A (spa) mutants in the community and hospitals in Oxfordshire. *BMC Microbiol.* 14, 63. doi:10.1186/1471-2180-14-63.

Walker, J. N., Crosby, H. A., Spaulding, A. R., Salgado-Pabón, W., Malone, C. L., Rosenthal, C. B., et al. (2013). The Staphylococcus aureus ArlRS Two-Component System Is a Novel Regulator of Agglutination and Pathogenesis. *PLoS Pathog.* 9, e1003819. doi:10.1371/journal.ppat.1003819.

Wang, X., and Zhao, X. (2009). Contribution of Oxidative Damage to Antimicrobial Lethality. *Antimicrob. Agents Chemother.* 53, 1395–1402. doi:10.1128/AAC.01087-08.

Warburg, O., and Christian, W. (1938). Bemerkung uber gelbe Fermente. *Biochem Zeitschr* 298, 368–377. Available at: https://eurekamag.com/research/024/230/024230052.php [Accessed January 3, 2022].

Wasil, M., Halliwell, B., Grootveld, M., Moorhouse, C. P., Hutchison, D. C., and Baum, H. (1987). The specificity of thiourea, dimethylthiourea and dimethyl sulphoxide as scavengers of hydroxyl radicals. Their protection of alpha 1-antiproteinase against inactivation by hypochlorous acid. *Biochem. J.* 243, 867. doi:10.1042/BJ2430867.

White, J. R., and Yeowell, H. N. (1982). Iron enhances the bactericidal action of streptonigrin. *Biochem. Biophys. Res. Commun.* 106, 407–411. doi:10.1016/0006-291X(82)91125-1.

Wieland, B., Feil, C., Gloria-Maercker, E., Thumm, G., Lechner, M., Bravo, J. M., et al. (1994). Genetic and biochemical analyses of the biosynthesis of the yellow carotenoid 4,4'-diaponeurosporene of Staphylococcus aureus. *J. Bacteriol.* 176, 7719–7726. doi:10.1128/jb.176.24.7719-7726.1994.

Wilding, E. I., Kim, D. Y., Bryant, A. P., Gwynn, M. N., Lunsford, R. D., McDevitt, D., et al. (2000). Essentiality, expression, and characterization of the class II 3-hydroxy-3-methylglutaryl coenzyme a reductase of Staphylococcus aureus. *J. Bacteriol.* 182, 5147–5152. doi:10.1128/JB.182.18.5147-5152.2000.

Williams, R. E., and Bruce, N. C. (2002). 'New uses for an Old Enzyme' – the Old Yellow Enzyme family of flavoenzymes. *Microbiology* 148, 1607–1614. doi:10.1099/00221287-148-6-1607.

Williams, R. E., Rathbone, D. A., Scrutton, N. S., and Bruce, N. C. (2004). Biotransformation of explosives by the old yellow enzyme family of flavoproteins. *Appl. Environ. Microbiol.* 70, 3566–3574. doi:10.1128/AEM.70.6.3566-3574.2004.

Wilson, D. N. (2009). The A–Z of bacterial translation inhibitors. *Crit. Rev. Biochem. Mol. Biol.* 44, 393–433. doi:10.3109/10409230903307311.

Wilson, D. N. (2014). Ribosome-targeting antibiotics and mechanisms of bacterial resistance. *Nat. Rev. Microbiol.* 12, 35–48. doi:10.1038/nrmicro3155.

Wolf, C., Hochgräfe, F., Kusch, H., Albrecht, D., Hecker, M., and Engelmann, S. (2008). Proteomic analysis of antioxidant strategies of Staphylococcus aureus: Diverse responses to different oxidants. *Proteomics* 8, 3139–3153. doi:10.1002/pmic.200701062.

Wu, S., de Lencastre, H., and Tomasz, A. (1996). Sigma-B, a putative operon encoding alternate sigma factor of Staphylococcus aureus RNA polymerase: molecular cloning and DNA sequencing. *J. Bacteriol.* 178, 6036–6042. doi:10.1128/jb.178.20.6036-6042.1996.

Wu, T., Hu, E., Xu, S., Chen, M., Guo, P., Dai, Z., et al. (2021). clusterProfiler 4.0: A universal enrichment tool for interpreting omics data. *Innov.* 2, 100141. doi:10.1016/j.xinn.2021.100141.

Wyllie, S., Roberts, A. J., Norval, S., Patterson, S., Foth, B. J., Berriman, M., et al. (2016). Activation of Bicyclic Nitro-drugs by a Novel Nitroreductase (NTR2) in Leishmania. *PLOS Pathog.* 12, e1005971. doi:10.1371/JOURNAL.PPAT.1005971.

Xiao, X., Li, Y., Li, L., and Xiong, Y. (2022). Identification of Methicillin-Resistant Staphylococcus aureus (MRSA) Genetic Factors Involved in Human Endothelial Cells Damage, an Important Phenotype Correlated with Persistent Endovascular Infection. *Antibiotics* 11, 316. doi:10.3390/antibiotics11030316.

Yu, G. (2020). Using ggtree to Visualize Data on Tree-Like Structures. *Curr. Protoc. Bioinforma.* 69, e96. doi:10.1002/cpbi.96.

Zeng, D., Debabov, D., Hartsell, T. L., Cano, R. J., Adams, S., Schuyler, J. A., et al. (2016). Approved Glycopeptide Antibacterial Drugs: Mechanism of Action and Resistance. *Cold Spring Harb. Perspect. Med.* 6, a026989. doi:10.1101/cshperspect.a026989.

7 Appendix

7.1 Transcriptomic analysis

Table 25: RNA-sequencing analysis comparing Δ*ofrA vs* JE2 (*n* = 3) at OD_{600} = 0.5 in RPMI medium (*P*-value < 0.05).

Locus tag	Gene symbol	Feature	log2FoldChange	*P*-value
SAUSA300_0107	*nptA*	CDS	0.529171	5.57E-05
SAUSA300_0170	*aldA*	CDS	-0.502329	6.55E-03
SAUSA300_0181	*ausA*	CDS	-0.233138	3.11E-02
SAUSA300_0185	*argJ*	CDS	-0.406380	2.40E-02
SAUSA300_0188	*brnQ1*	CDS	0.240291	2.18E-02
SAUSA300_0189	-	CDS	0.691455	2.88E-05
SAUSA300_0190	-	CDS	0.608584	3.05E-04
SAUSA300_0212	-	CDS	-0.453878	1.64E-03
SAUSA300_0213	-	CDS	-0.294745	2.92E-02
SAUSA300_0214	-	CDS	-0.342553	1.93E-02
SAUSA300_0221	*pflA*	CDS	-0.607220	4.10E-03
SAUSA300_0278	*esxA*	CDS	-0.338047	6.93E-03
SAUSA300_0283	*essC*	CDS	-0.358306	2.51E-02
SAUSA300_0339	-	CDS	-0.481196	1.90E-03
SAUSA300_0340	-	CDS	-0.552657	3.82E-03
SAUSA300_0358	*metF*	CDS	-0.395075	3.40E-02
SAUSA300_0372	-	CDS	-0.713585	2.71E-03
SAUSA300_0386	*xpt*	CDS	0.355888	1.05E-03
SAUSA300_0387	*pbuX*	CDS	0.271456	2.97E-03
SAUSA300_0424	*zagA*	CDS	0.457842	4.97E-02
SAUSA300_0429	-	CDS	-0.228977	3.55E-02
SAUSA300_0431	-	CDS	-0.558496	4.45E-02
SAUSA300_0445	*gltB*	CDS	-0.446180	8.17E-03
SAUSA300_0446	*gltD*	CDS	-0.390831	9.85E-03
SAUSA300_0455	*rrsA*	rRNA	-3.081901	3.16E-06
SAUSA300_0456	*rrl1*	rRNA	-2.349657	2.19E-05
SAUSA300_0469	*rnmV*	CDS	-0.324606	1.09E-02
SAUSA300_0470	*ksgA*	CDS	-0.279723	3.02E-02
SAUSA300_0476	-	CDS	0.358910	2.06E-02
SAUSA300_0499	*rrsB*	rRNA	-3.068966	3.55E-06
SAUSA300_0501	*rrlB*	rRNA	-2.329682	2.08E-05
SAUSA300_0566	-	CDS	-0.460741	5.52E-03
SAUSA300_0570	*pta*	CDS	0.293665	7.75E-03
SAUSA300_0571	*lipL*	CDS	0.213388	3.22E-02
SAUSA300_0591	-	CDS	0.310231	2.06E-02
SAUSA300_0595	-	CDS	0.327664	7.42E-03
SAUSA300_0629	*pbp4*	CDS	0.260920	4.31E-02
SAUSA300_0632	-	CDS	0.202688	4.72E-02
SAUSA300_0637	*dhaL*	CDS	-0.438330	1.70E-02

SAUSA300_0693	*saeP*	CDS	0.327637	7.58E-03
SAUSA300_0712	*dtpT*	CDS	0.288877	4.16E-03
SAUSA300_0718	*sstA*	CDS	0.424746	2.93E-03
SAUSA300_0719	*sstB*	CDS	0.381946	2.84E-02
SAUSA300_0774	*emp*	CDS	-0.384724	4.14E-02
SAUSA300_0815	*ear*	CDS	-0.902575	6.36E-05
SAUSA300_0841	-	CDS	0.351338	3.66E-03
SAUSA300_0856	*kapB*	CDS	0.362823	2.41E-02
SAUSA300_0857	*ppiB*	CDS	0.307918	1.60E-03
SAUSA300_0858	-	CDS	-0.893341	2.33E-05
SAUSA300_0859	-	CDS	-8.080708	2.15E-64
SAUSA300_0860	*rocD*	CDS	2.820476	1.35E-76
SAUSA300_0861	*gudB*	CDS	1.924808	2.87E-35
SAUSA300_0877	*clpB*	CDS	-0.312933	3.11E-02
SAUSA300_0897	*trpS*	CDS	0.215267	4.97E-02
SAUSA300_0964	-	CDS	0.350311	2.00E-03
SAUSA300_0971	*purL*	CDS	-0.325970	3.10E-02
SAUSA300_0972	*purF*	CDS	-0.329243	2.65E-02
SAUSA300_0973	*purM*	CDS	-0.353701	1.31E-02
SAUSA300_0974	*purN*	CDS	-0.378502	7.98E-03
SAUSA300_0975	*purH*	CDS	-0.386208	4.08E-03
SAUSA300_0976	*purD*	CDS	-0.349812	1.59E-02
SAUSA300_1005	*mntH*	CDS	-0.415872	3.06E-02
SAUSA300_1008	-	CDS	0.482818	1.25E-02
SAUSA300_1010	-	CDS	0.320503	4.15E-02
SAUSA300_1030	*isdC*	CDS	0.205684	4.27E-02
SAUSA300_1048	*sdhB*	CDS	-0.439766	8.33E-03
SAUSA300_1053	*flr*	CDS	-0.597587	2.22E-02
SAUSA300_1058	*hla*	CDS	-0.369417	7.84E-03
SAUSA300_1059	*ssl12*	CDS	-0.698406	1.45E-02
SAUSA300_1090	-	CDS	0.268964	3.77E-02
SAUSA300_1091	*pyrR*	CDS	0.977715	5.34E-04
SAUSA300_1092	*pyrP*	CDS	1.325441	2.22E-03
SAUSA300_1093	*pyrB*	CDS	1.160946	6.71E-06
SAUSA300_1094	*pyrC*	CDS	1.113761	3.38E-05
SAUSA300_1095	*carA*	CDS	1.093776	1.33E-05
SAUSA300_1096	*carB*	CDS	1.057255	5.10E-06
SAUSA300_1097	*pyrF*	CDS	1.057736	1.15E-05
SAUSA300_1098	*pyrE*	CDS	1.051715	3.79E-06
SAUSA300_1099	-	CDS	0.914792	2.71E-04
SAUSA300_1100	-	CDS	0.333136	6.28E-03
SAUSA300_1117	*rpmB*	CDS	0.343053	1.29E-02
SAUSA300_1131	*rpsP*	CDS	0.284702	9.43E-03
SAUSA300_1198	*hflX*	CDS	0.396897	4.02E-03
SAUSA300_1200	*glnR*	CDS	0.771931	2.66E-03
SAUSA300_1201	*glnA*	CDS	0.767979	5.03E-05

SAUSA300_1222	*nuc2*	CDS	0.377881	3.41E-02
SAUSA300_1231	-	CDS	0.243291	4.28E-02
SAUSA300_1233	*rpmG2*	CDS	0.458785	1.30E-03
SAUSA300_1241	-	CDS	0.294555	1.73E-02
SAUSA300_1244	*mscL*	CDS	0.322854	1.35E-02
SAUSA300_1245	*opuD1*	CDS	0.303888	2.15E-03
SAUSA300_1305	*sucB*	CDS	-0.268837	3.28E-02
SAUSA300_1309	-	CDS	-0.268157	4.80E-02
SAUSA300_1322	*cvfC*	CDS	0.187451	3.91E-02
SAUSA300_1323	-	CDS	0.340727	3.57E-03
SAUSA300_1329	-	CDS	-0.457359	9.36E-03
SAUSA300_1330	*ilvA1*	CDS	-0.542518	4.67E-04
SAUSA300_1331	*ald1*	CDS	-0.459418	9.73E-03
SAUSA300_1334	-	CDS	0.482534	3.04E-02
SAUSA300_1340	*recU*	CDS	0.276869	2.09E-02
SAUSA300_1341	*pbp2*	CDS	0.247509	2.43E-02
SAUSA300_1367	*cmk*	CDS	0.247354	3.38E-02
SAUSA300_1368	*ansA*	CDS	0.420570	6.91E-04
SAUSA300_1369	*ypdA*	CDS	0.240928	3.93E-02
SAUSA300_1456	*malA*	CDS	-0.426726	1.73E-02
SAUSA300_1495	-	CDS	0.283881	3.87E-03
SAUSA300_1525	*glyS*	CDS	0.187122	3.86E-02
SAUSA300_1545	*rpsT*	CDS	0.239290	3.63E-02
SAUSA300_1558	*mtnN*	CDS	0.250736	3.00E-02
SAUSA300_1581	-	CDS	-0.516195	1.38E-02
SAUSA300_1582	*csbD*	CDS	-0.489517	5.54E-03
SAUSA300_1583	*cymR*	CDS	0.309793	1.98E-03
SAUSA300_1607	-	CDS	0.291708	2.37E-02
SAUSA300_1653	-	CDS	0.292049	4.35E-02
SAUSA300_1666	*rpsD*	CDS	0.418813	1.93E-02
SAUSA300_1678	*fhs*	CDS	-0.384792	1.61E-02
SAUSA300_1680	*acuA*	CDS	-0.767489	3.32E-02
SAUSA300_1711	*putA*	CDS	-0.692700	2.60E-02
SAUSA300_1731	*pckA*	CDS	-0.369661	3.92E-02
SAUSA300_1760	*epiG*	CDS	-0.463894	2.46E-02
SAUSA300_1797	-	CDS	0.362438	7.77E-03
SAUSA300_1802	-	CDS	0.420807	7.16E-03
SAUSA300_1838	*rrl3*	rRNA	-2.348891	1.79E-05
SAUSA300_1841	*rrsD*	rRNA	-3.075666	3.50E-06
SAUSA300_1848	-	CDS	0.241942	1.07E-02
SAUSA300_1857	-	CDS	0.467007	8.24E-03
SAUSA300_1864	-	CDS	-0.333991	4.47E-02
SAUSA300_1873	*murT*	CDS	0.211002	4.01E-02
SAUSA300_1883	*putP*	CDS	0.308514	2.48E-02
SAUSA300_1940	-	CDS	0.458627	3.24E-02
SAUSA300_1941	-	CDS	0.645374	5.30E-03

SAUSA300_1943	-	CDS	0.878326	2.33E-02
SAUSA300_1975	*lukH*	CDS	-0.324336	3.93E-02
SAUSA300_1995	*scrR*	CDS	-0.354531	1.92E-02
SAUSA300_2016	*rrlE*	rRNA	-2.332242	2.18E-05
SAUSA300_2017	*rrsE*	rRNA	-3.018255	5.08E-06
SAUSA300_2022	*sigB*	CDS	-0.246278	3.73E-02
SAUSA300_2023	*rsbW*	CDS	-0.245474	2.23E-02
SAUSA300_2056	-	CDS	0.460628	4.56E-02
SAUSA300_2074	*rpmE2*	CDS	0.303758	9.37E-03
SAUSA300_2080	-	CDS	0.252262	4.63E-02
SAUSA300_2081	*pyrG*	CDS	0.379870	1.79E-02
SAUSA300_2097	-	CDS	-0.446302	4.56E-02
SAUSA300_2106	*mtlR*	CDS	-0.549376	3.13E-03
SAUSA300_2107	*mtlA*	CDS	-0.539293	1.40E-02
SAUSA300_2108	*mtlD*	CDS	-0.445857	8.29E-03
SAUSA300_2123	*rrlF*	rRNA	-2.335558	2.09E-05
SAUSA300_2124	*rrsF*	rRNA	-3.066793	3.48E-06
SAUSA300_2142	*asp23*	CDS	-0.534359	7.04E-04
SAUSA300_2144	*amaP*	CDS	-0.548346	3.36E-04
SAUSA300_2164	-	CDS	-1.579792	5.00E-03
SAUSA300_2171	*rpsI*	CDS	0.482163	1.63E-02
SAUSA300_2172	*rplM*	CDS	0.478093	5.94E-03
SAUSA300_2219	*moaA*	CDS	-0.267387	2.29E-02
SAUSA300_2223	*mobB*	CDS	-0.256143	2.90E-02
SAUSA300_2224	*moeA*	CDS	-0.280256	1.18E-02
SAUSA300_2235	*fhuD2*	CDS	0.321983	2.21E-02
SAUSA300_2261	-	CDS	-0.337063	1.71E-02
SAUSA300_2286	-	CDS	0.518715	5.04E-04
SAUSA300_2294	-	CDS	-0.244185	4.50E-02
SAUSA300_2298	*emrB*	CDS	0.320580	3.77E-02
SAUSA300_2300	-	CDS	0.271153	4.55E-02
SAUSA300_2327	-	CDS	-0.355997	3.32E-02
SAUSA300_2374	-	CDS	-0.286559	4.51E-02
SAUSA300_2385	*kimA*	CDS	0.343237	3.47E-03
SAUSA300_2392	*opuCB*	CDS	-0.496729	4.69E-02
SAUSA300_2396	*pnbA*	CDS	-0.460766	1.08E-02
SAUSA300_2417	-	CDS	0.273718	2.79E-02
SAUSA300_2443	*gntK*	CDS	-0.446052	1.13E-02
SAUSA300_2447	-	CDS	-0.596698	1.20E-03
SAUSA300_2455	*fbp*	CDS	-0.344012	9.80E-03
SAUSA300_2468	-	CDS	0.523080	3.06E-03
SAUSA300_2477	*cidC*	CDS	-0.325630	6.64E-03
SAUSA300_2498	*crtN*	CDS	-0.463055	3.73E-03
SAUSA300_2499	*crtM*	CDS	-0.670453	3.25E-03
SAUSA300_2500	*crtQ*	CDS	-0.580864	4.74E-03
SAUSA300_2501	*crtP*	CDS	-0.558134	5.83E-03

SAUSA300_2504	*oatA*	CDS	0.310238	9.12E-03
SAUSA300_2505	-	CDS	0.440882	3.28E-02
SAUSA300_2517	-	CDS	-0.362247	3.40E-02
SAUSA300_2518	-	CDS	-0.386245	2.92E-02
SAUSA300_2526	*pyrD*	CDS	0.597480	2.89E-04
SAUSA300_2527	-	CDS	0.512625	5.02E-03
SAUSA300_2541	*lqo*	CDS	0.189536	3.68E-02
SAUSA300_2548	-	CDS	-0.368208	2.15E-02
SAUSA300_2623	*pcp*	CDS	0.413689	3.24E-02
SAUSA300_2631	-	CDS	-0.386144	2.07E-02
SAUSA300_2647	*rnpA*	CDS	0.389345	2.25E-02

7.2 List of Figures

7.3 List of Tables

7.4 List of abbreviations

1C	One carbon metabolism	**MH**	Mueller–Hinton
ANOVA	Analysis of variance	**MHQ**	Methylhydroquinone
ATP	Adenosine triphosphate	**MIC**	Minimum inhibitory concentration
BHI	Brain-heart infusion	**MRSA**	Methicillin-resistant *S. aureus*
Brx	Bacilliredoxin	**MSCRAMM**	Microbial surface components recognizing adhesive matrix molecules
BSH	Bacillithiol	**MSSA**	Methicillin-sensitive *S. aureus*
CA-MRSA	Community acquired MRSA	**MUG**	4-Methylumbelliferyl-β-D-galactopyranoside
cDNA	Complementary DNA	**MVA**	Mevalonate pathway
CFU	Colony forming unit	**NAC**	*N*-acetyl cysteine
CHP	Cumene hydroperoxide	**NAD^+**	Nicotinamide adenine dinucleotide
CoASH	Coenzyme A	**$NADP^+$**	Nicotinamide adenine dinucleotide phosphate
co*lacZ*	Codon-optimised *lacZ*	**NEM**	*N*-ethylmaleimide
C_q	Quantification cycle	**NETs**	Neutrophil extracellular traps
dATP	Deoxyadenosine triphosphate	**OD**	Optical density
dCTP	Deoxycytidine triphosphate	**OYE**	Old yellow enzyme
dGTP	Deoxyguanosine triphosphate	**p.i.**	Post infection
Diamide	Tetramethylazodicarboxamide	**PBS**	Phosphate buffered saline
DNA	Deoxyribonucleic acid	**PCR**	Polymerase chain reaction
dNTPs	Deoxynucleoside triphosphate	**PNK**	Polynucleotide kinase
dTTP	Deoxythymidine triphosphate	**PPP**	Pentose phosphate pathway
EC buffer	Electrical conductivity buffer	**PSMs**	Phenol soluble modulins
ESKAPE	*Enterococcus faecium*, *Staphylococcus aureus*, *Klebsiella pneumoniae*, *Acinetobacter baumannii*, *Pseudomonas aeruginosa*, and *Enterobacter* spp.	**RCS**	Reactive chlorine species
ETC	Electron transport chain	**RES**	Reactive electrophilic species
FA	Formaldehyde	**RNA**	Ribonucleic acid
FAD	flavin adenine dinucleotide	**RNA-seq**	Ribonucleic acid sequencing
FBS	Fetal bovine serum	**RNS**	Reactive nitrogen species
Fe-S clusters	Iron-Sulfur cluster	**ROS**	Reactive oxygen species
FMN	Flavin mononucleotide	**RPMI**	Roswell Park Memorial Institute
Fosfo	Fosfomycin	**RSS**	Reactive sulfur species
FPP	Farnesyl pyrophosphate	**RT-qPCR**	Reverse transcription quantitative PCR

G+C	guanine and cytosine	***S. aureus***	*Staphylococcus aureus*
GAPDH	Glyceraldehyde 3-phosphate dehydrogenase	**STX**	Staphyloxanthin
Grx	Glutaredoxin	**TCA cycle**	tricarboxylic acid cycle
GSEA	Gene set enrichment analysis	**TCS**	Two component system
HA-MRSA	Hospital acquired MRSA	**Trx**	Thioredoxin
HMEC-1	Human microvascular endothelial cells	**TSB**	Tryptic soy broth
IPP	Isopentenyl pyrophosphate	**WT**	Wild type
LB	Lysogeny broth	**X-gal**	5-bromo-4-chloro-3-indolyl-β-D-galactopyranoside
LMW	Low molecular weight	**ϕ11**	Phage 11
MG	Methylglyoxal		

III. *Curriculum vitae* (CV)

IV. Affidavit

I hereby confirm that my thesis entitled **"Unraveling the function of the old yellow enzyme OfrA in *Staphylococcus aureus* stress response"** is the result of my own work. I did not receive any help or support from commercial consultants. All sources and / or materials applied are listed and specified in the thesis.

Furthermore, I confirm that this thesis has not yet been submitted as part of another examination process neither in identical nor in similar form.

Place, Date Signature

Eidesstattliche Erklärung

Hiermit erkläre ich an Eides statt, die Dissertation **Entschlüsselung der Funktion des "alten gelben Enzyms" OfrA in der Stressreaktion von *Staphylococcus aureus*** eigenständig, d.h. insbesondere selbständig und ohne Hilfe eines kommerziellen Promotionsberaters, angefertigt und keine anderen als die von mir angegebenen Quellen und Hilfsmittel verwendet zu haben.

Ich erkläre außerdem, dass die Dissertation weder in gleicher noch in ähnlicher Form bereits in einem anderen Prüfungsverfahren vorgelegen hat.

Ort, Datum Unterschrift